

Multi-aircraft Conflict Resolution using Velocity Obstacles

S. Balasoorian

October 31, 2017

Multi-aircraft Conflict Resolution using Velocity Obstacles

MASTER OF SCIENCE THESIS

For obtaining the degree of Master of Science in Aerospace Engineering
at Delft University of Technology

S. Balasooriyan

October 31, 2017



Delft University of Technology

Copyright © S. Balasooriyan
All rights reserved.

DELFT UNIVERSITY OF TECHNOLOGY
DEPARTMENT OF
CONTROL AND SIMULATION

The undersigned hereby certify that they have read and recommend to the Faculty of Aerospace Engineering for acceptance a thesis entitled “**Multi-aircraft Conflict Resolution using Velocity Obstacles**” by **S. Balasooriyan** in partial fulfillment of the requirements for the degree of **Master of Science**.

Dated: October 31, 2017

Supervisors:

prof.dr.ir J. M. Hoekstra

dr.ir. J. Ellerbroek

ir. E. Sunil

Reader:

prof.dr.ir H. A. P. Blom

Preface

Dear reader,

Thanks for showing an interest in this report that completes my MSc Thesis on “Multi-aircraft Conflict Resolution using Velocity Obstacles”. Working for ten months on a challenging problem, requiring extensive programming with a slight mathematical edge, turned out to be a very satisfactory time for me.

I would like to take the opportunity to thank the people who have been very helpful during my work on the thesis. First, I deeply thank my daily supervisors, Emmanuel Sunil and Joost Ellerbroek for their advice and guidance. Not only their expertise, but also their enthusiasm on many aspects of my thesis kept me encouraged to work with discipline on the thesis. I would also like to acknowledge Jacco Hoekstra for his insights and excellent motivating capabilities in the meetings we had together.

I am thanking my parents for their love and support, not only during the five years at university, but throughout my whole life. And my sister, Awani, who actually contributed to this thesis even though the topic is completely out of her field of study. The support of friends that have shown genuine interest during the thesis should also not be forgotten. And last, but certainly not least, the people at the faculty that contributed to the great working atmosphere.

This work not only signifies the end of my graduation project at the department of Control & Simulation, but also the end of my five years as a student at the Faculty of Aerospace Engineering at Delft University of Technology. I can honestly look back at this time with great memories.

Suthes Balasooriyan
October 2017
Schiedam, The Netherlands

Contents

| | |
|--|-------------|
| Preface | v |
| List of Tables | xi |
| List of Figures | xv |
| List of Abbreviations | xvii |
| List of Symbols | xix |
| Thesis Outline | xxi |
| | |
| I Scientific Paper | 1 |
| | |
| II Appendices | 19 |
| | |
| A Additional Results | 21 |
| A-1 Safety Metrics Charts | 22 |
| A-2 Stability Metrics Charts | 26 |
| A-3 Efficiency Metrics Charts | 27 |
| A-4 Safety Metrics Normality Test | 30 |
| A-5 Stability Metrics Normality Test | 34 |
| A-6 Efficiency Metrics Normality Test | 35 |
| A-7 Safety Metrics Wilcoxon Signed-Rank Test | 38 |
| A-8 Stability Metrics Wilcoxon Signed-Rank Test | 42 |
| A-9 Efficiency Metrics Wilcoxon Signed-Rank Test | 43 |

| | |
|---|-----------|
| B Unit Tests of the SSD in BlueSky | 47 |
| | |
| III Preliminary Report [already graded] | 49 |
| | |
| 1 Introduction | 51 |
| 1-1 Thesis Objective and Research Questions | 52 |
| 1-2 Research Approach | 55 |
| 1-3 Research Scope | 56 |
| 1-3-1 Assumptions | 56 |
| 1-3-2 Further considerations | 57 |
| 1-4 Outline of the Preliminary Thesis Report | 58 |
| | |
| 2 Literature Review | 59 |
| 2-1 Detecting, Preventing and Resolving Conflicts | 59 |
| 2-1-1 The Definition of Conflicts | 59 |
| 2-1-2 Conflict Detection, Prevention and Resolution | 61 |
| 2-2 Conflict Resolution Methods | 62 |
| 2-2-1 Kuchar and Yang's Taxonomy | 62 |
| 2-2-2 Jenie's Taxonomy | 63 |
| 2-2-3 TCAS | 65 |
| 2-2-4 The Modified Voltage Potential | 67 |
| 2-3 Velocity Obstacles | 68 |
| 2-3-1 Basics of a Velocity Obstacle | 68 |
| 2-3-2 Methods using Velocity Obstacles | 69 |
| 2-3-3 Set theory representation | 70 |
| 2-3-4 The Solution Space Diagram | 72 |
| 2-4 ADS-B characteristics | 73 |
| | |
| 3 Experiment Design | 75 |
| 3-1 Simulations in BlueSky | 75 |
| 3-2 Independent Variables | 76 |
| 3-2-1 Coordination rules | 76 |
| 3-2-2 Conflict Scenarios | 77 |
| 3-2-3 Maneuvering Space | 78 |
| 3-3 Dependent Variables | 78 |
| 3-3-1 Safety | 78 |
| 3-3-2 Efficiency | 79 |
| 3-3-3 Stability | 79 |
| 3-4 Hypothesis | 81 |
| | |
| 4 Conclusion | 83 |

| | | |
|----------|---|-----------|
| A | Deriving a Solution Space Diagram | 85 |
| A-1 | Deriving the legs of a Velocity Obstacle | 85 |
| A-2 | Set operations on the Velocity Obstacle and Velocity Limits | 88 |
| A-3 | BlueSky implementation | 89 |
| A-3-1 | Initial module | 89 |
| A-3-2 | External module | 92 |
| B | Examples of Simulated Conflict Scenarios | 95 |
| | Bibliography | 97 |

List of Tables

| | | |
|------|--|----|
| A-1 | Change of x-axis labels between scientific paper and appendix. | 21 |
| A-2 | P-values for Shapiro-Wilk (top) and Kolmogorov-Smirnov (bottom) tests for number of conflicts with small maneuvering space. | 30 |
| A-3 | P-values for Shapiro-Wilk (top) and Kolmogorov-Smirnov (bottom) tests for number of conflicts with large maneuvering space. | 30 |
| A-4 | P-values for Shapiro-Wilk (top) and Kolmogorov-Smirnov (bottom) tests for number of intrusions with small maneuvering space. | 30 |
| A-5 | P-values for Shapiro-Wilk (top) and Kolmogorov-Smirnov (bottom) tests for number of intrusions with large maneuvering space. | 30 |
| A-6 | P-values for Shapiro-Wilk (top) and Kolmogorov-Smirnov (bottom) tests for the IPR with small maneuvering space. | 31 |
| A-7 | P-values for Shapiro-Wilk (top) and Kolmogorov-Smirnov (bottom) tests for the IPR with large maneuvering space. | 31 |
| A-8 | P-values for Shapiro-Wilk (top) and Kolmogorov-Smirnov (bottom) tests for the intrusion severity with small maneuvering space. | 31 |
| A-9 | P-values for Shapiro-Wilk (top) and Kolmogorov-Smirnov (bottom) tests for the intrusion severity with large maneuvering space. | 31 |
| A-10 | P-values for Shapiro-Wilk (top) and Kolmogorov-Smirnov (bottom) tests for the time to resolve conflicts with small maneuvering space. | 32 |
| A-11 | P-values for Shapiro-Wilk (top) and Kolmogorov-Smirnov (bottom) tests for the time to resolve conflicts with large maneuvering space. | 32 |
| A-12 | P-values for Shapiro-Wilk (top) and Kolmogorov-Smirnov (bottom) tests for the time to resolve intrusions with small maneuvering space. | 32 |
| A-13 | P-values for Shapiro-Wilk (top) and Kolmogorov-Smirnov (bottom) tests for the time to resolve intrusions with large maneuvering space. | 32 |

| | |
|---|----|
| A-14 P-values for Shapiro-Wilk (top) and Kolmogorov-Smirnov (bottom) tests for the time spent in conflict with small maneuvering space. | 33 |
| A-15 P-values for Shapiro-Wilk (top) and Kolmogorov-Smirnov (bottom) tests for the time spent in conflict with large maneuvering space. | 33 |
| A-16 P-values for Shapiro-Wilk (top) and Kolmogorov-Smirnov (bottom) tests for the time spent in LoS with small maneuvering space. | 33 |
| A-17 P-values for Shapiro-Wilk (top) and Kolmogorov-Smirnov (bottom) tests for the time spent in LoS with large maneuvering space. | 33 |
| A-18 P-values for Shapiro-Wilk (top) and Kolmogorov-Smirnov (bottom) tests for the DEP with small maneuvering space. | 34 |
| A-19 P-values for Shapiro-Wilk (top) and Kolmogorov-Smirnov (bottom) tests for the DEP with large maneuvering space. | 34 |
| A-20 P-values for Shapiro-Wilk (top) and Kolmogorov-Smirnov (bottom) tests for the multi-aircraft conflicts with small maneuvering space. | 34 |
| A-21 P-values for Shapiro-Wilk (top) and Kolmogorov-Smirnov (bottom) tests for the multi-aircraft conflicts with large maneuvering space. | 34 |
| A-22 P-values for Shapiro-Wilk (top) and Kolmogorov-Smirnov (bottom) tests for the extra expended energy with small maneuvering space. | 35 |
| A-23 P-values for Shapiro-Wilk (top) and Kolmogorov-Smirnov (bottom) tests for the extra expended energy with large maneuvering space. | 35 |
| A-24 P-values for Shapiro-Wilk (top) and Kolmogorov-Smirnov (bottom) tests for the extra travel time with small maneuvering space. | 35 |
| A-25 P-values for Shapiro-Wilk (top) and Kolmogorov-Smirnov (bottom) tests for the extra travel time with large maneuvering space. | 35 |
| A-26 P-values for Shapiro-Wilk (top) and Kolmogorov-Smirnov (bottom) tests for the extra travel distance with small maneuvering space. | 36 |
| A-27 P-values for Shapiro-Wilk (top) and Kolmogorov-Smirnov (bottom) tests for the extra travel distance with large maneuvering space. | 36 |
| A-28 P-values for Shapiro-Wilk (top) and Kolmogorov-Smirnov (bottom) tests for the density with small maneuvering space. | 36 |
| A-29 P-values for Shapiro-Wilk (top) and Kolmogorov-Smirnov (bottom) tests for the density with large maneuvering space. | 36 |
| A-30 P-values for Shapiro-Wilk (top) and Kolmogorov-Smirnov (bottom) tests for the magnitude of the resolution vector with small maneuvering space. | 37 |
| A-31 P-values for Shapiro-Wilk (top) and Kolmogorov-Smirnov (bottom) tests for the magnitude of the resolution vector with large maneuvering space. | 37 |
| A-32 Test statistic (top) and p-values (bottom) for Wilcoxon signed-rank test for number of conflicts with small maneuvering space. | 38 |

| | |
|--|----|
| A-33 Test statistic (top) and p-values (bottom) for Wilcoxon signed-rank test for number of conflicts with large maneuvering space. | 38 |
| A-34 Test statistic (top) and p-values (bottom) for Wilcoxon signed-rank test for number of intrusions with small maneuvering space. | 38 |
| A-35 Test statistic (top) and p-values (bottom) for Wilcoxon signed-rank test for number of intrusions with large maneuvering space. | 38 |
| A-36 Test statistic (top) and p-values (bottom) for Wilcoxon signed-rank test for the IPR with small maneuvering space. | 39 |
| A-37 Test statistic (top) and p-values (bottom) for Wilcoxon signed-rank test for the IPR with large maneuvering space. | 39 |
| A-38 Test statistic (top) and p-values (bottom) for Wilcoxon signed-rank test for the intrusion severity with small maneuvering space. | 39 |
| A-39 Test statistic (top) and p-values (bottom) for Wilcoxon signed-rank test for the intrusion severity with large maneuvering space. | 39 |
| A-40 Test statistic (top) and p-values (bottom) for Wilcoxon signed-rank test for the time to resolve conflicts with small maneuvering space. | 40 |
| A-41 Test statistic (top) and p-values (bottom) for Wilcoxon signed-rank test for the time to resolve conflicts with large maneuvering space. | 40 |
| A-42 Test statistic (top) and p-values (bottom) for Wilcoxon signed-rank test for the time to resolve intrusions with small maneuvering space. | 40 |
| A-43 Test statistic (top) and p-values (bottom) for Wilcoxon signed-rank test for the time to resolve intrusions with large maneuvering space. | 40 |
| A-44 Test statistic (top) and p-values (bottom) for Wilcoxon signed-rank test for the time spent in conflict with small maneuvering space. | 41 |
| A-45 Test statistic (top) and p-values (bottom) for Wilcoxon signed-rank test for the time spent in conflict with large maneuvering space. | 41 |
| A-46 Test statistic (top) and p-values (bottom) for Wilcoxon signed-rank test for the time spent in LoS with small maneuvering space. | 41 |
| A-47 Test statistic (top) and p-values (bottom) for Wilcoxon signed-rank test for the time spent in LoS with large maneuvering space. | 41 |
| A-48 Test statistic (top) and p-values (bottom) for Wilcoxon signed-rank test for the DEP with small maneuvering space. | 42 |
| A-49 Test statistic (top) and p-values (bottom) for Wilcoxon signed-rank test for the DEP with large maneuvering space. | 42 |
| A-50 Test statistic (top) and p-values (bottom) for Wilcoxon signed-rank test for the multi-aircraft conflicts with small maneuvering space. | 42 |
| A-51 Test statistic (top) and p-values (bottom) for Wilcoxon signed-rank test for the multi-aircraft conflicts with large maneuvering space. | 42 |

| | |
|--|----|
| A-52 Test statistic (top) and p-values (bottom) for Wilcoxon signed-rank test for the extra expended energy with small maneuvering space. | 43 |
| A-53 Test statistic (top) and p-values (bottom) for Wilcoxon signed-rank test for the extra expended energy with large maneuvering space. | 43 |
| A-54 Test statistic (top) and p-values (bottom) for Wilcoxon signed-rank test for the extra travel time with small maneuvering space. | 43 |
| A-55 Test statistic (top) and p-values (bottom) for Wilcoxon signed-rank test for the extra travel time with large maneuvering space. | 43 |
| A-56 Test statistic (top) and p-values (bottom) for Wilcoxon signed-rank test for the extra travel distance with small maneuvering space. | 44 |
| A-57 Test statistic (top) and p-values (bottom) for Wilcoxon signed-rank test for the extra travel distance with large maneuvering space. | 44 |
| A-58 Test statistic (top) and p-values (bottom) for Wilcoxon signed-rank test for the density with small maneuvering space. | 44 |
| A-59 Test statistic (top) and p-values (bottom) for Wilcoxon signed-rank test for the density with large maneuvering space. | 44 |
| A-60 Test statistic (top) and p-values (bottom) for Wilcoxon signed-rank test for the magnitude of the resolution vector with small maneuvering space. | 45 |
| A-61 Test statistic (top) and p-values (bottom) for Wilcoxon signed-rank test for the magnitude of the resolution vector with large maneuvering space. | 45 |
| 2-1 Relationship between the range and look-ahead time of maneuvers | 65 |
| 3-1 Maneuvering Space ranges used in the simulations | 78 |
| 3-2 Safety metrics | 79 |
| 3-3 Efficiency metrics | 80 |
| 3-4 Stability metrics | 81 |

List of Figures

| | | |
|------|--|----|
| A-1 | Effect of traffic density on conflicts. | 22 |
| A-2 | Effect of traffic density on intrusions. | 22 |
| A-3 | Effect of traffic density on the IPR. | 23 |
| A-4 | Effect of traffic density on intrusion severity. | 23 |
| A-5 | Effect of traffic density on time to resolve conflicts. | 24 |
| A-6 | Effect of traffic density on time to resolve intrusions. | 24 |
| A-7 | Effect of traffic density on time spent in conflict. | 25 |
| A-8 | Effect of traffic density on time spent in LoS. | 25 |
| A-9 | Effect of traffic density on the DEP. | 26 |
| A-10 | Effect of traffic density on multi-aircraft conflicts. | 26 |
| A-11 | Effect of traffic density on the extra expended energy. | 27 |
| A-12 | Effect of traffic density on the extra travel time. | 27 |
| A-13 | Effect of traffic density on the extra travel distance. | 28 |
| A-14 | Effect of traffic density on the density. | 28 |
| A-15 | Effect of traffic density on the magnitude of the resolution vector. | 29 |
| | | |
| B-1 | Resolution points for basic coordination rulesets. | 47 |
| B-2 | Resolution points for coordination rulesets incorporating priority rules | 47 |
| B-3 | Resolution point for OPT or RS1 corresponding to Figure B-1. | 47 |
| B-4 | Resolution point for RIGHT or RS2 corresponding to Figure B-1. | 47 |
| B-5 | Resolution point for HDG or RS3 corresponding to Figure B-1. | 48 |

| | | |
|------|--|----|
| B-6 | Resolution point for SPD or RS4 corresponding to Figure B-1. | 48 |
| B-7 | Resolution point for DEST or RS5 corresponding to Figure B-1. | 48 |
| B-8 | Resolution point for ROTA or RS6 corresponding to Figure B-2. | 48 |
| B-9 | Resolution point for OPT+ or RS7 corresponding to Figure B-2. | 48 |
| B-10 | Resolution point for DEST+ or RS8 corresponding to Figure B-2. | 48 |
| B-11 | Resolution point for OPT or RS1 corresponding to Figure B-2. | 48 |
| B-12 | Resolution point for DEST or RS5 corresponding to Figure B-2. | 48 |
| 1-1 | Differences in the set of VOs and the SSD | 52 |
| 1-2 | Research framework | 55 |
| 2-1 | The PZ and protection minima | 60 |
| 2-2 | The conflict geometry for a conflict involving two aircraft | 61 |
| 2-3 | Different types of state propagation methods | 63 |
| 2-4 | Overview of categorization criteria in Kuchar and Yang's taxonomy | 64 |
| 2-5 | Overview of categorization criteria in Jenie's taxonomy | 66 |
| 2-6 | Construction of the avoidance vector in the MVP | 68 |
| 2-7 | The CC and VO in the different velocity spaces of the conflict geometry | 69 |
| 2-8 | The FV | 71 |
| 2-9 | The RV | 71 |
| 2-10 | Combining the FRV and the ARV into the SSD | 71 |
| 3-1 | Resolution points under different coordination rules | 77 |
| 3-2 | The Maneuvering Space within a given heading change | 80 |
| A-1 | The CC and VO in the different velocity spaces of the conflict geometry | 86 |
| A-2 | Relevant angles and distances in the CC | 86 |
| A-3 | Extreme VO | 87 |
| A-4 | Intersecting edges of the concave polygon (red) and the convex polygon (blue) | 90 |
| A-5 | Removing vertices outside the ring-shaped RV | 92 |
| B-1 | A small-scale conflict scenario | 95 |
| B-2 | Scenario of Figure B-1 simulated using the MVP | 96 |
| B-3 | Scenario of Figure B-1 simulated using the SSD with the shortest-way-out rule | 96 |
| B-4 | Scenario of Figure B-1 simulated using the SSD with the clockwise-turning rule | 96 |

List of Abbreviations

| | |
|--------------|--|
| ACAS | Airborne Collision Avoidance System |
| ADS-B | Automatic Dependent Surveillance - Broadcast |
| ARV | Allowed Reachable Velocities |
| ASAS | Airborne Separation Assurance System |
| ATC | Air Traffic Control |
| ATCo | Air Traffic Controller |
| ATM | Air Traffic Management |
| CC | Collision Cone |
| CD | Conflict Detection |
| CP | Conflict Prevention |
| CPA | Closest Point of Approach |
| CR | Conflict Resolution |
| DEP | Domino Effect Parameter |
| FRV | Forbidden Reachable Velocities |
| FV | Forbidden Velocities |
| GPWS | Ground Proximity Warning System |
| IFR | Instrument Flight Rules |
| IPR | Intrusion Prevention Rate |
| LoS | Loss of Separation |
| MER | Maneuver Efficiency Rate |
| MS | Maneuvering Space |
| MVP | Modified Voltage Potential |
| PASAS | Predictive ASAS |
| PR | Primary Radar |
| PZ | Protected Zone |
| RA | Resolution Advisory |
| RV | Reachable Velocities |

| | |
|-----------------|------------------------------------|
| SESAR | Single European Sky ATM Research |
| SSD | Solution Space Diagram |
| SSR | Secondary Surveillance Radar |
| SVO | Selective Velocity Obstacle |
| TA | Traffic Advisory |
| TCAS | Traffic Collision Avoidance System |
| TU Delft | Delft University of Technology |
| UAV | Unmanned Aerial Vehicle |
| VFR | Visual Flight Rules |
| VO | Velocity Obstacle |

List of Symbols

Greek Symbols

| | |
|-----------|-----------------------------------|
| α | Half-angle of a Velocity Obstacle |
| φ | Bearing angle |
| χ | Heading angle |

Roman Symbols

| | |
|--------------|---|
| d | Distance |
| R | Radius of the Protected Zone or horizontal separation |
| \mathbf{s} | Displacement vector |
| \mathbf{T} | Thrust vector |
| T | Duration |
| L | Length |
| t | Time |
| \mathbf{V} | Velocity vector |
| V | Velocity magnitude |
| W | Work done |
| \mathbf{x} | Position vector |

Thesis Outline

This report gives an overview of the work performed during this MSc Thesis. The report is divided into three parts:

I Scientific Paper

The findings of the research are presented in the scientific paper contained within this part.

II Appendices

Additional results that were not presented in the scientific paper are presented in the second part. Furthermore the results of a unit test of the implemented methods are given.

III Preliminary Report

The MSc Thesis has two distinctive phases. The preliminary phase and main phase, of which the former was already reported in the Preliminary Report. This report is already graded contained with the third and last part as reference material. This report also includes the literature study carried out at the beginning of the research.

Part I

Scientific Paper

Are Velocity Obstacles the Solution to Multi-aircraft Conflicts?

Author: Suthes Balasooriyan

Supervisors: Emmanuel Sunil, Joost Ellerbroek and Jacco Hoekstra

Abstract—In an effort to increase airspace capacity, new decentralized, implicitly coordinated conflict resolution methods are investigated. The behavior of existing conflict resolution methods is not completely understood in multi-aircraft conflict scenarios. This paper shows the usage of the Solution Space Diagram as an automated, horizontal conflict resolution method. The Solution Space Diagram, constructed from velocity obstacles, indicates the combinations of headings and velocities that will lead to trajectories with or without conflicts. Furthermore, the Solution Space Diagram overviews all nearby aircraft simultaneously, which makes it suitable to use in the resolution of multi-aircraft conflicts. To identify the strengths and weaknesses of the novel conflict resolution method a comparison is made with a successfully proven pairwise conflict resolution method, the Modified Voltage Potential. This comparison is done using fast-time simulations, where eight different coordination rulesets were employed in unison with the Solution Space Diagram. The simulations have shown that the Modified Voltage Potential outperforms the proposed conflict resolution method in terms of safety, stability and efficiency. It is suggested to develop a new ruleset to improve the performance of the novel conflict resolution method. The dynamic behavior of the Solution Space Diagram due to the movement of aircraft should be taken into account in this ruleset.

Index Terms—Conflict resolution, Airborne Separation Assurance System (ASAS), self-separation, Velocity Obstacle (VO), Solution Space Diagram (SSD), Modified Voltage Potential (MVP)

I. INTRODUCTION

WITH further globalization and technological advancements, air traffic is expected to grow tremendously in the coming decades and the airspace will start to reach its limits in terms of capacity [1]. The emergence of Unmanned Aerial Vehicles (UAVs) and the recovering economic growth put a greater burden on the limited capacity [2], [3]. To increase airspace capacity, new Air Traffic Management (ATM) concepts are continuously being researched, in line with the goals of the Single European Sky ATM Research (SESAR) [4].

One of the constraints of airspace capacity is Air Traffic Controller (ATCo) workload. The Free Flight concept, proposed in 1995, aims to reduce this workload by delegating the responsibility of separation between aircraft from the ATCo on the ground towards the crew in the air [5], [6]. This moves the separation task of Air Traffic Control (ATC) from the current centralized approach towards a decentralized approach with airborne self-separation.

An important interaction treated in the aforementioned research within ATM are aircraft conflicts. By propagating

state information, such as speed, direction and altitude, an aircraft is said to be in conflict when an intrusion, or a Loss of Separation (LoS), is expected in the near future. An intrusion occurs when two aircraft are separated at less than the minimum horizontal separation of 5 NM and vertical separation of 1,000 ft [7]. Automatic Dependent Surveillance - Broadcast (ADS-B) is the technology used to determine the required state information. In general, aircraft conflicts are dealt with in three main components: Conflict Detection (CD), Conflict Prevention (CP) and Conflict Resolution (CR) [8]. In the context of conflicts and airborne separation in ATM a lot of research has already been conducted. For this reason, Kuchar and Yang and Jenie et al. have made an effort to make proper surveys of existing CD- and CR-methods [9], [10].

The Modified Voltage Potential (MVP)-method is a proven CR-method in three dimensions, which is a slight modification of Eby's original voltage potential method by Hoekstra et al. [11]–[13]. One of the unknowns with this and other CR-methods is the behavior in conflicts involving three or more aircraft resulting in possible coordination issues. These type of conflicts are also referred to as multi-aircraft conflicts. The MVP-method resolves these multi-aircraft conflicts by calculating resolution maneuvers for each individual conflict pair separately. Afterwards, all the calculated resolution maneuvers are combined by vector addition.

In order to resolve the coordination issues in the unknown behavior in multi-aircraft conflicts, it is suggested to develop a CR-method that considers all nearby aircraft simultaneously to calculate a resolution maneuver. For this reason, the Solution Space Diagram (SSD) is proposed as a supporting tool for a novel CR-method, since it provides insight into existing and potential conflicts surrounding an aircraft. The aforementioned leads to the following question. How does a SSD-based, two-dimensional CR-method perform in the airborne self-separation task in general and in multi-aircraft conflicts in terms of safety, stability and efficiency?

In an effort to answer this question, a CR-method using the SSD is developed and implemented in BlueSky, an ATC simulator [14]. Accompanied with the SSD are eight coordination rulesets that prescribe how resolution maneuvers are selected from the SSD. The analysis is done using 3,000 fast-time simulations. The simulations consists of an experiment area with differing levels of traffic demand where aircraft fly at cruise altitude without defined airways and each aircraft having different destinations, similar to the Free Flight concept. Besides the SSD, the MVP-method is used in the simulations to form a baseline for the performance.

The design and analysis into the performance of the proposed conflict resolution method that provides automated resolution advisories is outlined in this paper. First, previous work is discussed in Section II. This is followed by an elaboration upon the design of the SSD-based CR-method in Section III. To measure the performance of the novel method, fast-time simulations are designed as well in Section IV. In Section V the results are presented and subsequently discussed in the following section. Lastly, the main conclusions are drawn in Section VII.

II. PREVIOUS WORK

In this section the fundamental idea behind the MVP-method is explained. Subsequently, the work that has already been carried out concerning the SSD is briefly presented.

A. Modified Voltage Potential

Force field, or voltage potential methods are often introduced as an analogy where aircraft are related to charged particles. However, this analogy is not very practical and accordingly Eby has developed this original voltage potential method into a feasible conflict resolution method in 1994 [11]. This was slightly modified by Hoekstra et al. and subsequently called the MVP [12], [13]. The essence of the MVP-method is that intruder aircraft will be pushed away from the Protected Zone (PZ) of the ownship. The reverse is also true, the ownship will be pushed away from the PZ of intruders, retaining the analogy of a force field method.

Figure 1 is used to illustrate the construction of the resolution maneuver in the MVP-method. The traffic situation is depicted in the relative velocity space, which means that the velocity vector of the intruder is subtracted from both aircraft. This makes the PZ of the intruder a static obstacle and the velocity of the ownship relative towards the intruder. Furthermore, only the one-sided case is depicted, with the ownship moving towards the PZ of the intruder.

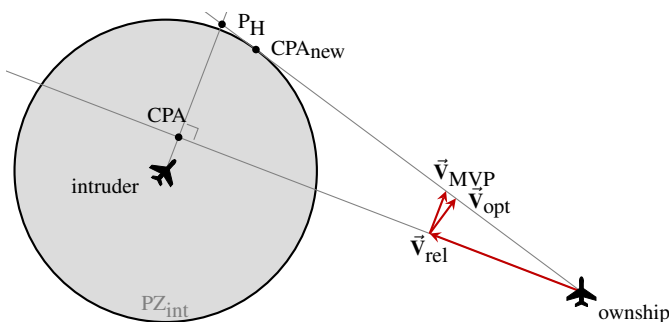


Fig. 1. The resolution maneuver in the MVP-method [12], [15]

The aircraft are in conflict since the Closest Point of Approach (CPA) lies within the PZ. The conflict is resolved when the CPA is moved outside the PZ, indicated by CPA_{new} in the figure. The path of the ownship becomes tangential to the PZ of the intruder. In order to follow this path, a resolution vector is added to \vec{V}_{rel} . In the MVP-method the resolution vector is perpendicular to the initial path and denoted by

\vec{V}_{MVP} in the figure. Note that a shorter avoidance vector is also available, which is perpendicular to the tangential path instead and denoted by \vec{V}_{opt} [16].

In similar fashion the vertical resolution maneuver can be computed [12]. The MVP-method is implicitly coordinated, which means that the intruder will resolve by performing the opposite maneuver. Another advantage is that the MVP-method can handle multi-aircraft conflicts, since resolution vectors can be summed for each conflict pair, thus solving multi-aircraft conflicts pairwise.

B. Solution Space Diagram

This research focuses on improving the performance in multi-aircraft conflicts using the SSD as a CR-method. The SSD was first conceptualized by Hermes et al. who proposed it as an alternative metric to predict workload for an ATCo [17]. Following this study, more research has been conducted into the usage of the SSD as a workload metric [18]–[20]. Other applications are decision-support tools based on the SSD. Mercado Velasco et al. investigated the possibility of reducing ATCo-workload in separating air traffic by using a visualization of the SSD [21]. The acceptance of automated resolutions by ATCos using the SSD as supporting tool was studied by Borst et al. [22], [23]. Likewise, pilots can benefit from the capabilities of the SSD, which can be projected as a visual aid for a possible airborne separation task on the navigational display in the cockpit [24], [25].

The main difference with the aforementioned MVP-method is that a SSD-based CR-method cannot be considered a force field method as categorized by Kuchar and Yang [9]. It should be regarded as an optimized method. Moreover, the novel CR-method resolves conflicts by considering all aircraft in the vicinity, contrary to the pairwise resolution in the MVP-method.

III. DESIGN OF THE SOLUTION SPACE DIAGRAM

The proposed conflict resolution method uses Velocity Obstacles (VOs) and combines them into the SSD, which is used to find an appropriate resolution maneuver. This section describes the construction of a VO and the SSD. Afterwards, it explains considerations regarding the numerical implementation of the SSD and the eight different coordination rulesets that can be followed to select the resolution maneuvers.

A. Velocity Obstacles

The principles of VOs originate from research into motion planning in robotics. Fiorini and Shiller eventually gave the principle its definitive terminology of *Velocity Obstacle* [26]–[28].

Each intruder in the vicinity of an ownship results in a separate VO. Figure 2a illustrates a traffic situation in which an ownship is in conflict with an intruder.

By subtracting the intruder velocity from the ownship and the intruder Figure 2b is obtained in the relative velocity space. In this velocity space the intruder is static, whereas the ownship will have a relative velocity. Here the Collision

Cone (CC) can be constructed, which is an infinitely extending triangular area bounded by two lines tangent to the PZ. One of these lines is identical to the tangential path illustrated in Figure 1. The ownship and the intruder are in conflict, since the relative velocity of the ownship towards the intruder is inside the CC. Resolving this conflict is accomplished by adding a resolution vector which moves the relative velocity vector outside CC. This notion is also used in the MVP method.

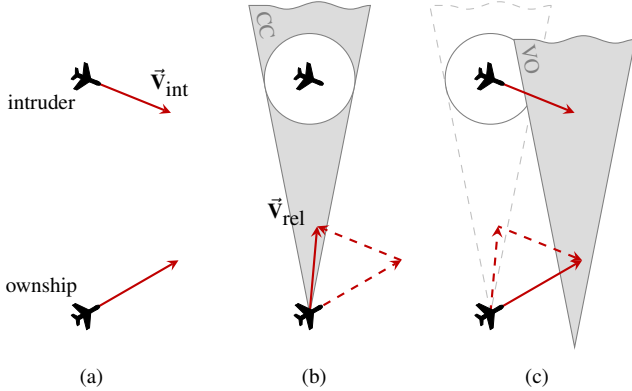


Fig. 2. The construction of a single VO by moving between absolute and relative velocity spaces.

With the CC defined in the relative velocity space, it is desirable to move back towards the absolute velocity space. Figure 2c performs this translation by adding the intruder velocity to the cone, which results in the VO. The advantage of a VO is that it is more intuitive to move an absolute velocity vector outside the VO instead of moving a relative velocity vector. Another advantage of VOs is the summation possibility, due to their identical reference frames. CCs have different reference frames depending on the movement of the intruders [28]. As a consequence, the VOs are suitable for use in multi-aircraft conflicts.

B. Solution Space Diagram

The summation of VOs is essentially taking the union set as shown in (1) with N intruders and VO_i corresponding to the VO of each intruder i . Having a velocity vector inside the resulting set of Forbidden Velocities (FV) implies a conflict. Ideally, the velocity vector is moved inside the complement of the set of FV.

$$FV = \bigcup_{i=1}^N VO_i \quad (1)$$

However, not all velocities can be reached due to speed constraints of the considered aircraft. This is expressed in (2) as the set of Reachable Velocities (RV).

$$RV = \{V, \psi \mid V_{\min} \leq V \leq V_{\max}, 0^\circ \leq \psi < 360^\circ\} \quad (2)$$

The SSD is obtained by combining both sets of FV and RV as shown in (3) and (4) respectively. The set of Forbidden Reachable Velocities (FRV) is a set intersection of RV and FV, whereas the set of Allowed Reachable Velocities (ARV) is a set intersection of RV and the complement of FV. The

latter set intersection can also be written as a set difference of RV and FV, which is preferred for computational purposes.

$$FRV = RV \cap FV \quad (3)$$

$$ARV = RV \cap FV^C = RV \setminus FV \quad (4)$$

The presented equations are also illustrated in Figure 3. The set of FV shown in Figure 3a is the result of joining the VOs of four intruding aircraft. The ring-shaped set of RV in Figure 3b indicates the speed limits of the ownship. The combination of both sets is shown in the ring-shaped SSD in Figure 3c.

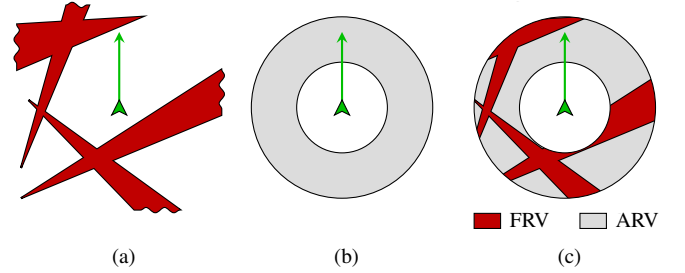


Fig. 3. The construction of the SSD in (c) by combining the sets of FV in (a) and the RV in (b).

An ownship is in conflict when $\vec{V}_{own} \in FRV$ and is not in conflict when $\vec{V}_{own} \in ARV$. In other words, any velocity vector within the set of ARV corresponds to a combination of speed and heading that will result in a conflict-free trajectory.

C. Numerical Implementation

Even though the set functions in (1) to (4) are relatively straightforward, their numerical implementation proves to be more difficult. The VOs can be constructed as sufficiently large triangles using information on the position and velocity of aircraft within the minimum ADS-B range of 80NM [12]. These triangles are convex polygons for which the vertices have been calculated.

Subsequently, the set operations must be performed. These operations are also known as boolean operations on polygons or clipping within the field of computer science. For a fast and precise implementation in the simulation software a clipping library by Angus Johnson has been used, which is based on a clipping algorithm by Vatti [29]. The clipping process results in the set of ARV, on which all possible resolution points can be calculated.

D. Coordination Rulesets

An aircraft in conflict can utilize the SSD to select a conflict-free velocity vector from the set of ARV. The logic behind this selection is encompassed in the coordination ruleset. This ruleset is a set of predefined rules that are intended to allow for implicit coordination in the self-separation task of aircraft. In order to describe the considered rulesets, the traffic situation illustrated in Figure 4 is used. It consists of an ownship that has four intruders nearby of which two are within 40NM. Based on the presented traffic situation and without knowledge of the velocities, the ownship might be in conflict with two of

the four aircraft. It is clearly not in conflict with the other two, since the distance at the CPA is more than the minimum horizontal separation of 5 NM. From the viewpoint of the ownship, the CPA of the aircraft on the right has passed, whereas the CPA with the leftmost aircraft still has to be reached.

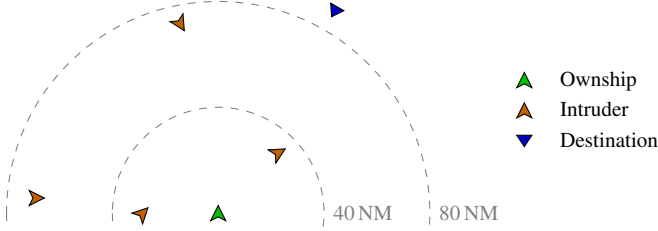


Fig. 4. Traffic situation.

For this research eight rulesets are considered, divided into five basic rulesets and three more advanced rulesets that incorporate priority. An overview of these rulesets has been in listed in Table I.

TABLE I
COORDINATION RULESETS WITH LABELS AND DESCRIPTIONS.

| Label | Priority | Description |
|----------|----------|--|
| 1. OPT | ✗ | Resolve by taking the shortest way out. |
| 2. RIGHT | ✗ | Resolve by only turning right. |
| 3. HDG | ✗ | Resolve by only changing heading. |
| 4. SPD | ✗ | Resolve by only changing speed. |
| 5. DEST | ✗ | Resolve towards the target heading. |
| 6. ROTA | ✓ | Resolve by adhering to the rules of the air. |
| 7. OPT+ | ✓ | Resolve sequentially while adhering to OPT. |
| 8. DEST+ | ✓ | Resolve sequentially while adhering to DEST. |

1) *Basic Coordination Rulesets*: For more elaboration on the basic coordination rulesets Figure 5 is used, in which a SSD is constructed corresponding to the traffic situation in Figure 4. It also shows that the ownship is currently in conflict with only one aircraft. Furthermore, it indicates that two aircraft have little influence on the conflict resolution since their VOs are relatively far from the current velocity vector in the SSD.

After the set of ARV has been calculated, the first ruleset (OPT) selects the closest point on the set of ARV measured from the current velocity vector. For conflicts involving only two aircraft, Ellerbroek refers to this resolution as geometrically optimal [16]. The second ruleset (RIGHT) reduces the set of ARV to only include right-turning resolution maneuvers by performing an additional boolean operation. Afterwards, it also selects the closest point measured from the current velocity vector. HDG and SPD perform an equivalent ARV-reducing operation to contain resolution maneuvers that only alter heading or speed respectively. Similarly, the closest point is selected from this reduced set of ARV. The last ruleset without priority (DEST) selects the closest point on the set of ARV measured from the target heading and speed. Note that it is possible to have an empty set of ARV. In that case, RIGHT,

HDG and SPD will default to OPT. When OPT continues to result in an empty set of ARV, no resolution maneuver will be performed, effectively maintaining the current heading and speed.

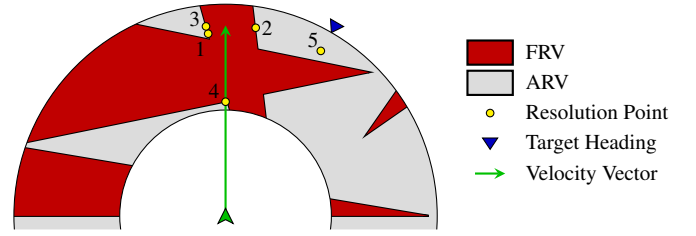


Fig. 5. Basic coordination rulesets.

2) *Coordination Rulesets With Priority*: Figure 6 is referred to for the explanation of the rulesets with priority rules. The differences with the previously used Figure 5 are the lower speed of the ownship, causing a multi-aircraft conflict and a distinction with a lighter color for the VOs of aircraft that are at a distance more than half the minimum ADS-B range.

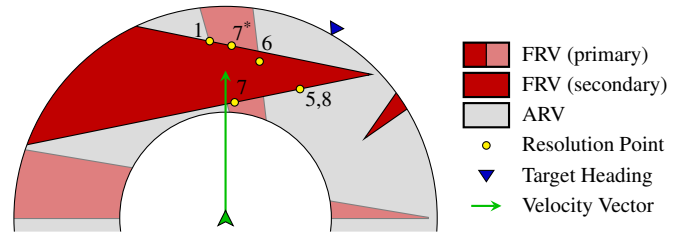


Fig. 6. Coordination rulesets incorporating priority rules.

The sixth ruleset (ROTA) is based on the rules of the air, which comprises three priority rules [30]. Head-on conflicts are resolved cooperatively by both turning right, overtaking must happen to the right of the slower aircraft and traffic approaching from the left has to give way. This explains how the sixth resolution maneuver in Figure 6 is still inside the set of FRV. It is expected that the nearby intruder on the left shall give way and the head-on conflict must be solved by turning to the right.

The last two coordination rulesets follow from preliminary results of simulations with the aforementioned coordination rulesets. In high density traffic, the set of ARV tends to be very small, which limits the choice in resolution maneuvers. To account for this, a secondary SSD can be constructed with a select group of intruders based on spatial or temporal proximity. Similar to how the primary SSD is based on spatial proximity, the secondary SSD is constructed exclusively with intruders that are closer than 40 NM, which is half the minimum ADS-B range. Resolution points are calculated on this secondary SSD according to OPT and DEST. Afterwards, a comparison of the resolution points can be made using their respective time to LoS. Choosing a resolution point from either of the primary and secondary SSD explains the sequential property of the seventh and eighth rulesets (OPT+ and DEST+).

In Figure 6 it is shown how OPT+ prioritizes the resolution point on the secondary SSD. OPT indicates that the shortest

resolution maneuver will be an acceleration and a heading change to the left. The sequential property of OPT+ prescribes the usage of the secondary SSD, which disregards the aircraft that is approaching head-on at a distance larger than 40 NM. Because of this, two resolution points (7 and 7*) are closer than the resolution point provided by OPT. OPT+ selects the resolution point that leads to a larger time to LoS, which is resolution point 7 as it requires a deceleration.

It is a possibility to have identical resolution points for the primary and secondary SSD. This happens when the aircraft at a distance between 40 to 80 NM have a negligible influence on the resolution maneuver. This is the case for DEST+ in Figure 6, since DEST would have provided the same resolution point based on the primary SSD. Note that the resolution point for DEST is different in Figure 5 due to different magnitudes of velocity.

IV. SIMULATION DESIGN

Fast-time simulation experiments were conducted to evaluate the performance of the proposed conflict resolution method using the SSD. The design of these simulations is described in further detail in this section.

A. Simulation Environment

The simulation environment in which the experiments were conducted is provided by BlueSky, an open data and open source ATC simulator project developed by students and researchers of the Aerospace faculty at TU Delft [14]. BlueSky is a promising simulator that allows for simple modifications due to its modular structure, which is advantageous when new ATM concepts are being researched.

BlueSky already had a functioning Airborne Separation Assurance System (ASAS) that uses state-based CD and multiple CR-methods, including an implementation of the MVP-method. Note that the automated resolution provided by this MVP-implementation does not contain the CP-component or Predictive ASAS (PASAS). In this case, the MVP-method only makes an effort to maneuver out of conflicts. An SSD-based CR-method shall intrinsically encompass CP as it aims to resolve towards a conflict-free trajectory.

The implementation of the SSD-based resolution within BlueSky was accomplished with an existing clipping library as was explained in Section III-C. Even though the library is written in C++, it is nevertheless significantly slower than the implementation of the MVP-method in Bluesky. The reason is that for every aircraft in conflict at least two clipping operations must be executed for the sets of FRV and ARV respectively, whereas the MVP are completely vectorized calculations for each aircraft.

The aircraft model used during the simulations is based on the Boeing 747-400. Its characteristics are listed in Table II.

Furthermore, in an effort to limit the research scope, wind and turbulence are considered to be absent. The presence of wind and turbulence can be disruptive for estimating velocities from ADS-B data, which should be acknowledged when interpreting the results [16, p.7].

TABLE II
RELEVANT DATA OF THE BOEING 747-400 IN CRUISE.

| Characteristic | Value |
|--------------------------|----------------------------|
| Speed | 450–500 kts |
| Mach | 0.784–0.871 |
| Mass | 285,700 kg |
| Load Factor in Turns | 1.22 |
| Turn rate | 1.53–1.70° s ⁻¹ |
| Acceleration and Braking | 1.0 kts s ⁻¹ |

Information on the aircraft's identification, surface position, airborne position and airborne velocity is relayed through ADS-B messages [31]. It is assumed that state information will be continuously available. In reality the messages are transmitted with an interval of at least 0.5 s and relaying the messages will actually exhibit other delays as well [32], [33].

B. Traffic Scenarios

Taking into account the intended aircraft density, flight time and cruise speed, a square area of 455,625 NM² is considered to be the experiment area. Aircraft are allowed to leave this area, but have to remain within the simulation area that is an extension of the experiment area by 225 NM on all sides. For completeness, all aircraft are set at an altitude of 36,000 ft in BlueSky. Aircraft at different altitudes are considered to have left the simulation area and will be deleted from the simulation as a result.

The aircraft spawn at an interval depending on the specified aircraft density. The scenarios are designed to have a flight time of 1,800 s for each aircraft that cruise at a true airspeed chosen uniformly between 450 to 500 kts. The aircraft are spawned at cruise altitude in the first two hours of the scenario, which implies that the scenarios have a theoretical duration of 2.5 h. Moreover, the designed density will be reached after 0.5 h from the start of the simulation. The aircraft shall fly towards a destination that is between 225 and 250 NM away at a heading that is uniformly chosen between 0° to 360°. After reaching the destination an aircraft shall start to descend from cruise altitude, which causes it to be deleted as soon as it has left the simulation area.

Another important aspect of the traffic scenario are the spawn locations of the aircraft. Ideally, spawning aircraft do not immediately cause intrusions. For the generation of the scenarios this is accounted for by nominally propagating existing aircraft along their respective path for every spawn time. This provides insight into the location of all existing aircraft when a new aircraft is about to spawn. In turn, it is possible to spawn aircraft at a location that does not immediately lead to an intrusion. This procedure assumes that aircraft will fly along their nominal trajectory. Accordingly, aircraft will deviate from this path when the ASAS is switched on. This will potentially cause intrusions due to spawning of aircraft, which should be taken into account when interpreting the results.

C. Independent Variables

During the experiment three categories of independent variables are used to simulate different conditions. Different resolution methods and coordination rulesets are considered, varying traffic volumes are simulated and also the influence of the maneuvering space is investigated.

1) *Resolution Methods and Coordination Rulesets*: Naturally, the resolution method that uses the SSD to resolve conflicts will be used during the simulations. As explained in Section III-D and listed in Table I, a total of eight coordination rulesets are considered in the aforementioned SSD-method. Besides the novel method of this research, the horizontal part of the existing MVP-method is used in the simulations as a baseline. Lastly, the simulations are also performed without a functioning resolution method to aid in the verification of the designed experiments and to calculate certain dependent variables. As a result, ten combinations of resolution methods and coordination rulesets are experimented with. The three resolution methods are summarized in Table III.

TABLE III
CONFLICT RESOLUTION METHODS WITH LABELS AND DESCRIPTIONS.

| Label | Description |
|---------|---|
| MVP | Resolve using the MVP-method. |
| various | Resolve using the SSD with a ruleset listed in Table I. |
| NO CR | No conflict resolution method selected. |

2) *Traffic Volume*: Another important condition of the experiment is the traffic volume or density of aircraft. In general, more conflicts will arise with larger traffic densities. This makes it beneficial to resolve conflicts in shorter time to preserve the stability of the airspace. For that reason three densities ranging from 2.5 AC/10,000 NM² have been used in the simulations. The used aircraft density directly determines the spawn rate of new aircraft in the scenarios. Due to the experiment area being 455,625 NM², this would lead to a designed instantaneous traffic volume between 113 and 341. Note that the actual volume will be a higher as it is expected that aircraft will fly longer due to path deviations caused by conflict avoidance maneuvers.

TABLE IV
TRAFFIC VOLUME IN THE TRAFFIC SCENARIOS.

| Label | Density | Instantaneous |
|----------|-------------------------------|---------------|
| Low | 2.5 AC/10,000 NM ² | 113 |
| Moderate | 5.0 AC/10,000 NM ² | 227 |
| High | 7.5 AC/10,000 NM ² | 341 |

3) *Maneuvering Space*: It has been shown that the SSD is constructed by incorporating the minimum and maximum true airspeed, which explains the shape of a ring. The minimum is due to the stall behavior, whereas the maximum comes from structural constraints and available thrust provided by the engine. The difference in the performance limits effectively determines the maneuvering space for the aircraft. The smaller the space, the smaller the set of ARV and thus limiting the possibilities to resolve a conflict. To this end, two true airspeed

ranges are chosen and listed in Table V. A factor that affects this variable is the altitude. At higher altitudes the stall speed increases, which decreases the maneuvering space. The smaller range listed in the table emulates the case in which aircraft remain in the clean configuration suited for cruise. In contrast, the larger range resembles the situation in which aircraft are allowed to take more drastic measures to resolve conflicts.

TABLE V
THE MANEUVERING SPACE RANGES USED IN SIMULATIONS.

| Range [kts] | V _{min} [kts] | V _{max} [kts] |
|-------------|------------------------|------------------------|
| 50 | 450 | 500 |
| 200 | 300 | 500 |

Ten combinations of resolution methods and coordination rulesets, three aircraft densities and two maneuvering spaces are considered in this research. This means that 60 different simulation settings are available. Each setting is repeated 50 times, which implies that in total 3,000 simulations are carried out during this study.

D. Dependent Variables

During the simulations dependent variables can be observed to assess the performance of different conflict resolution strategies under varying conditions. The dependent variables are divided into three categories with metrics on safety, stability and efficiency, similar to earlier studies [34]–[36].

1) *Safety*: Ideally, the proposed resolution method is safe by keeping aircraft separated at a distance of at least their separation minimum. Eight metrics are used to assess the safety. The number of conflicts (n_{cf}) and the number of intrusions (n_{int}) are possible metrics to assess the safety. Conflicts occur when an intrusion, or a LoS, is predicted, where a LoS means that an aircraft has actually intruded another aircraft's PZ. From these metrics the Intrusion Prevention Rate (IPR) is derived by Sunil et al., a measure of the ability to resolve conflicts as shown in (5) [34].

$$IPR = \frac{n_{\text{cf}} - n_{\text{int}}}{n_{\text{cf}}} \quad (5)$$

Every LoS can also be characterized. This leads to two other metrics, the severity (LoS_{sev}) and duration (T_{LoS}) of the intrusion. Since this research concerns horizontal resolution maneuvers only, the severity of intrusion can be computed with (6). Here, R is the minimum horizontal separation and d_{CPA} the closest distance between two aircraft.

$$LoS_{\text{sev}} = \frac{R - d_{\text{CPA}}}{R} \quad (6)$$

Similarly, the duration of the conflict (T_{cf}) can be considered, which is simply the duration for which a conflict has existed. In other words, it is the time it takes to resolve conflicts. Since resolving conflicts can cause secondary conflicts due to the domino effect, it is considered less safe to take a relatively long time to resolve conflicts. Another time-based metric would be the time in conflict (t_{inCF}) and the time in LoS (t_{inLoS}) per aircraft.

2) *Stability*: Resolution methods can potentially lead to new conflicts when performing maneuvers. The stability of such methods partially depends on the amount of new conflicts it has created. An often used principle to describe the instability of a method is the domino effect [12], [37]. Bilimoria et al. devised a metric to measure this effect, the Domino Effect Parameter (DEP) [38].

Although Bilimoria et al. used the number of aircraft in conflict to describe the effect, this research will follow the approach of Sunil et al. and use the number of conflict pairs (n_{cfl}) [34]. This subtle difference describes multi-aircraft conflict scenarios more accurately as aircraft with multiple conflicts are included multiple times. The DEP is computed in (7). The number of encountered conflicts without CR ($n_{\text{cfl}}^{\text{OFF}}$) is found by simulating without any resolution. Subsequently, the number of encountered conflicts with CR ($n_{\text{cfl}}^{\text{ON}}$) allows the calculation of the DEP. Generally, a resolution method with a low DEP is considered to be more stable.

$$DEP = \frac{n_{\text{cfl}}^{\text{ON}}}{n_{\text{cfl}}^{\text{OFF}}} - 1 \quad (7)$$

Another metric that could describe the stability is the number of aircraft experiencing multi-aircraft conflicts (N_{mcfl}). A low number would indicate a more stable airspace. It should be noted that instability for this dependent variable should not always be viewed negatively. In fact, Hoekstra argues that a moderately positive DEP is beneficial as it creates more airspace in the sense that it spreads the aircraft out in the available airspace [12].

3) *Efficiency*: The performance of the resolution methods in economic, workload and environmental aspects can be measured by its efficiency. The efficiency can be viewed in multiple manners. First, the work done (W) by all aircraft in the scenario can be used as a global efficiency metric. Since the work done is strongly correlated with the fuel consumption, this can advocate the economic and environmental benefits of a certain resolution method. The metric for a single aircraft is calculated using (8), in which \vec{T} is the thrust vector and \vec{s} the displacement vector along the path.

$$W = \int_{\text{path}} \vec{T} \cdot d\vec{s} \quad (8)$$

Besides the work done, or the expended energy, the flight duration and travel distance can be observed as well. Especially the travel distance is interesting due to the insight it gives into the path deviations of the different conditions.

In total thirteen metrics are considered as dependent variables, divided into three categories of safety, stability and efficiency. The metrics have been summarized in Table VI.

E. Hypotheses

The MVP is a decentralized force field method, whereas a method based on the SSD can be considered as a decentralized optimized method. Reviewing the nature of aforementioned resolution methods can prompt hypotheses on the performance of these methods.

TABLE VI
DEPENDENT VARIABLES.

| Variable | Type | Description |
|--------------------|------------|---------------------------------------|
| n_{cfl} | Safety | Number of conflicts. |
| n_{int} | Safety | Number of intrusions. |
| IPR | Safety | Intrusion Prevention Rate. |
| LoS_{sev} | Safety | Severity of an intrusion. |
| T_{cfl} | Safety | Duration of a conflict. |
| T_{LoS} | Safety | Duration of an intrusion. |
| t_{incfl} | Safety | Time in conflict for an AC. |
| t_{inLoS} | Safety | Time in LoS for an AC. |
| DEP | Stability | Domino Effect Parameter. |
| N_{mcfl} | Stability | Number of AC with multi-AC conflicts. |
| W | Efficiency | Work done during a flight. |
| T | Efficiency | Duration of a flight. |
| D | Efficiency | Travel distance of a flight. |

A property of force field methods is that new conflicts are created as individual aircraft push their way through towards the target. The expectation is that SSD-based methods will have a less significant domino effect as they search for solutions with no conflicts with the aid of its CP-component. It is hypothesized that resolution methods based on the SSD have a relatively low DEP compared to the MVP-method.

It is also expected that the work done is lower when many aircraft have to perform small resolution maneuvers. Opposed to the case where fewer aircraft resolve, but make larger resolution maneuvers. The latter is typical for the SSD-method, whereas the former is characteristic for the MVP-method. This leads to the second hypothesis where it is posed that the resolution methods based on the SSD have a relatively high W compared to the MVP-method.

V. RESULTS

The results of the 2.735 million simulated aircraft spread out over 3,000 simulations are outlined in the upcoming section. The results are presented with box-and-whisker plots to visualize the sample distribution. For clarity purposes the outliers are not presented. Some graphs exclude the case where the ASAS is switched off when it does not provide further insight.

Since some samples did not pass the normality tests by Shapiro-Wilk and Kolmogorov-Smirnov [39], a nonparametric test was required to compare samples. For this reason, the two-tailed Wilcoxon signed-rank test (test statistic z) was used with the null hypothesis that two dependent samples are selected from populations having the same distribution. When comparing two samples, the difference was considered significant when $p \leq 0.01$ and marginally significant when $0.01 < p \leq 0.05$. A certain sample of 50 repetitions can be compared with nine other rulesets and CR-methods, two other aircraft densities and one other maneuvering space. Thus, twelve comparisons were possible, requiring a Bonferroni correction of 12 to the significance levels. Hence, after the correction the difference was considered significant when $p \leq 8.33\text{e-}4$ and marginally significant when $8.33\text{e-}4 < p \leq 4.17\text{e-}3$.

1) *Influence of the Maneuvering Space:* In Section IV-C3 it was suggested to consider two speed ranges to model a small and large maneuvering space. The percentage increase or decrease in the number of conflicts and intrusions are depicted in Figures 7 and 8. This indicates that the MVP-method and HDG do not utilize the additional maneuvering space to improve their performance. For HDG this can be explained as the ruleset considers heading changes only for its resolution maneuvers. It can be recognized that for high level of traffic more conflicts are created. However, this effect is less present for the extra number of intrusions. In the remainder of this section it is chosen to present the results with the smaller maneuvering space only.

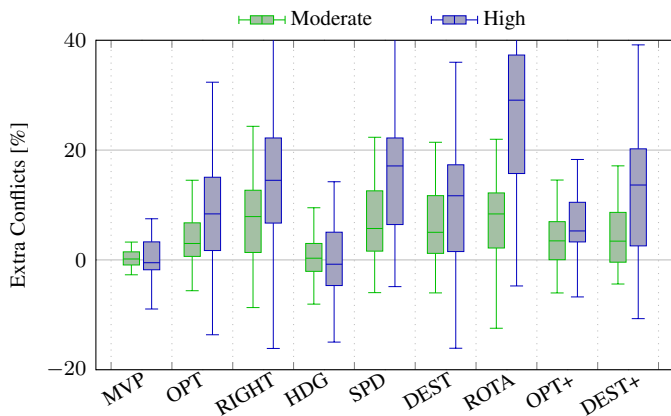


Fig. 7. Extra conflicts due to smaller maneuvering space under moderate and high traffic density.

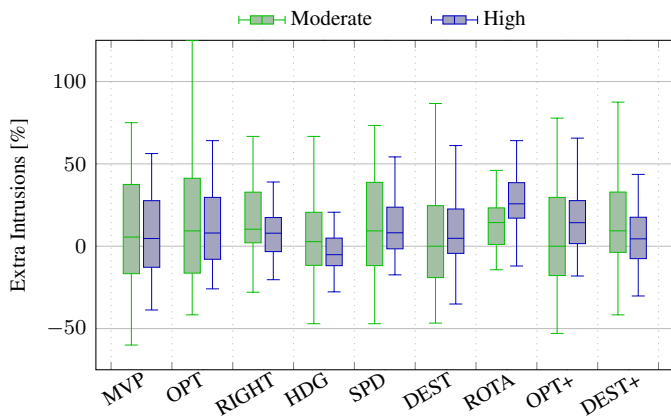


Fig. 8. Extra intrusions due to smaller maneuvering space under moderate and high traffic density.

2) *Safety:* As listed in Table VI, numerous metrics are considered to assess the safety in different simulation conditions. Figures 9 and 10 illustrate the number of conflicts and intrusions respectively. Both figures show that having more aircraft involved in the traffic scenario also leads to more conflicts and intrusions. It can be discerned that the MVP-method creates fewer conflicts and intrusions for all traffic levels compared with the SSD-based resolution method, since all coordination rulesets show a significantly larger number of conflicts ($z \leq -3.692, p \leq 2.214e-4$) and intrusions

($z \leq -3.377, p \leq 5.227e-4$). It can also be noted that the case with no conflict resolution (NO CR) is not incorporated in the number of intrusions as this method does not actively aims to reduce this number.

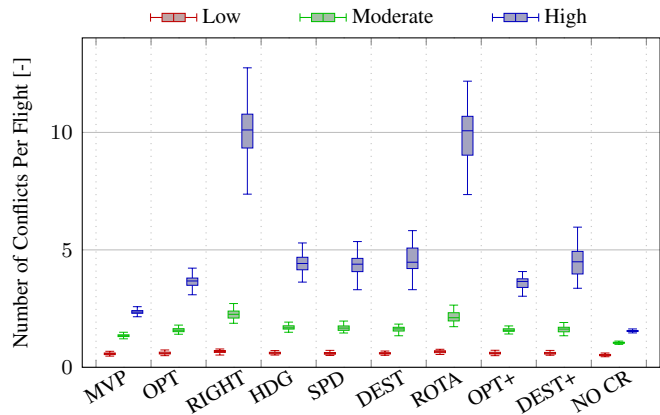


Fig. 9. Effect of traffic density on conflicts.

Within the different rulesets the figures show that RIGHT and ROTA perform significantly worse than other rulesets and methods in terms of number of conflicts ($z \leq -5.396, p \leq 6.735e-8$) and intrusions ($z \leq -5.686, p \leq 1.174e-8$). To recapitulate, these rulesets are the right-turning and based on the rules of the air respectively. Whereas the other rulesets and methods do not show relatively large differences at the lower traffic volume, these two rulesets already start to perform worse, especially in terms of the number of intrusions. It is worth to mention that the number of intrusions for the ruleset based on the rules of the air under high traffic is approximately as high as 0.5 per aircraft and not made visible in the figure. This can be explained as aircraft in this ruleset expect to have the right of way and might not resolve urgent conflicts. OPT, based on the shortest way out, and its sequential variant OPT+ are the better performing rulesets in these metrics, which is more apparent in the high aircraft density.

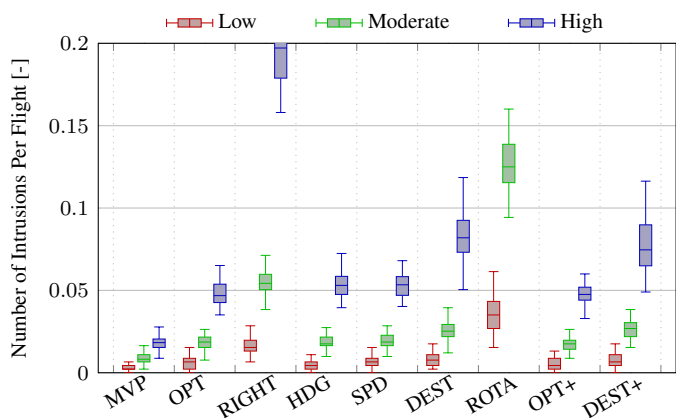


Fig. 10. Effect of traffic density on intrusions.

The number of conflicts and intrusions can also be combined into the IPR, which is shown in Figure 11. Similar to the previous figures it indicates that RIGHT and ROTA have a significantly less performance ($z \leq -4.744, p \leq 2.089e-6$).

Since the number of conflicts and intrusions increases with the aircraft density, more samples will be used to calculate the IPR. Hence, the variability of the IPR becomes smaller, which is visible as the spread of the boxes in the figure becomes smaller. For this reason, no further significant results follow from the low density case. However, for the high density case it shows that MVP is significantly better at preventing intrusions than the SSD-based rulesets ($z \leq -6.144, p \leq 8.031e-10$).

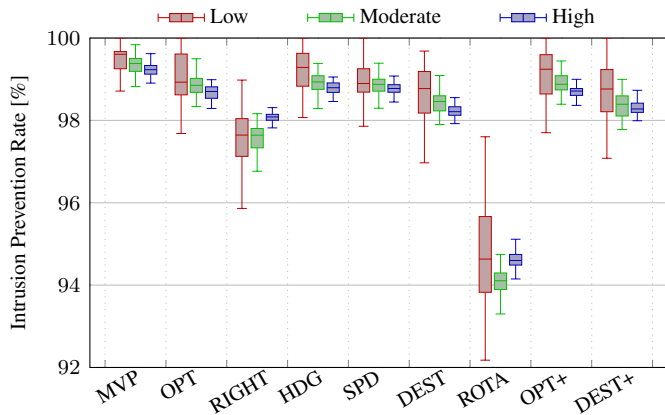


Fig. 11. Effect of traffic density on the IPR.

Figure 12 depicts the intrusion severity. It shows a trend for more severe intrusions as more traffic is involved for the whole range of resolution methods and rulesets. Similar to the IPR the lower aircraft density exhibits a larger spread than the higher aircraft densities. Once more it can be observed that ROTA has an inferior performance, which is significant at the highest aircraft density ($z \leq -6.086, p \leq 1.155e-9$). On the contrary, the ruleset with right-turning resolution maneuvers (RIGHT) does not behave significantly different ($z \leq -0.400, p \leq 0.689$) from the other methods and rulesets, with the exception of ROTA.

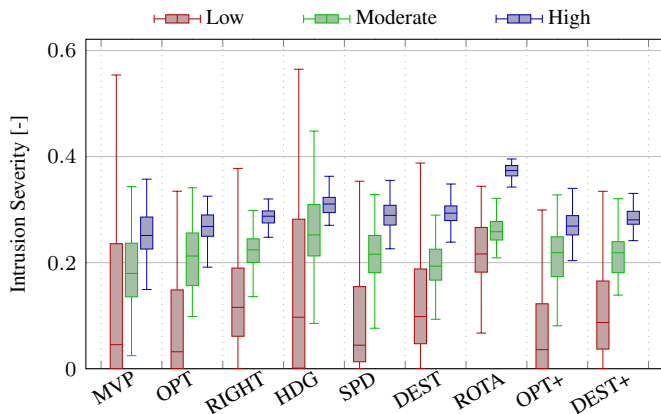


Fig. 12. Effect of traffic density on intrusion severity.

Table VI listed four time-based metrics that have been split in two categories. One category measures the duration of individual events, whereas the other measures the time spent in such event for each aircraft. Herein, the events are conflicts and intrusions.

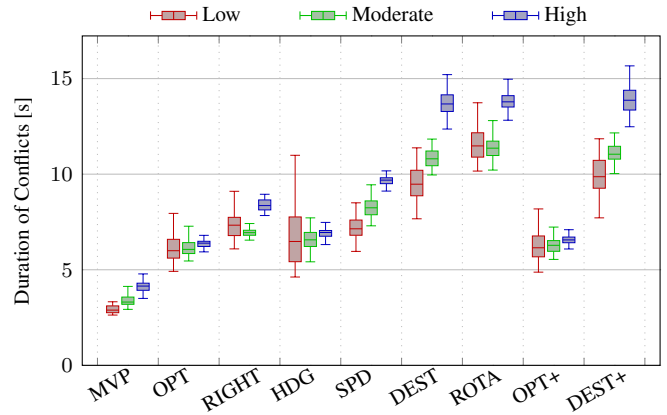


Fig. 13. Effect of traffic density on time to resolve conflicts.

Figure 13 visualizes the average duration of individual conflicts that range from 3 to 15s depending on the resolution method and aircraft density. Once more, the number of conflicts increases with the aircraft density, which leads to a decrease in the spread of the box plot with increasing aircraft density. Additionally, this figure shows the strength of the MVP as it resolves conflicts significantly faster than the SSD-based rulesets ($z \leq -6.153, p \leq 7.557e-10$). Comparing HDG and SPD where it is only allowed to alter heading or speed, it becomes apparent that it takes longer to resolve conflicts by altering the speed only. Accordingly, it is slower to accelerate or decelerate out of conflicts opposed to turning out of these conflicts. The rulesets based on resolving towards the target, DEST and the sequential DEST+, exhibit long resolving times. The short explanation is the influence of the changing SSD over time, which leads to alternating resolution points. This will be elaborated upon in the discussion. The change of the SSD over time is also referred to as the dynamic behavior of the SSD.

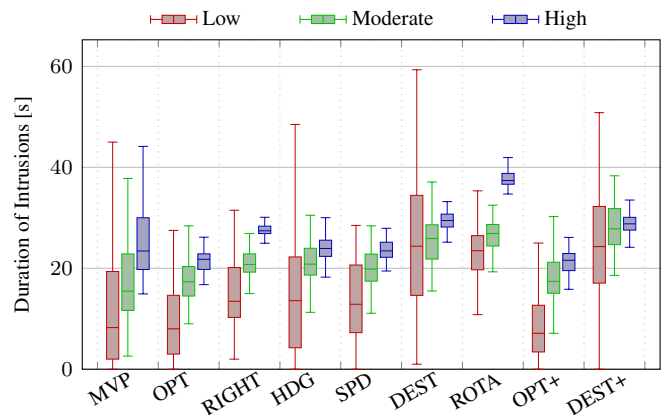


Fig. 14. Effect of traffic density on time to resolve intrusions.

The average duration of individual intrusions in Figure 14 has a large variability in comparison with the duration of individual conflicts as there are fewer intrusions than conflicts. Again, the variability decreases, whereas the duration of intrusions increases with higher traffic levels. It is worth to mention that it takes longer to escape intrusions compared

with the time it takes to resolve conflicts. The reason for this is that aircraft in the majority of conflicts are at a large distance apart requiring relatively small resolution maneuvers. On the contrary, in an intrusion aircraft are within 5 NM, which requires large and therefore long-lasting resolution maneuvers.

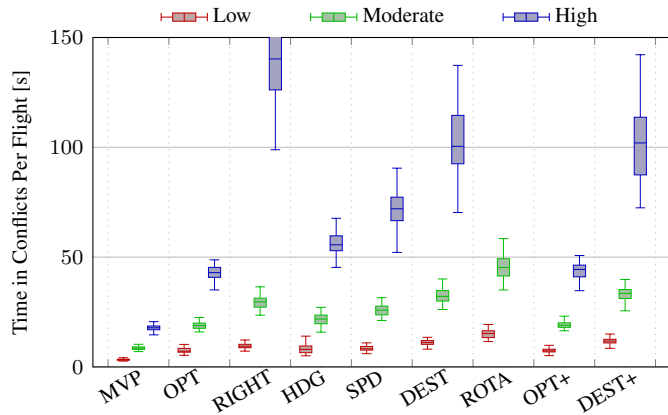


Fig. 15. Effect of traffic density on time spent in conflict.

Figures 15 and 16 provide another time-based view on the conflicts and intrusions. Essentially, the figures combine the number of events per aircraft and the duration of each event. RIGHT, DEST, ROTA and DEST+ were performing poorly in these previous metrics, which can be derived from the time spent in conflicts and intrusions as well.

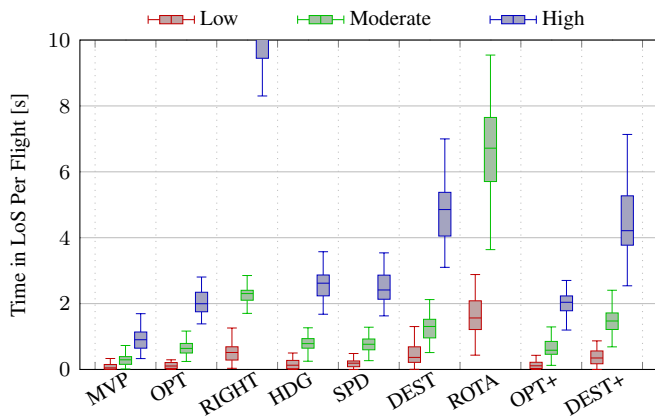


Fig. 16. Effect of traffic density on time spent in LoS.

Based on the safety metrics the MVP has a better performance than any of the rulesets using the SSD. Within the variety of rulesets there are large differences. OPT and its sequential form OPT+ function comparatively well, closely followed by HDG and SPD. It should be pointed out that HDG and SPD are set to default to OPT when there is no resolution maneuver available, which partly explains their performance. DEST and DEST+ are rated slightly worse, whereas RIGHT and ROTA can be viewed as the worst performers in terms of safety.

3) *Stability*: The second category of dependent variables are the stability metrics. The DEP is used to observe the

tendency to create secondary conflicts while resolving conflicts. The results of this metric are visualized in Figure 17. As expected, the same trends from the number of conflicts in Figure 9 can be observed. With increasing density the DEP also increases. Due to the vertical scaling of the figure, it is hard to discern differences in the low traffic density. However, the MVP-method has a significantly lower DEP for all aircraft densities ($z \leq -3.656, p \leq 2.548e-4$). It is also remarkable that the median DEP of RIGHT and ROTA is as high as 5.73 and 5.71 respectively.

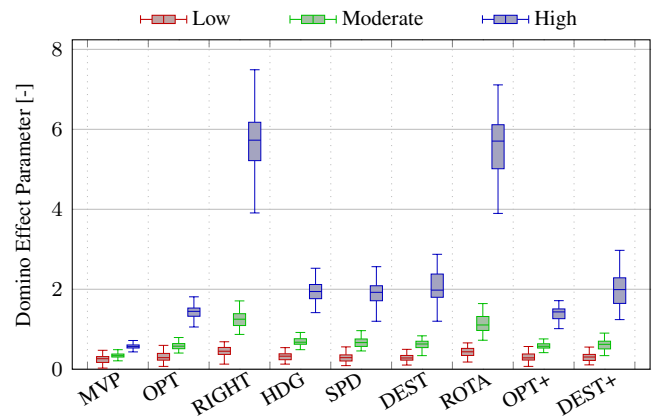


Fig. 17. Effect of traffic density on the DEP.

The number of aircraft encountering multi-aircraft conflicts is the second and last stability metric. This is visualized in Figure 18 where the portion of aircraft that have experienced a multi-aircraft conflict during their flight can be observed. The portion of aircraft is positively correlated with the aircraft density as more multi-aircraft conflicts are to be expected in denser traffic. It is remarkable that a significantly lower portion of aircraft comes across multi-aircraft conflict for low to moderate levels of air traffic in OPT, HDG and OPT+ compared to the MVP-method ($z \leq -6.134, p \leq 8.500e-10$). An obvious reason is that the SSD-based method has a CP-component built in, whereas the implementation in BlueSky of the MVP-method lacks CP. For high levels of traffic this effect is not visible.

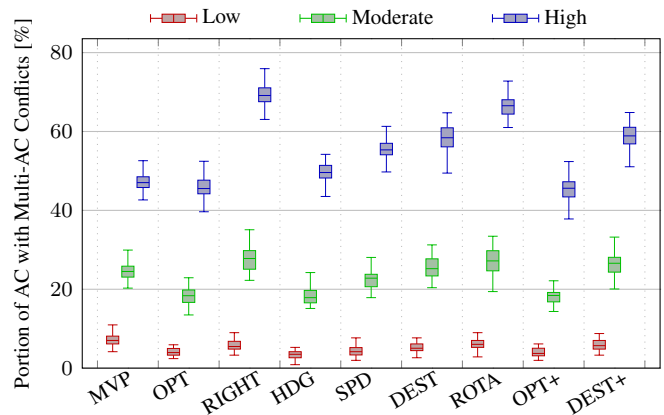


Fig. 18. Effect of traffic density on multi-aircraft conflicts.

4) *Efficiency*: Three metrics were considered regarding the efficiency, being the work done, the travel time and the travel distance. The nominal expended energy, time and distance can be extracted from the simulations with the ASAS switched off (NO CR). This leads to values of 63.2 ± 0.1 GJ, 0.500 ± 0.001 h and 237.0 ± 0.2 NM, which verifies that the scenarios have been designed correctly.

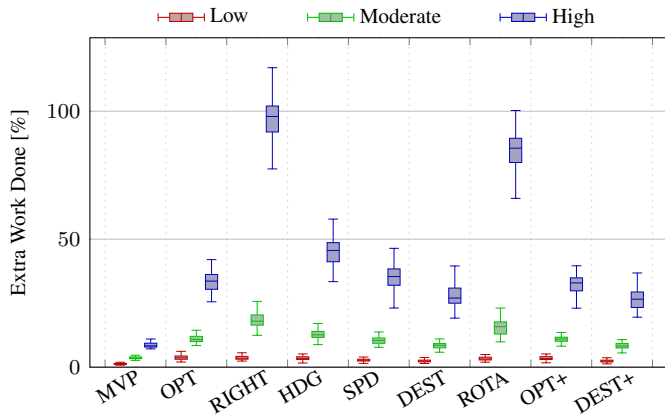


Fig. 19. Effect of traffic density on the extra expended energy.

Figures 19, 20 and 21 visualize the metrics on efficiency. The figures suggest a strong correlation between the metrics, which can be confirmed by calculating the correlation for all pairs ($R^2 > 0.999$). It shows that the MVP-method is the most optimal in terms of efficiency for the whole range of aircraft densities. Furthermore, rulesets resolving towards the target are likely to be more efficient in the case with a high aircraft density. OPT, SPD and OPT+ are very similar in efficiency, while HDG is slightly less efficient. RIGHT and ROTA are the least efficient rulesets.

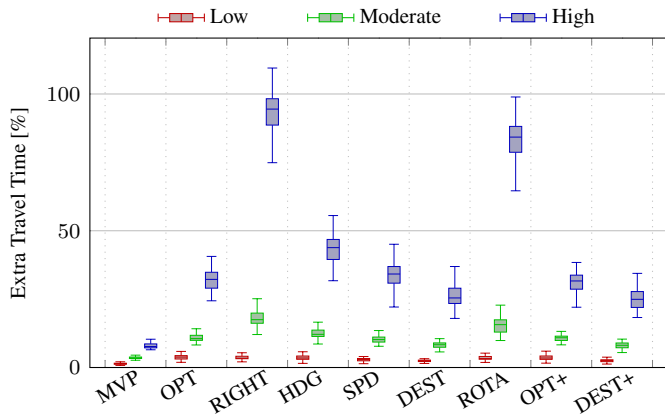


Fig. 20. Effect of traffic density on the extra travel time.

It is worth to mention the excessive rise in extra travel time and distance when the traffic volumes increase for the SSD-method. For example, the highest aircraft density leads to a 7.7% and 7.9% increase in travel time and distance in the MVP-method against 24.9% and 25.1% for the most efficient coordination ruleset (DEST+). For the least efficient ruleset this is even 94.5% and 94.7%.

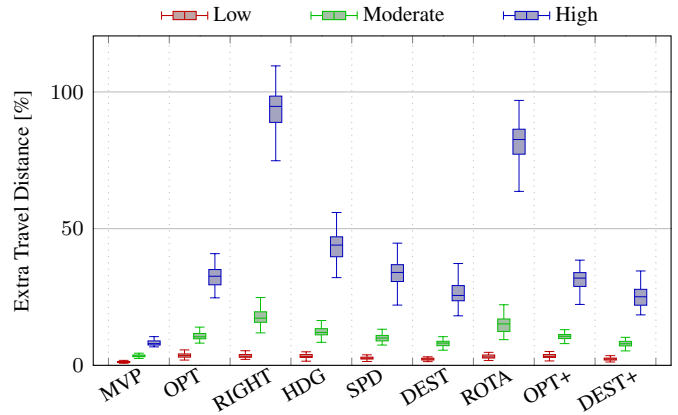


Fig. 21. Effect of traffic density on the extra travel distance.

The three efficiency metrics show that the rulesets generally have larger path deviations, leading to a longer travel time and distance. In other words, it takes longer for an aircraft to reach its destination in the simulations. As fewer aircraft reach their destination on time, the deletion rate is lower than the spawn rate since the spawn rate of aircraft is independent of the resolution method. This explains the increase in aircraft density with respect to the designed densities listed in Table IV. Figure 22 visualizes the density measured from 0.5 to 2.0 h.

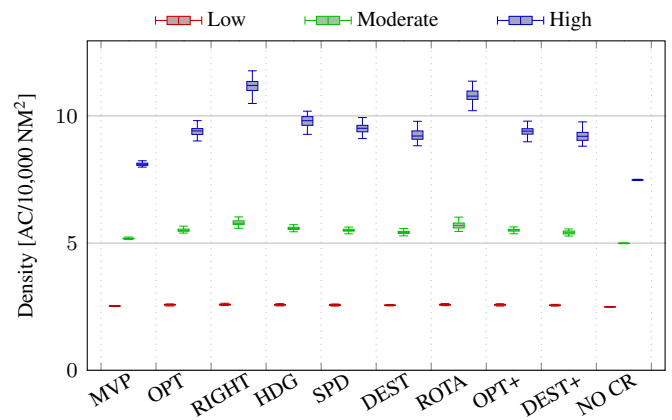


Fig. 22. Effect of traffic density on the actual density.

The figure confirms that the ASAS causes an increase in aircraft density, which becomes significant from the moderate traffic level and upwards. The condition without conflict resolution (NO CR) is in fact on the designed densities of 2.5, 5.0 and 7.5 AC/10,000 NM². It is remarkable that the MVP-method does not deviate much from the designed density, whereas the SSD-based rulesets all show a significant increase in density ($z \leq -6.134$, $p \leq 8.534e-10$).

The previous would lead to the conclusion that resolution maneuvers are shorter in MVP-method. Surprisingly, this is initially not the case under several conditions as shown in Figure 23 where the magnitude of the initial resolution vector is depicted. The explanation for this unusual result is detailed in the upcoming discussion.

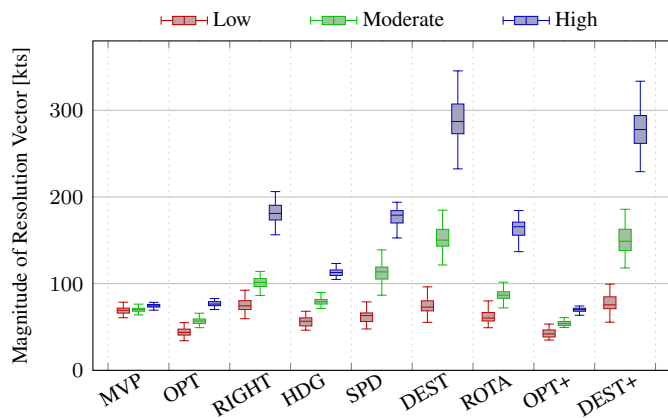


Fig. 23. Effect of traffic density on the magnitude of the resolution vector.

Table VII is used to summarize the performance of the rulesets by ranking the medians of the three categories of dependent variables. The MVP-method has not been included as it outperforms the SSD-method on almost all metrics. It is evident that RIGHT and ROTA are the worst performing rulesets. OPT and its sequential variant OPT+ are the best performing rulesets. DEST and DEST+ are likely more efficient at the expense of safety and stability.

TABLE VII
RULESETS RANKED BY MEDIANS OF THE DEPENDENT VARIABLES.

| Ruleset | Safety | Stability | Efficiency |
|----------|--------|-----------|------------|
| 1. OPT | 1 | 2 | 5 |
| 2. RIGHT | 7 | 8 | 8 |
| 3. HDG | 4 | 3 | 6 |
| 4. SPD | 3 | 4 | 3 |
| 5. DEST | 5 | 5 | 2 |
| 6. ROTA | 8 | 7 | 7 |
| 7. OPT+ | 2 | 1 | 4 |
| 8. DEST+ | 6 | 6 | 1 |

VI. DISCUSSION

The research question asked how a SSD-based CR-method performs in general and in multi-aircraft conflicts in terms of safety, stability and efficiency. In this section the resulting performance of the novel CR-method is discussed. First the results on a macroscopic scale are further clarified, after which examples of microscopic effects are shown. At last, the research question is briefly answered and recommendations for possible future research are made.

A. Macroscopic Effects

From the results it can be concluded that the MVP-method is overall a better resolution method compared to the coordination rulesets used in the SSD-method. In terms of safety and efficiency, the MVP performed significantly better, whereas for the stability some rulesets with the SSD-method had fewer aircraft that encounter multi-aircraft conflicts for low and moderate traffic density.

An explanation for the increased density in Figure 22 can be found in the time it takes to resolve conflicts in Figure 13. The average duration is significantly longer for the SSD-based rulesets, indicating that the resulting path deviations shall be greater as well. The reason for the fast conflict resolution in the MVP-method is that the implementation lacks CP and its resolution maneuver being the sum of all pairwise calculated resolution vectors.

Aircraft in the MVP-method approach multi-aircraft conflicts with minimal maneuvering, resulting in a spreading-out of aircraft, which is closely tied with its nature as a force field method. In contrast, the SSD-based rulesets approach multi-aircraft conflicts with large resolution maneuvers, preferably avoiding the multi-aircraft conflicts altogether. This is possible due to its CP-component.

An analogy can be made with the airborne pulse-Doppler weather radar equipped on aircraft. One can use the radar to avoid adverse weather conditions with large avoidance maneuvers. However, the situation behind the first wall of clouds is unknown. Furthermore, one must account for the dynamics of weather, such as wind.

Coming back to the SSD, a common weakness of the investigated rulesets becomes clear. After calculating the resolution maneuver, it takes time to complete the maneuver. These maneuver dynamics are unaccounted for in the construction of the SSD. During the time to complete a resolution maneuver, the SSD changes, also referred to as the dynamic behavior of the SSD. A CR-method is said to exhibit uncoordinated behavior when it is possible that aircraft resolve towards each other. In this case, the dynamic behavior has a negative impact and additional corrections to the resolution maneuvers are required. This uncoordinated behavior is more present in the SSD-based CR-method than in the MVP-method, which can be observed in Figure 23 where the magnitude of the resolution vector is shown. It shows that some rulesets in the SSD initially have shorter resolutions, especially at lower aircraft densities. However, as Figure 13 indicates, the average duration of conflicts is longer. This can be explained by the additional corrections required while resolving the conflict due to more uncoordinated behavior in the SSD-based CR-method.

In short, the dynamic behavior of the SSD is not considered and it is unknown how the SSD changes when resolving towards a conflict-free point on the set of ARV. This is further illustrated with examples in the next section on microscopic effects. The result is that larger path deviations occur, leading to more conflicts.

It should be mentioned that the increased aircraft density of the coordination rulesets in combination with the SSD result in a worse performance with respect to the MVP-method as there are simply more aircraft in the simulation. However, this is a consequence of the SSD-based method being slower at resolving conflicts. Essentially, these two effects amplify each other. It is therefore desirable for CR-methods to exhibit small path deviations and short conflict durations such that aircraft can reach their destinations sooner.

In Section IV-E two hypotheses were formulated. The first hypothesis regarding the DEP should be rejected. For moderate and high traffic volumes the MVP-method has a significantly

lower DEP, as Figure 17 shows. The second hypothesis regarding the efficiency should be accepted. Figure 19 depicts a significantly lower expended energy, or work done, for the MVP-method.

B. Microscopic Effects

It is already discussed how the MVP-method performs better on a macroscopic scale. In this part the weaknesses of both methods on a microscopic scale are further detailed.

1) *Uncoordinated Behavior and Conflict Prevention*: Section IV-A explained that the implementation of the MVP-method did not have CP, whereas a SSD-based method intrinsically has CP. The CP-component should theoretically reduce the number of conflicts. The discussion on the macroscopic effects reasoned the absence of this reduction.

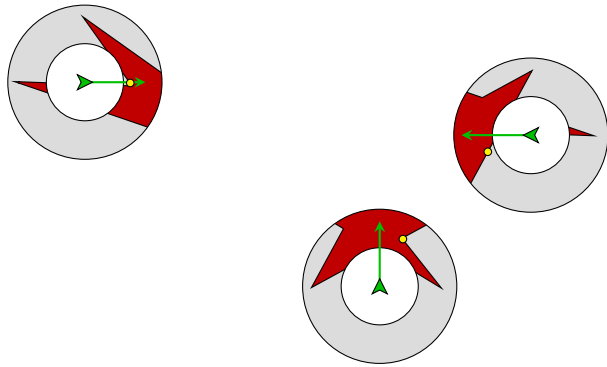


Fig. 24. Uncoordinated behavior in the SSD-based method.

A disadvantage of having CP is illustrated with the traffic situation in Figure 24. The southern aircraft is in a multi-aircraft conflict with the two other aircraft. The aircraft flying towards the east and the west are not in conflict with each other, which is not clearly visibly in the figure. However, the presence of the nearby aircraft influences which resolution point is selected due to the CP. The resolution points are drawn as small yellow circles in the SSD. Under the shown conditions OPT resolves the southern and eastern aircraft towards each other. In fact, following OPT will eventually lead to an intrusion in this case.

The provided example indicates how the CP-component of the SSD-method could potentially lead to intrusions. In this case OPT led to an intrusion, though similar simplistic traffic situations can expose the same uncoordinated behavior for the other rulesets as well. RIGHT and ROTA are exceptions to this as they are designed to be implicitly coordinated, except these rulesets have other shortcomings. In contrast, the MVP-method resolves the conflict with minimal path deviations in a relatively short time due to the lack of CP. The uncoordinated behavior that leads to intrusions is one of the emergent issues in multi-aircraft conflicts that is not solved by the considered SSD-based rulesets.

2) *ARV Reduction*: The set of ARV as presented in Figure 25a is calculated for all coordination rulesets. OPT, DEST, OPT+ and DEST+ use this set to select a resolution maneuver. RIGHT, HDG, SPD and ROTA reduce the set first before selecting a resolution maneuver. The resulting SSD of three rulesets are visualized in Figures 25b, 25c and 25d.

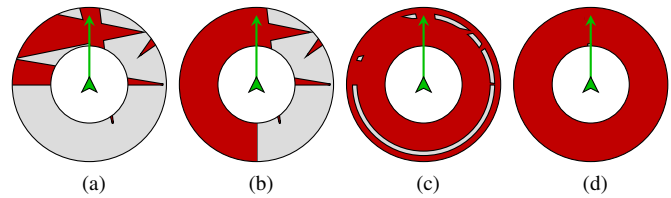


Fig. 25. The set of ARV in (a) is reduced due to rulesets RIGHT in (b), HDG in (c) and SPD in (d).

RIGHT clips half of the SSD such that only right-turning resolutions remain. The third ruleset (HDG) clips a larger area by only considering a very small ring with the same speed for the resolution maneuvers. The set of ARV in SPD is further reduced, leaving only resolution maneuvers with the current heading. SPD clearly indicates, and HDG to a lesser extent, the reason it is necessary that these rulesets default to OPT when no resolution maneuvers are available. The reduction of the set of ARV often leads to very illogical or no resolution maneuvers at all. This is not an issue for the second coordination ruleset.

Having a reduced set of ARV inevitably causes longer conflict durations as less optimal resolution maneuvers are selected. In turn, the longer conflict durations lead to a larger domino effect and a larger path deviation.

Even though the improvement in performance was insignificant, the sequential rulesets, OPT+ and DEST+, were actually devised to increase the set of ARV. This was achieved by disregarding aircraft at a distance between 40 and 80 NM under certain circumstances.

3) *Alternating Resolution Points*: All coordination rulesets in the SSD-method select a resolution point based on the traffic situation at that moment. However, traffic is not static and will change the resulting SSD slightly over time. This is also referred to as the dynamic behavior of the SSD. As nearby aircraft also make an effort to resolve conflicts, this dynamic behavior is even stronger.

Figure 26 demonstrates a negative aspect of the dynamic behavior. In this case it is applicable for OPT, SPD, DEST, OPT+ and DEST+. From the SSD it can be derived that the traffic situation involves two intruding aircraft in the northeast and northwest that are flying respectively to the west and to the east. In Figure 26a a left-turning resolution is proposed. The SSD changes marginally due to the other aircraft flying and resolving. The rulesets now propose a different resolution point in Figure 26b that is opposite to the initial resolution point. The SSD keeps changing, after which a third closer resolution point appears in Figure 26c which eventually resolves the conflict completely.

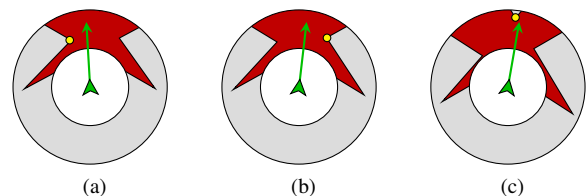


Fig. 26. The resolution point alternate due to the changing set of ARV.

The oscillating or alternating of resolution points leads to a longer conflict duration. It has been discussed already that a long conflict duration is undesirable. The rulesets based on the shortest path towards the target, DEST and DEST+, are more prone to this oscillating behavior.

4) *Rules of the Air*: The ruleset based on the rules of the air actually combines multiple negative aspects on the microscopic scale. First of all, it reduces the ARV as resolution maneuvers should be right-turning only. Furthermore, it incorporates priority rules where only one aircraft resolves the conflict. This increases the duration of conflicts for which the consequences have already been discussed and explains the adverse performance of ROTA.

5) *Shallow angle conflicts*: Another effect that was observed in both the MVP- as the SSD-method was undesired behavior in very shallow angle conflicts. These occur when two aircraft, that need to pass each other, are on nearly parallel tracks. The aircraft are not able to pass each other when the angle of conflict is sufficiently low. This results in two aircraft flying outside the experiment area towards the edge of the simulation area. The aircraft are deleted when the edge is reached. Even though these deleted aircraft will have flown for a much longer distance and time, they are considered to be outliers as this type of behavior does not occur often.

C. Recommendations

The results have shown that the MVP-method performed better than the SSD-based CR-method on almost every metric in terms of safety, stability and efficiency. However, the SSD as a CR-method should not be dismissed yet. Other coordination rulesets can potentially perform better.

In the discussion of the microscopic effects, one of the significant weaknesses was the lack of insight into the dynamic behavior of the SSD. For future work it is recommended to look into using a secondary SSD constructed from nominally propagated positions and velocities. The usage of a secondary SSD is similar to the functioning of the sequential rulesets, OPT+ and DEST+. By utilizing the time-propagated secondary SSD, some of the dynamics of the SSD, or change of the SSD, can be used to select a resolution maneuver. In the end, a well-functioning ruleset should aim for a short conflict duration and small path deviations. Furthermore, the turn dynamics could be included in the SSD as was shown by van Dam et al. [40].

Another aspect that should be taken into account is the design of the scenario. The objective of aircraft in the scenarios was to fly towards a destination. However, the simulations have shown that the SSD-based method had more difficulties in reaching the destination. Future studies could be more lenient by allowing approximate destinations that can be reached with parallel tracks as well. This is more in line with the Free Flight principle.

Lastly, during the research many assumptions were made. The resolution method neglected wind and turbulence, was chosen to be two-dimensional and used one type of aircraft. It could be interesting to revoke one or more of these assumptions to investigate whether the SSD-method has a better relative performance.

VII. CONCLUSION

The research presented in this paper has investigated the usage of the SSD in an automated CR-method. To achieve this, the SSD was combined with eight coordination rulesets, encompassing a set of rules that select an appropriate resolution maneuver. These coordination rulesets were experimented with in fast-time simulations. The MVP-method is used to interpret the resulting performance in the landscape of existing conflict resolution methods. The following conclusions can be drawn from the study:

- The SSD-based CR-method performed less than the MVP-method on almost every metric in terms of safety, stability and efficiency. However, in low to moderate traffic densities the SSD reduced the number of multi-aircraft conflicts.
- Small path deviations and short conflict durations are properties of a well-performing CR-method. The MVP-method performed better on both of these properties compared to the SSD-based coordination rulesets.
- The SSD-based CR-method showed more uncoordinated behavior than the MVP-method, which means that the selected resolution maneuver did not contribute to the resolution of a conflict. This effectively extended the duration of conflicts.
- The previous three points do not imply that the SSD should be rejected as a CR-method. It is possible that other coordination rulesets function better.
- In between the coordination rulesets used with the SSD, the ones based on the shortest path out of conflict were the most promising. The rulesets based on the shortest path from the target heading showed a higher efficiency. However, this was at the expense of the conflict duration, which makes these rulesets less promising.

REFERENCES

- [1] ICAO, *Global Air Transport Outlook to 2030 and Trends to 2040*. Montréal, Quebec: ICAO, 2013, vol. CIR 333.
- [2] FAA, "FAA Aerospace Forecast: Fiscal Years 2016-2036," FAA, Washington DC, Tech. Rep., March 2016.
- [3] EUROCONTROL, "Challenges of Growth 2013, Task 4: European Air Traffic in 2035," EUROCONTROL, Brussels, Tech. Rep., June 2013.
- [4] SESAR, *European ATM Master Plan*. Brussels: SESAR, 2015.
- [5] RTCA, Inc., "Final Report of RTCA Task Force 3 on Free Flight Implementation," RTCA, Inc., Washington DC, Tech. Rep., October 1995.
- [6] J. M. Hoekstra, R. C. J. Ruigrok, and R. N. H. W. Van Gent, "Free flight in a crowded airspace?" *3rd USA/Europe Air Traffic Management R&D Seminar*, no. June, 2000.
- [7] ICAO, "Doc 4444: PANS-ATM," ICAO, November 2007.
- [8] T. W. Rand and M. S. Eby, "Algorithms for airborne conflict detection, prevention, and resolution," *The 23rd Digital Avionics Systems Conference*, no. 3.B.1, pp. 1–17, 2004.
- [9] J. K. Kuchar and L. C. Yang, "A review of conflict detection and resolution modeling methods," *IEEE Transactions on Intelligent Transportation Systems*, vol. 1, no. 4, pp. 179–189, 2000.
- [10] Y. I. Jenie, E.-J. van Kampen, J. Ellerbroek, and J. M. Hoekstra, "Taxonomy of Conflict Detection and Resolution Approaches for Unmanned Aerial Vehicle in an Integrated Airspace," *IEEE Transactions on Intelligent Transportation Systems*, vol. PP, no. 99, pp. 1–11, 2016.
- [11] M. S. Eby, "A Self-Organizational Approach for Resolving Air Traffic Conflicts," *The Lincoln Laboratory Journal*, vol. 7, no. 2, pp. 239–253, 1994.
- [12] J. M. Hoekstra, "Designing for Safety: the Free Flight Air Traffic Management Concept," PhD Thesis, Delft University of Technology, 2001.

- [13] J. M. Hoekstra, R. N. H. W. van Gent, and J. Groeneweg, "Airborne separation assurance validation with multiple humans-in-the-loop," *5th USA/Europe Air Traffic Management R&D seminar*, vol. 251, pp. 1–10, 2003.
- [14] J. M. Hoekstra and J. Ellerbroek, "BlueSky ATC Simulator Project: an open Data and Open Source Approach," *Proceedings of the 7th International Conference on Research in Air Transportation*, no. June, 2016.
- [15] J. Maas, "A Quantitative Comparison of Conflict Resolution Strategies for Free Flight," MSc Thesis, Delft University of Technology, 2015.
- [16] J. Ellerbroek, "Airborne Conflict Resolution In Three Dimensions," PhD Thesis, Delft University of Technology, 2013.
- [17] P. Hermes, M. Mulder, M. M. Van Paassen, J. H. L. Boering, and H. Huisman, "Solution-Space-Based Analysis of the Difficulty of Aircraft Merging Tasks," *Journal of Aircraft*, vol. 46, no. 6, pp. 1995–2015, 2009.
- [18] M. M. van Paassen, J. G. D'Engelbronner, and M. Mulder, "Towards an Air Traffic Control Complexity Metric based on Workspace Constraints," *IEEE Systems, Man and Cybernetics International Conference*, pp. 654–660, 2010.
- [19] S. M. B. Abdul Rahman, M. M. van Paassen, and M. Mulder, "Using the Solution Space Diagram in Measuring the Effect of Sector Complexity During Merging Scenarios," *AIAA Guidance, Navigation, and Control Conference*, no. August, pp. 1–25, 2011.
- [20] J. G. d'Engelbronner, C. Borst, J. Ellerbroek, M. M. van Paassen, and M. Mulder, "Solution-Space-Based Analysis of Dynamic Air Traffic Controller Workload," *Journal of Aircraft*, vol. 52, no. 4, pp. 1146–1160, 2015.
- [21] G. A. Mercado Velasco, M. Mulder, and M. M. Van Paassen, "Analysis of Air Traffic Controller Workload Reduction Based on the Solution Space for the Merging Task," *AIAA Guidance, Navigation, and Control Conference*, no. August, pp. 1–18, 2010.
- [22] C. Westin, B. Hilburn, and C. Borst, "Mismatches between Automation and Human Strategies: An Investigation into Future Air Traffic Management (ATM) Decision Aiding," *Proceedings of the First SESAR Innovation Days*, 2011.
- [23] C. Borst, C. Westin, and B. Hilburn, "An Investigation into the Use of Novel Conflict Detection and Resolution Automation in Air Traffic Management," *Proceedings of the Second SESAR Innovation Days*, 2012.
- [24] J. Ellerbroek, K. C. R. Brantegem, M. M. van Paassen, and M. Mulder, "Design of a coplanar airborne separation display," *IEEE Transactions on Human-Machine Systems*, vol. 43, no. 3, pp. 277–289, 2013.
- [25] J. Ellerbroek, K. C. R. Brantegem, M. M. van Paassen, M. Mulder, and N. de Gelder, "Experimental evaluation of a co-planar airborne separation display," *IEEE Transactions on Human-Machine Systems*, vol. 43, no. 3, pp. 290–301, 2013.
- [26] L. Tychonievich, D. Zaret, J. Mantegna, R. Evans, E. Muehle, and S. Martin, "A Maneuvering-Board Approach to Path Planning with Moving Obstacles," *Proceedings of the 11th international joint conference on Artificial Intelligence*, vol. 2, pp. 1017–1021, 1989.
- [27] P. Fiorini and Z. Shiller, "Motion planning in dynamic environments using the relative velocity paradigm," *1993 IEEE International Conference on Robotics and Automation*, vol. 1, pp. 560–566, 1993.
- [28] —, "Motion planning in dynamic environments using velocity obstacles," *The International Journal of Robotics Research*, vol. 17, no. 7, pp. 760–772, 1998.
- [29] B. R. Vatti, "A Generic Solution to Polygon Clipping," *Communications of the ACM*, vol. 35, no. 7, pp. 56–63, 1992.
- [30] ICAO, "Annex 2: Rules of the Air," ICAO, July 2005.
- [31] J. Sun, *ADS-B Decoding Guide*, Delft University of Technology, May 2017.
- [32] *ADS-B Implementation and Operations Guidance Document*, 7th ed., ICAO, September 2014.
- [33] J. Ellerbroek, M. M. van Paassen, and M. Mulder, "Coordination in airborne conflict resolution," May 2013, presented at the 17th International Symposium on Aviation Psychology.
- [34] E. Sunil, J. Ellerbroek, J. M. Hoekstra, A. Vidosavljevic, M. Arntzen, F. Bussink, and D. Nieuwenhuisen, "Analysis of Airspace Structure and Capacity for Decentralized Separation Using Fast-Time Simulations," *Journal of Guidance, Control, and Dynamics*, vol. 40, no. 1, pp. 38–51, 2017.
- [35] M. A. P. Tra, "The Effect of a Layered Airspace Concept on Conflict Probability and Capacity," MSc Thesis, Delft University of Technology, 2016.
- [36] T. P. Langejan, "Effect of ADS-B Limitations and Inaccuracies on CD&R Performance," MSc Thesis, Delft University of Technology, 2016.
- [37] K. D. Bilimoria, H. Q. Lee, Z.-H. Mao, and E. M. Feron, "Comparison of Centralized and Decentralized Conflict Resolution Strategies for Multiple-Aircraft Problems," *AIAA Guidance, Navigation, and Control Conference*, no. 2000-4268, 2000.
- [38] K. D. Bilimoria, K. S. Sheth, H. Q. Lee, and S. R. Grabbe, "Performance Evaluation of Airborne Separation Assurance for Free Flight," *AIAA Guidance, Navigation, and Control Conference*, no. 2000-4265, 2000.
- [39] S. S. Shapiro and M. B. Wilk, "An Analysis of Variance Test for Normality (Complete Samples)," *Biometrika*, vol. 52, pp. 591–611, 1965.
- [40] S. B. J. van Dam, M. Mulder, and M. M. van Paassen, "Airborne self-separation display with turn dynamics and intruder intent-information," *Proceedings of IEEE International Conference on Systems, Man and Cybernetics*, pp. 1445–1454, 2007.

Part II

Appendices

Appendix A

Additional Results

During the experimental-phase of the research, 3,000 simulations were performed. Only a select group of the results are included in the scientific paper of Part I. In this appendix first the boxplots for the large maneuvering space are presented. This is followed by the results of the Shapiro-Wilk and Kolmogorov-Smirnov normality tests. This appendix is concluded by the results of the Wilcoxon signed-rank test for the comparison between the MVP-method and SSD-based rulesets. For the normality tests, the null-hypothesis is rejected when $p \leq 0.05$, which is indicated with underlined values. The differences in the comparison with the Wilcoxon signed-rank test are considered marginally significant (italicized) when $0.01 < p \leq 0.05$ and significant (underlined) when $p \leq 0.01$. A Bonferroni correction of 12 is applied, which reduces the significance levels.

Note that the labels are more simplistic for the rulesets in contrast to the descriptive labels in the paper of Part I. The differences have been listed in Table A-1.

Table A-1: Change of x-axis labels between scientific paper and appendix.

| Appendix | Scientific Paper |
|----------|------------------|
| RS1 | OPT |
| RS2 | RIGHT |
| RS3 | HDG |
| RS4 | SPD |
| RS5 | DEST |
| RS6 | ROTA |
| RS7 | OPT+ |
| RS8 | DEST+ |

A-1 Safety Metrics Charts

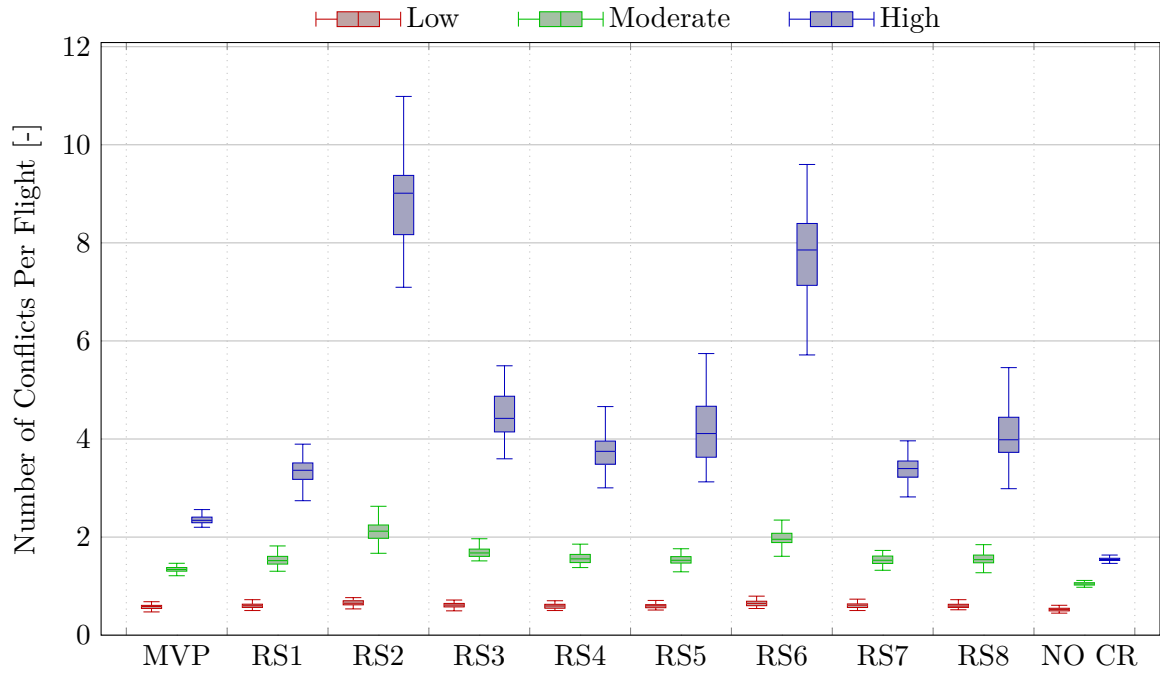


Figure A-1: Effect of traffic density on conflicts.

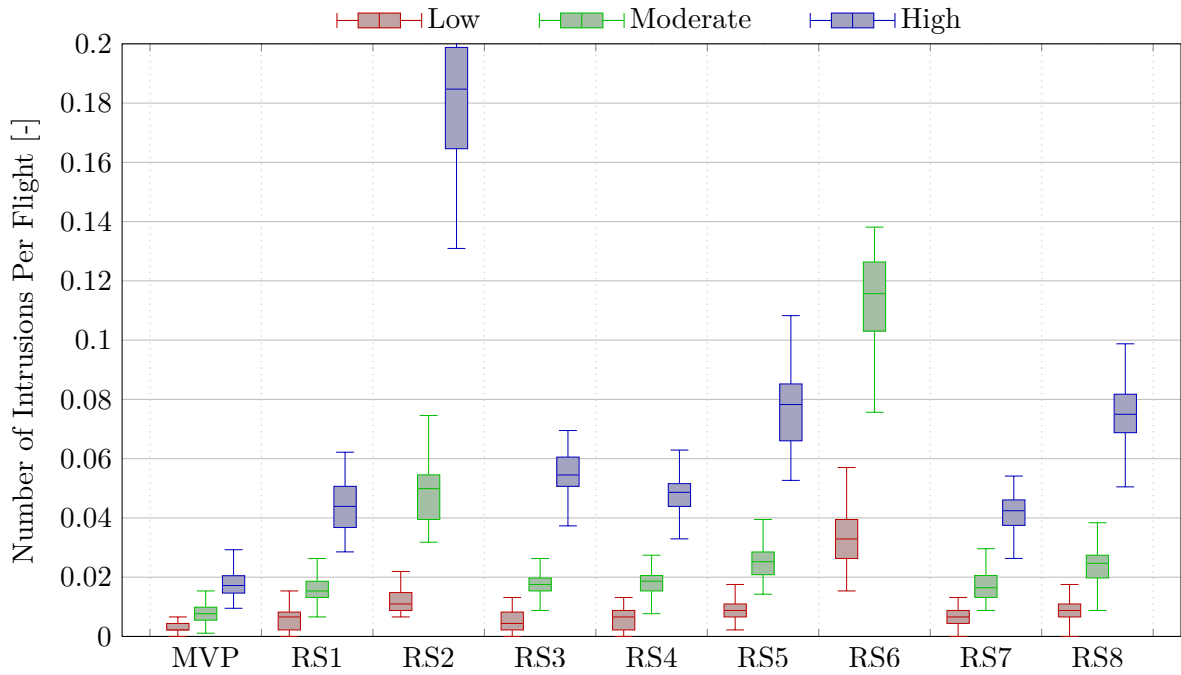


Figure A-2: Effect of traffic density on intrusions.

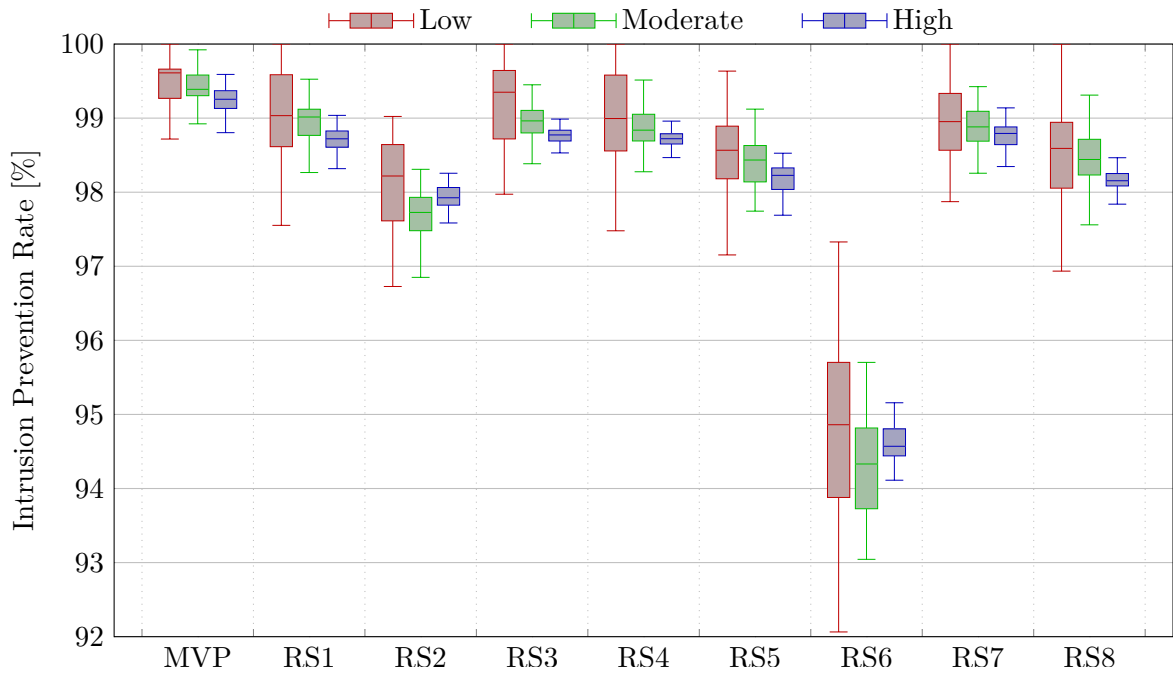


Figure A-3: Effect of traffic density on the IPR.

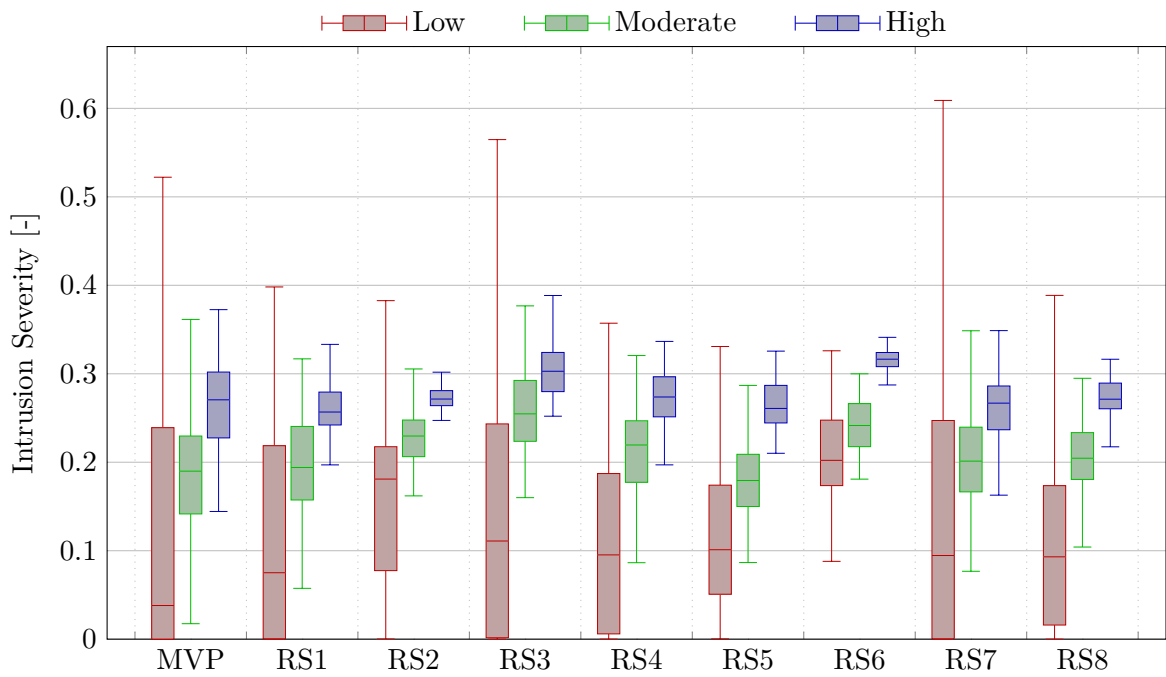


Figure A-4: Effect of traffic density on intrusion severity.

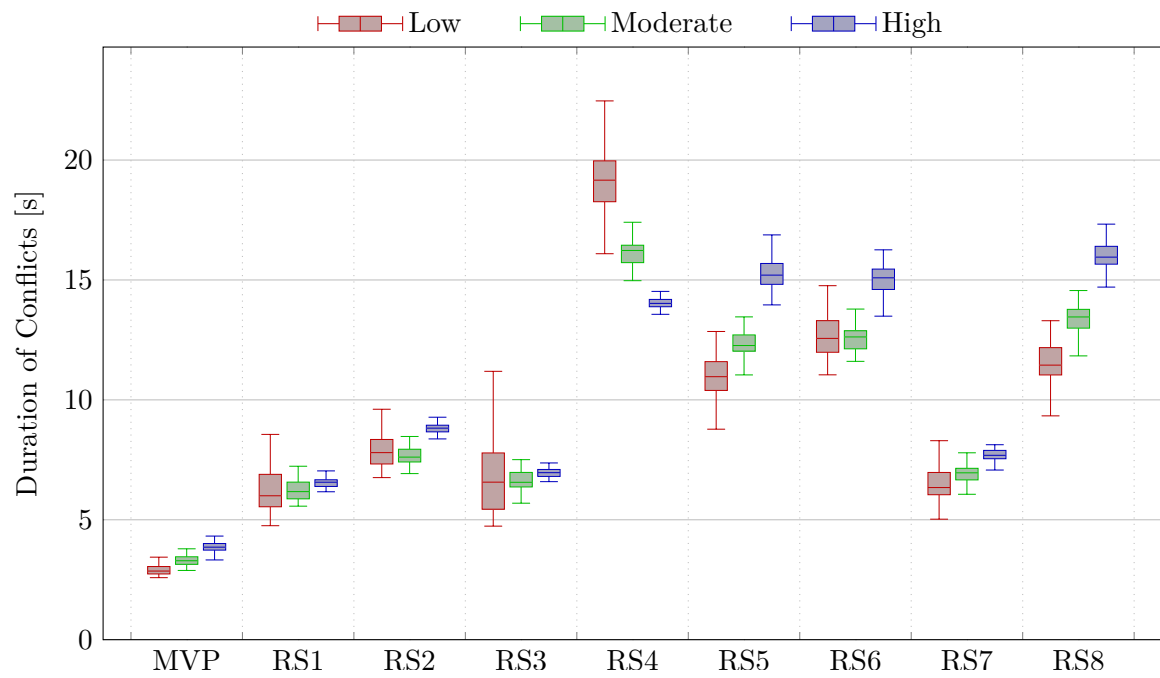


Figure A-5: Effect of traffic density on time to resolve conflicts.

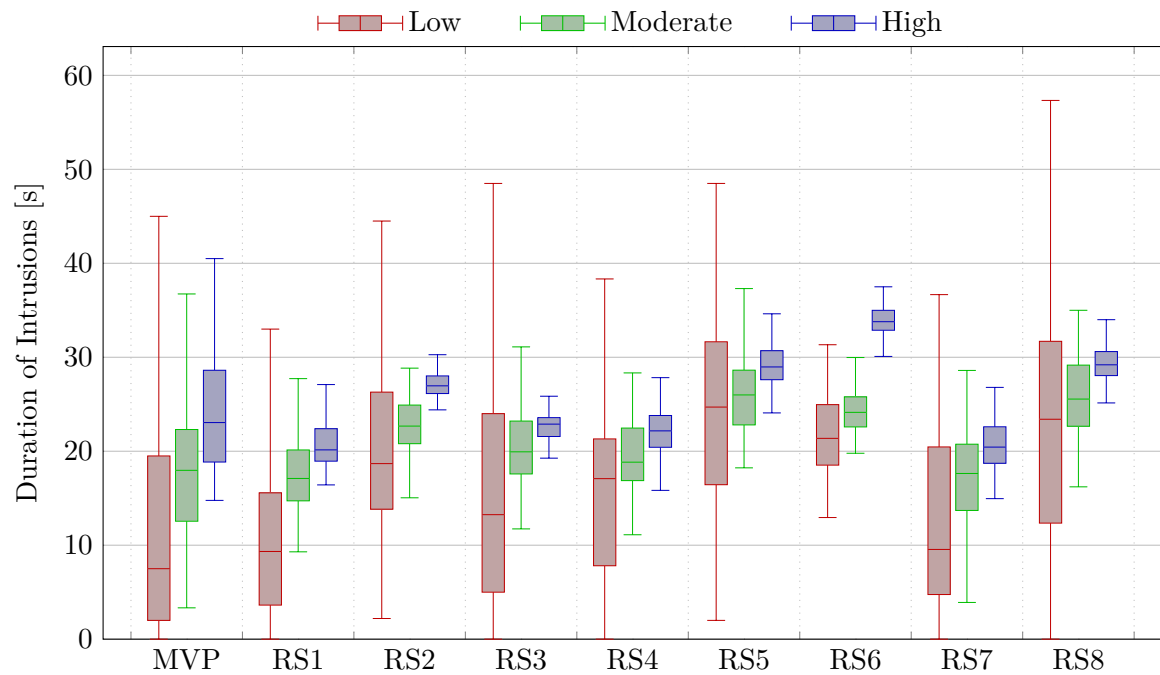


Figure A-6: Effect of traffic density on time to resolve intrusions.

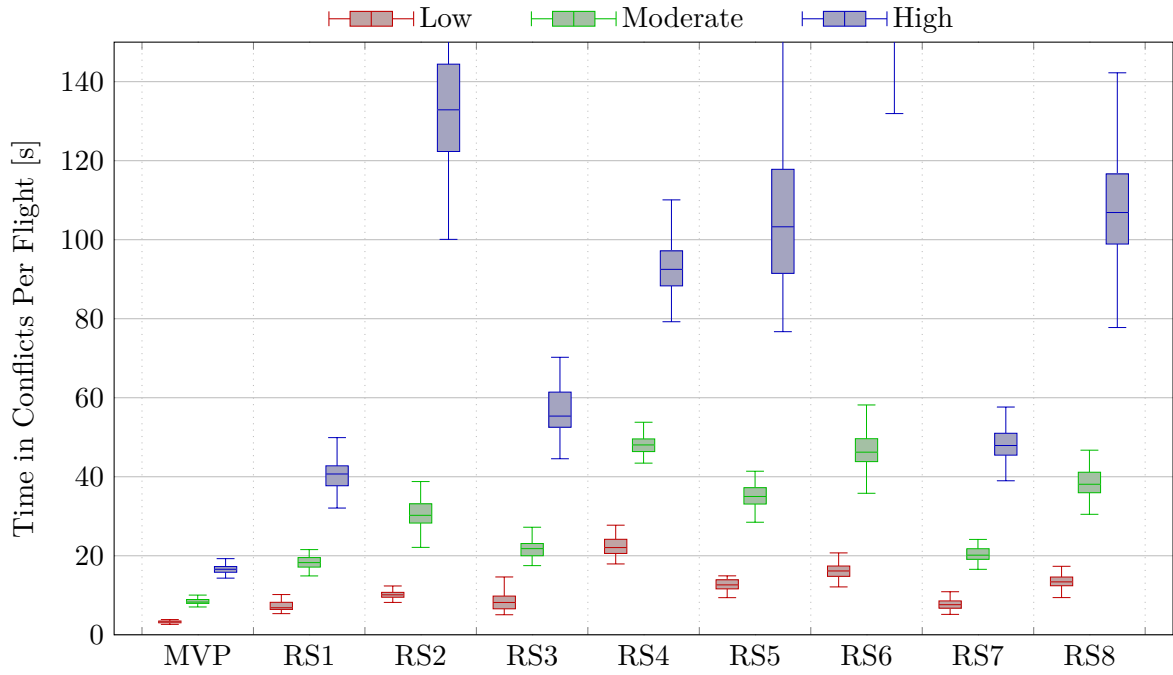


Figure A-7: Effect of traffic density on time spent in conflict.

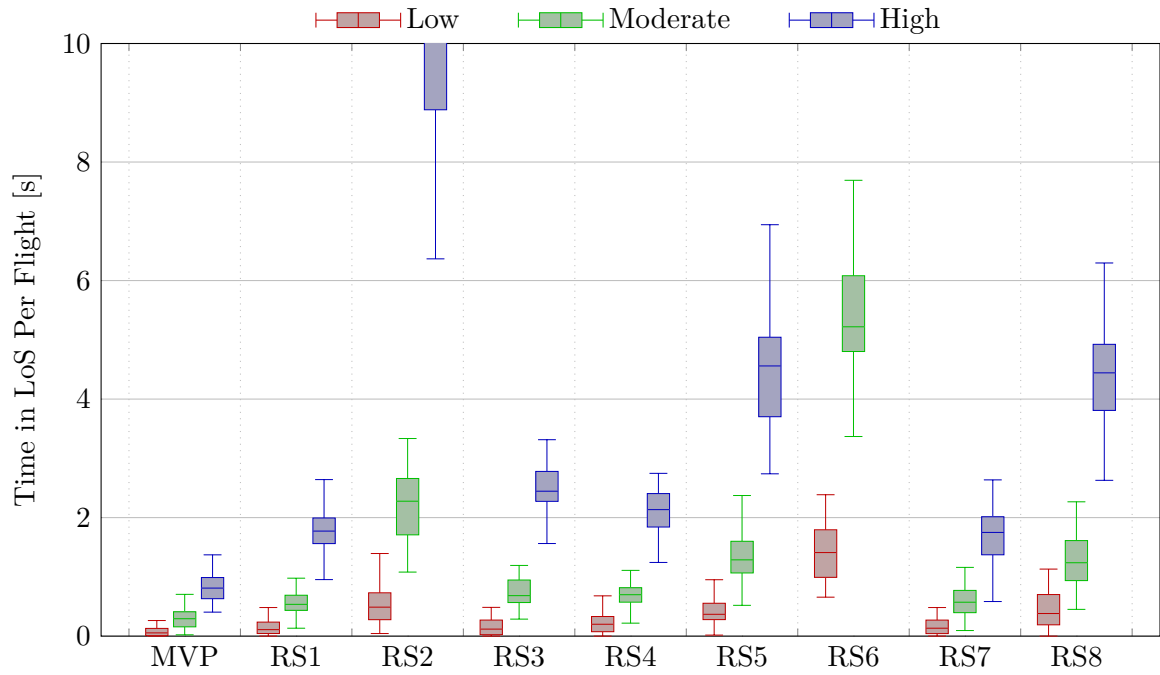


Figure A-8: Effect of traffic density on time spent in LoS.

A-2 Stability Metrics Charts

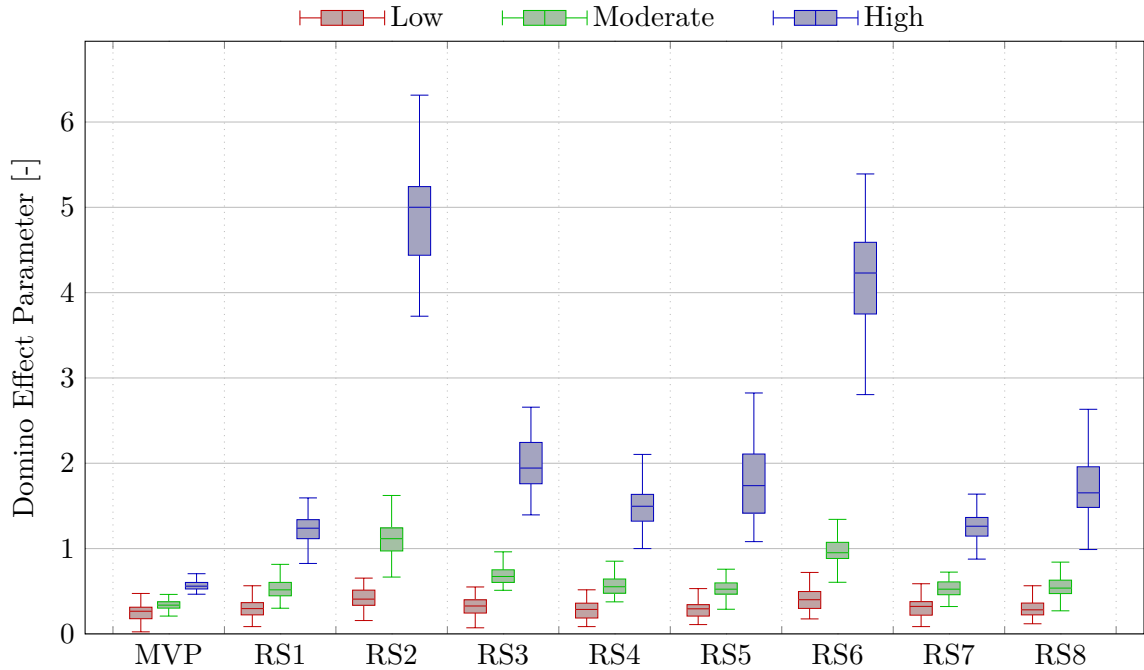


Figure A-9: Effect of traffic density on the DEP.

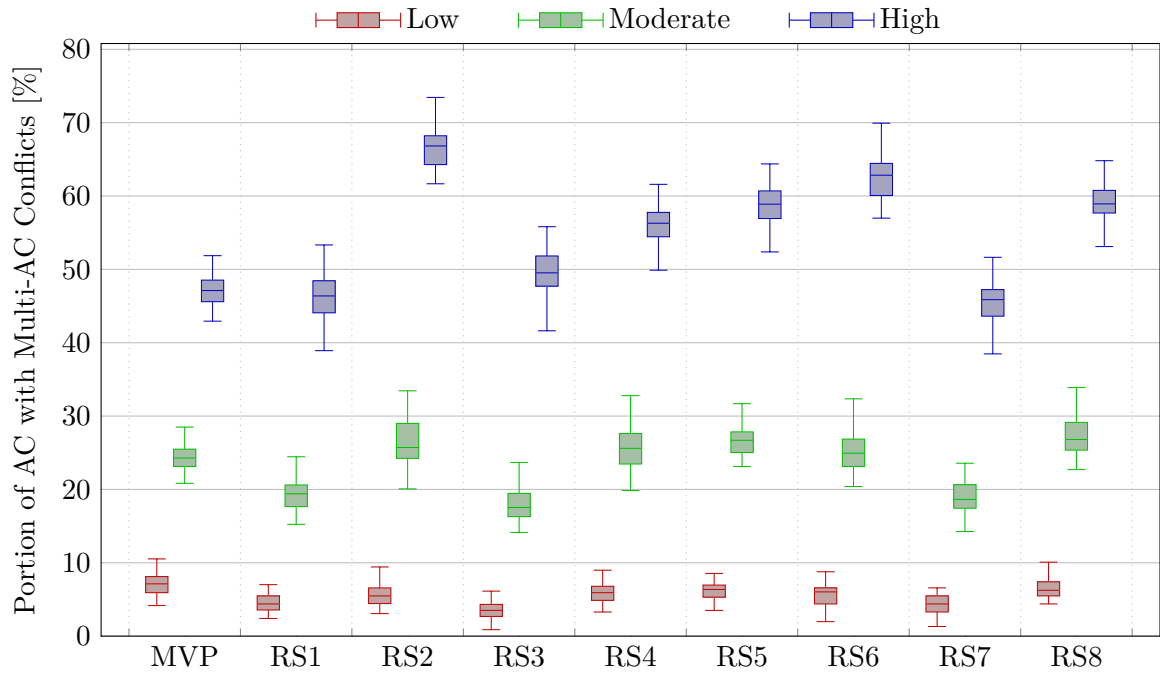


Figure A-10: Effect of traffic density on multi-aircraft conflicts.

A-3 Efficiency Metrics Charts

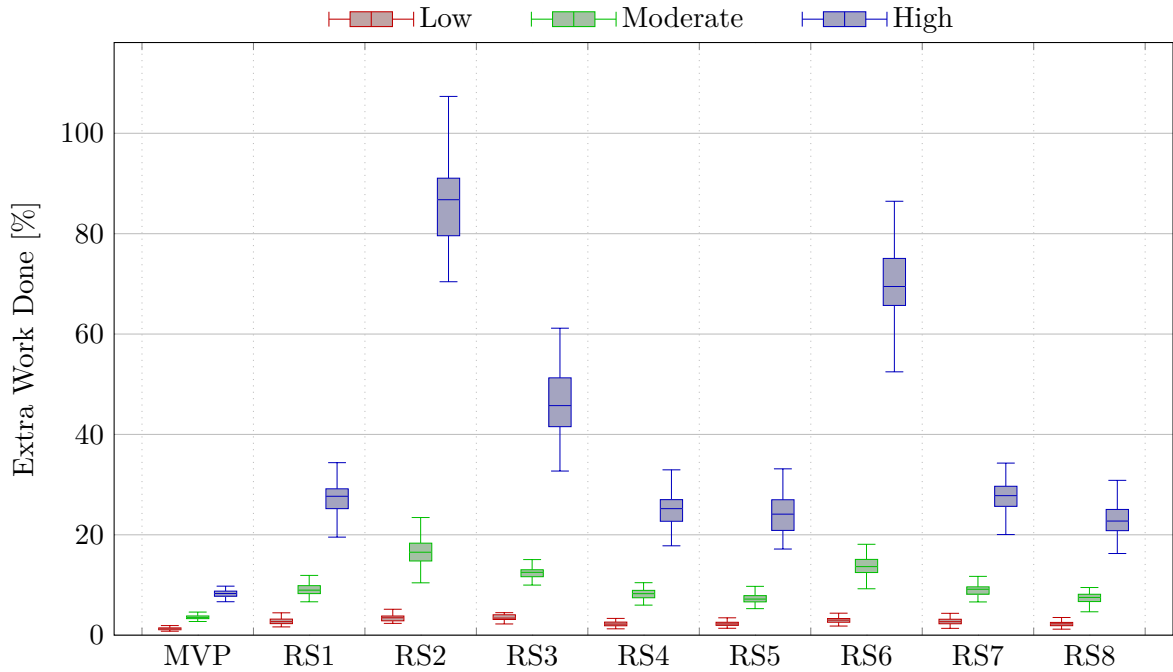


Figure A-11: Effect of traffic density on the extra expended energy.

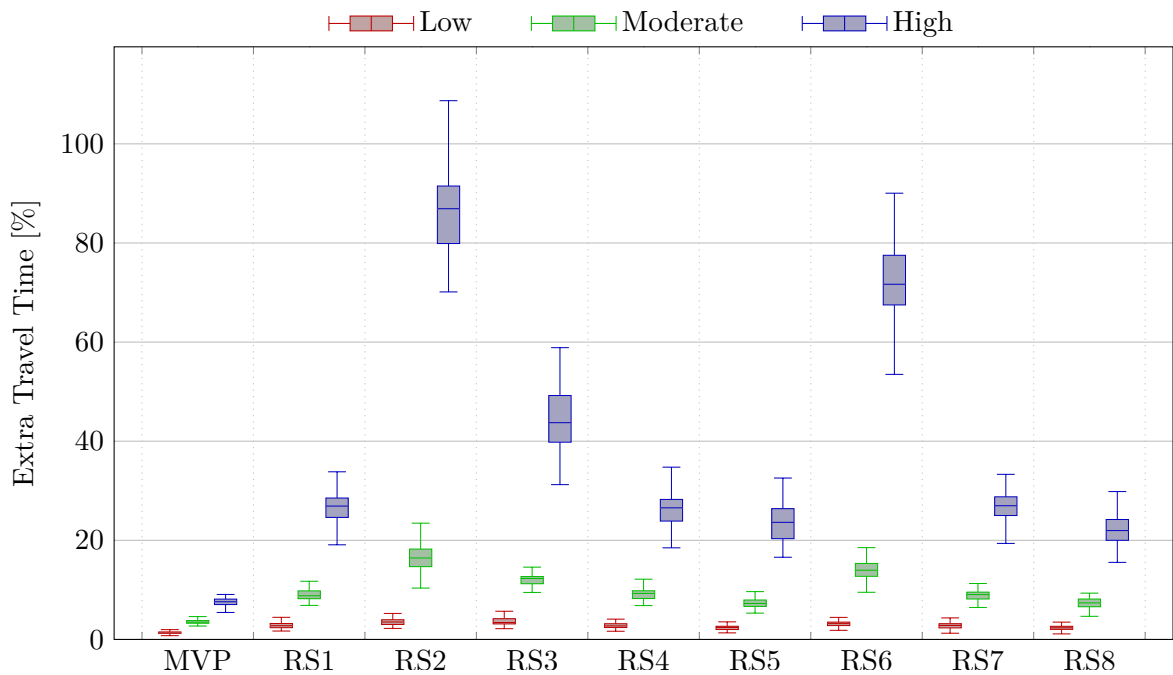


Figure A-12: Effect of traffic density on the extra travel time.

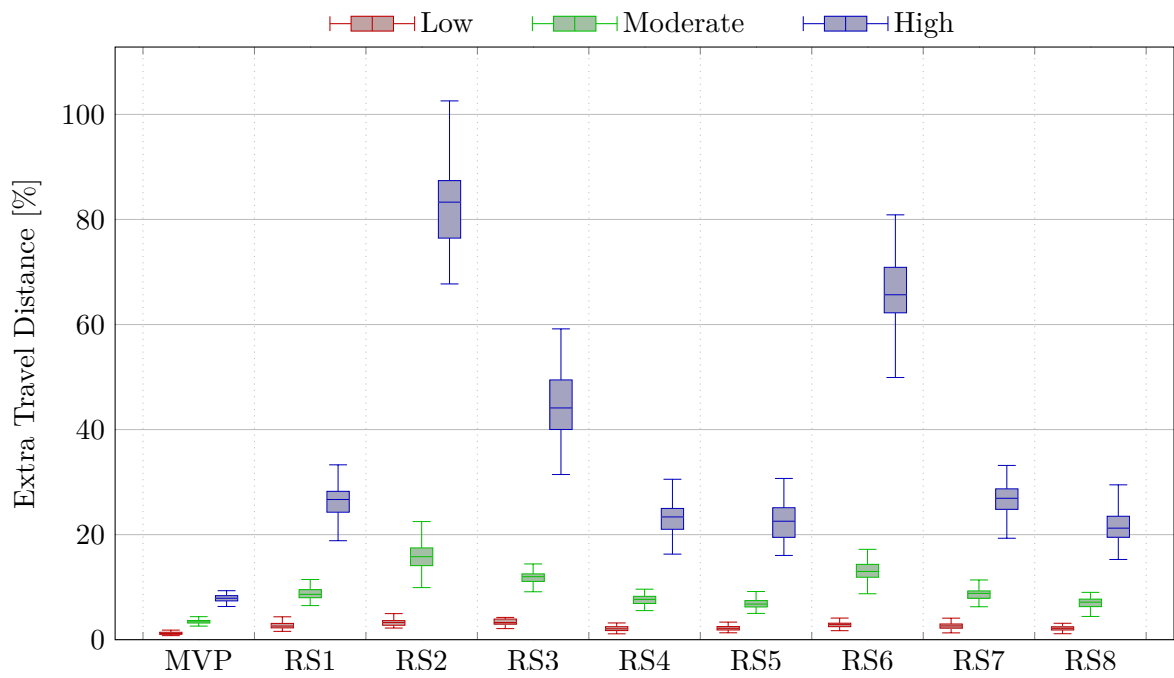


Figure A-13: Effect of traffic density on the extra travel distance.

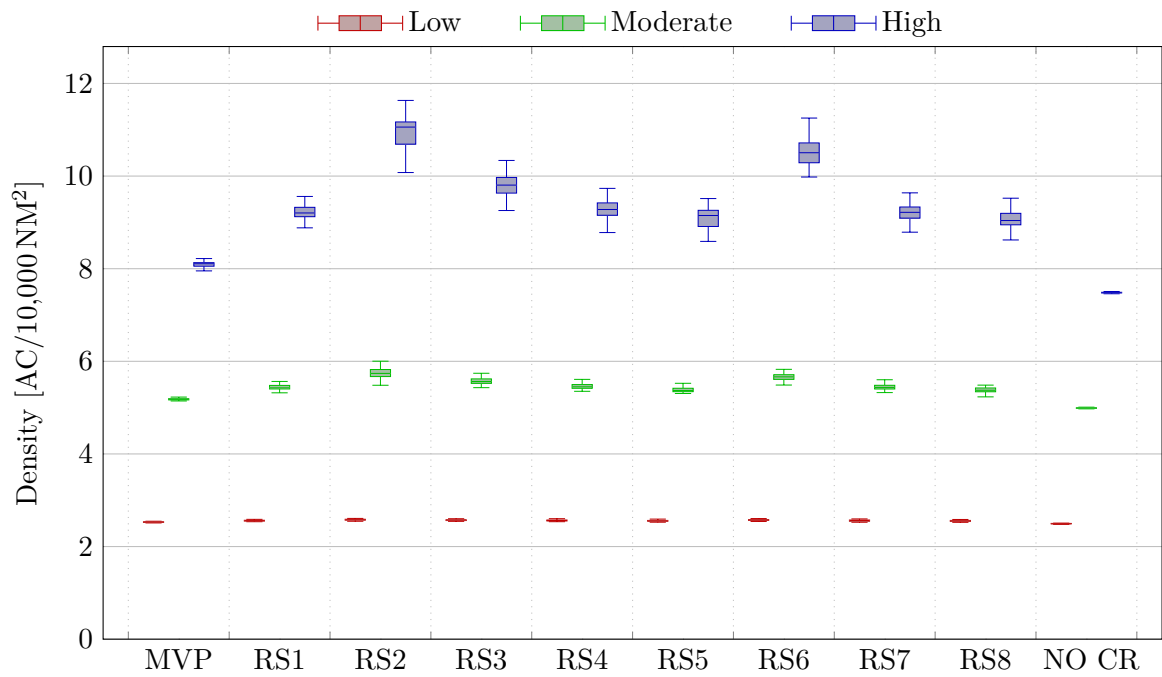


Figure A-14: Effect of traffic density on the actual density.

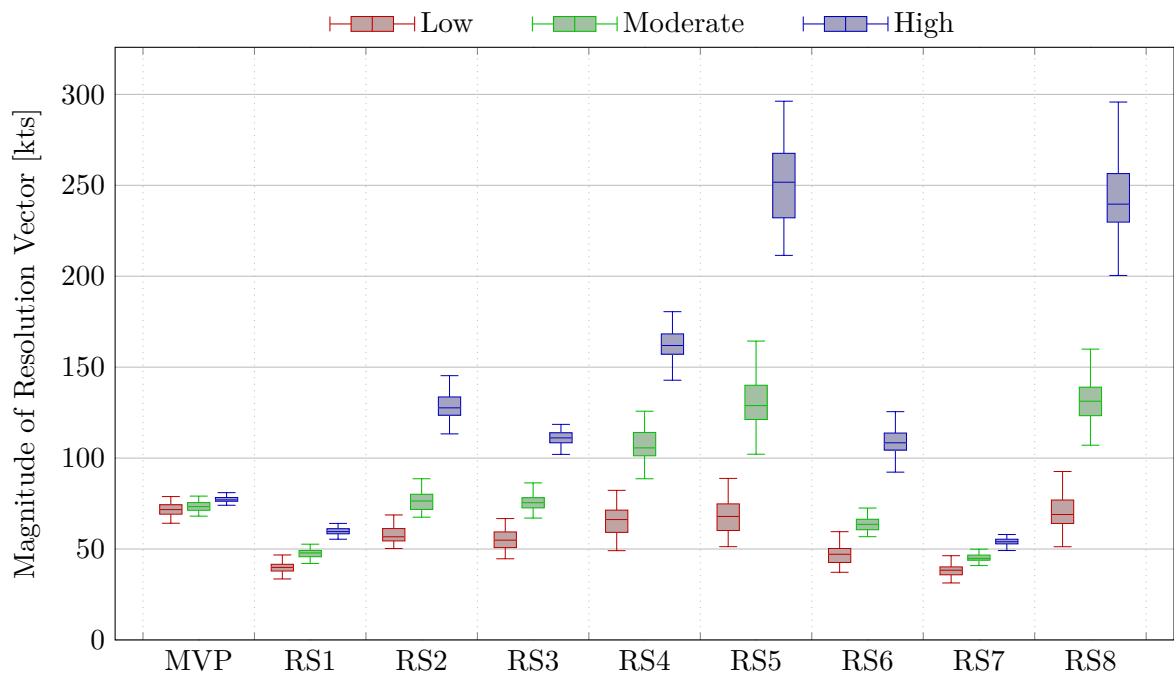


Figure A-15: Effect of traffic density on the magnitude of the resolution vector.

A-4 Safety Metrics Normality Test

Table A-2: P-values for Shapiro-Wilk (top) and Kolmogorov-Smirnov (bottom) tests for number of conflicts with small maneuvering space.

| ρ | MVP | RS1 | RS2 | RS3 | RS4 | RS5 | RS6 | RS7 | RS8 | NO CR |
|--------|--------|--------|---------------|---------------|--------|--------|--------|---------------|---------------|--------|
| 2.5 | 0.8538 | 0.2899 | 0.2724 | 0.5201 | 0.8589 | 0.3180 | 0.3568 | 0.4876 | 0.8278 | 0.7908 |
| 5.0 | 0.7931 | 0.5920 | <u>0.0486</u> | <u>0.0486</u> | 0.3326 | 0.8572 | 0.4021 | 0.0792 | 0.6414 | 0.9789 |
| 7.5 | 0.5567 | 0.6671 | 0.9969 | 0.9001 | 0.9413 | 0.2548 | 0.0756 | <u>0.0419</u> | <u>0.0279</u> | 0.8402 |
| 2.5 | 0.8528 | 0.6838 | 0.8822 | 0.7961 | 0.9869 | 0.9494 | 0.9486 | 0.7815 | 0.9957 | 0.9329 |
| 5.0 | 0.9975 | 0.9317 | 0.7717 | 0.3123 | 0.9679 | 0.9386 | 0.8474 | 0.8013 | 0.6902 | 0.9919 |
| 7.5 | 0.8906 | 0.8901 | 0.9991 | 0.9719 | 0.9997 | 0.5865 | 0.7564 | 0.3579 | 0.4088 | 0.9705 |

Table A-3: P-values for Shapiro-Wilk (top) and Kolmogorov-Smirnov (bottom) tests for number of conflicts with large maneuvering space.

| ρ | MVP | RS1 | RS2 | RS3 | RS4 | RS5 | RS6 | RS7 | RS8 | NO CR |
|--------|--------|--------|--------|---------------|---------------|--------|--------|--------|--------|--------|
| 2.5 | 0.8922 | 0.2442 | 0.6226 | 0.9778 | 0.1631 | 0.4414 | 0.4666 | 0.6568 | 0.2727 | 0.7908 |
| 5.0 | 0.8347 | 0.9126 | 0.9970 | <u>0.0013</u> | 0.1069 | 0.6790 | 0.4900 | 0.6352 | 0.3898 | 0.9789 |
| 7.5 | 0.1434 | 0.8926 | 0.7531 | 0.4120 | <u>0.0463</u> | 0.0518 | 0.6944 | 0.6685 | 0.0692 | 0.8402 |
| 2.5 | 0.9764 | 0.5884 | 0.9374 | 0.9973 | 0.6031 | 0.6771 | 0.9598 | 0.7244 | 0.3931 | 0.9329 |
| 5.0 | 0.9998 | 0.9978 | 0.9999 | 0.2917 | 0.6606 | 0.9312 | 0.9388 | 0.9577 | 0.7429 | 0.9919 |
| 7.5 | 0.7494 | 0.9516 | 0.5493 | 0.7631 | 0.6244 | 0.5816 | 0.9109 | 0.7408 | 0.4335 | 0.9705 |

Table A-4: P-values for Shapiro-Wilk (top) and Kolmogorov-Smirnov (bottom) tests for number of intrusions with small maneuvering space.

| ρ | MVP | RS1 | RS2 | RS3 | RS4 | RS5 | RS6 | RS7 | RS8 |
|--------|---------------|---------------|--------|---------------|---------------|---------------|--------|---------------|---------------|
| 2.5 | <u>0.0000</u> | <u>0.0076</u> | 0.0642 | <u>0.0052</u> | <u>0.0171</u> | <u>0.0134</u> | 0.6207 | <u>0.0013</u> | <u>0.0399</u> |
| 5.0 | 0.1055 | 0.7174 | 0.2905 | 0.0585 | 0.1403 | 0.5967 | 0.5861 | 0.6032 | 0.2115 |
| 7.5 | 0.6763 | 0.2161 | 0.1345 | 0.1427 | 0.3398 | 0.8421 | 0.1164 | 0.8907 | 0.1299 |
| 2.5 | <u>0.0060</u> | 0.0929 | 0.2102 | 0.1799 | 0.0776 | 0.1030 | 0.8415 | <u>0.0446</u> | 0.0518 |
| 5.0 | 0.4165 | 0.7946 | 0.5161 | 0.2431 | 0.2195 | 0.8482 | 0.7975 | 0.7828 | 0.9094 |
| 7.5 | 0.5601 | 0.3270 | 0.7249 | 0.5549 | 0.9696 | 0.9177 | 0.9364 | 0.9833 | 0.3911 |

Table A-5: P-values for Shapiro-Wilk (top) and Kolmogorov-Smirnov (bottom) tests for number of intrusions with large maneuvering space.

| ρ | MVP | RS1 | RS2 | RS3 | RS4 | RS5 | RS6 | RS7 | RS8 |
|--------|---------------|---------------|---------------|---------------|---------------|---------------|--------|---------------|--------|
| 2.5 | <u>0.0000</u> | <u>0.0046</u> | <u>0.0000</u> | <u>0.0003</u> | <u>0.0236</u> | <u>0.0091</u> | 0.1637 | <u>0.0210</u> | 0.1576 |
| 5.0 | 0.0538 | 0.4812 | 0.3656 | <u>0.0226</u> | 0.7183 | 0.5466 | 0.1674 | 0.1653 | 0.9756 |
| 7.5 | 0.1005 | 0.5330 | 0.8479 | 0.8161 | 0.7751 | 0.2001 | 0.6931 | 0.9743 | 0.9108 |
| 2.5 | <u>0.0054</u> | 0.0823 | <u>0.0103</u> | <u>0.0074</u> | 0.2881 | <u>0.0416</u> | 0.7059 | 0.1881 | 0.5859 |
| 5.0 | 0.2503 | 0.3409 | 0.5191 | 0.1494 | 0.3469 | 0.9234 | 0.7891 | 0.5409 | 0.8951 |
| 7.5 | 0.8299 | 0.9036 | 0.9576 | 0.9385 | 0.7722 | 0.7212 | 0.9572 | 0.9936 | 0.9192 |

Table A-6: P-values for Shapiro-Wilk (top) and Kolmogorov-Smirnov (bottom) tests for the IPR with small maneuvering space.

| ρ | MVP | RS1 | RS2 | RS3 | RS4 | RS5 | RS6 | RS7 | RS8 |
|--------|---------------|---------------|--------|---------------|--------|--------|--------|---------------|--------|
| 2.5 | <u>0.0003</u> | <u>0.0449</u> | 0.4629 | 0.0615 | 0.0779 | 0.0544 | 0.6804 | <u>0.0163</u> | 0.3237 |
| 5.0 | 0.3541 | 0.9590 | 0.4041 | 0.8121 | 0.3845 | 0.5746 | 0.0705 | 0.7773 | 0.1549 |
| 7.5 | 0.6663 | 0.1599 | 0.2023 | <u>0.0349</u> | 0.7271 | 0.6183 | 0.7622 | 0.2296 | 0.2643 |
| 2.5 | 0.0706 | 0.2490 | 0.5725 | 0.4510 | 0.5528 | 0.4435 | 0.9920 | 0.1876 | 0.9082 |
| 5.0 | 0.9158 | 0.9959 | 0.4972 | 0.9850 | 0.4978 | 0.7722 | 0.6225 | 0.9831 | 0.7886 |
| 7.5 | 0.9724 | 0.4489 | 0.3339 | 0.2742 | 0.9946 | 0.6750 | 0.9468 | 0.4854 | 0.7856 |

Table A-7: P-values for Shapiro-Wilk (top) and Kolmogorov-Smirnov (bottom) tests for the IPR with large maneuvering space.

| ρ | MVP | RS1 | RS2 | RS3 | RS4 | RS5 | RS6 | RS7 | RS8 |
|--------|---------------|---------------|---------------|---------------|--------|---------------|--------|--------|--------|
| 2.5 | <u>0.0001</u> | <u>0.0445</u> | <u>0.0001</u> | <u>0.0019</u> | 0.2077 | 0.1066 | 0.3709 | 0.2726 | 0.6547 |
| 5.0 | 0.1438 | 0.5571 | 0.7919 | 0.3312 | 0.8234 | 0.6614 | 0.3004 | 0.5666 | 0.7243 |
| 7.5 | 0.8349 | 0.3034 | 0.0968 | 0.3644 | 0.1587 | <u>0.0237</u> | 0.1677 | 0.7284 | 0.5995 |
| 2.5 | 0.0758 | 0.6027 | 0.2049 | <u>0.0486</u> | 0.7492 | 0.8810 | 0.9911 | 0.6528 | 0.9754 |
| 5.0 | 0.3159 | 0.6589 | 0.9787 | 0.7971 | 0.6911 | 0.6509 | 0.7254 | 0.7645 | 0.8557 |
| 7.5 | 0.9481 | 0.8250 | 0.7686 | 0.8588 | 0.8043 | 0.1677 | 0.5293 | 0.8510 | 0.8988 |

Table A-8: P-values for Shapiro-Wilk (top) and Kolmogorov-Smirnov (bottom) tests for the intrusion severity with small maneuvering space.

| ρ | MVP | RS1 | RS2 | RS3 | RS4 | RS5 | RS6 | RS7 | RS8 |
|--------|---------------|---------------|---------------|---------------|---------------|---------------|--------|---------------|---------------|
| 2.5 | <u>0.0000</u> | <u>0.0000</u> | <u>0.0006</u> | <u>0.0000</u> | <u>0.0000</u> | <u>0.0004</u> | 0.2439 | <u>0.0000</u> | <u>0.0001</u> |
| 5.0 | 0.6366 | 0.5066 | 0.2588 | 0.3086 | 0.9044 | 0.4493 | 0.9651 | 0.7498 | 0.4934 |
| 7.5 | 0.7291 | 0.2193 | 0.9019 | 0.0564 | 0.9782 | 0.9547 | 0.3897 | 0.9578 | 0.1261 |
| 2.5 | <u>0.0072</u> | <u>0.0077</u> | 0.3409 | 0.1041 | <u>0.0132</u> | 0.3508 | 0.9649 | <u>0.0166</u> | 0.1096 |
| 5.0 | 0.6755 | 0.7215 | 0.7670 | 0.2591 | 1.0000 | 0.7957 | 0.9889 | 0.7902 | 0.6954 |
| 7.5 | 0.9875 | 0.9672 | 0.9574 | 0.5850 | 0.9995 | 0.9975 | 0.8682 | 0.9998 | 0.3837 |

Table A-9: P-values for Shapiro-Wilk (top) and Kolmogorov-Smirnov (bottom) tests for the intrusion severity with large maneuvering space.

| ρ | MVP | RS1 | RS2 | RS3 | RS4 | RS5 | RS6 | RS7 | RS8 |
|--------|---------------|---------------|---------------|---------------|---------------|---------------|---------------|---------------|---------------|
| 2.5 | <u>0.0000</u> | <u>0.0000</u> | <u>0.0320</u> | <u>0.0000</u> | <u>0.0000</u> | <u>0.0017</u> | 0.5753 | <u>0.0000</u> | <u>0.0000</u> |
| 5.0 | <u>0.0000</u> | 0.8983 | 0.3403 | 0.8532 | 0.5347 | 0.3346 | 0.1346 | 0.8580 | 0.0756 |
| 7.5 | 0.4814 | 0.0554 | 0.7019 | 0.0696 | 0.4199 | 0.4012 | <u>0.0321</u> | 0.3897 | 0.3205 |
| 2.5 | <u>0.0045</u> | <u>0.0310</u> | 0.3600 | 0.0567 | <u>0.0231</u> | 0.5249 | 0.8878 | 0.0865 | 0.1651 |
| 5.0 | <u>0.0391</u> | 0.7995 | 0.8588 | 0.9488 | 0.7258 | 0.8879 | 0.9655 | 0.9027 | 0.7057 |
| 7.5 | 0.5013 | 0.5530 | 0.6772 | 0.9139 | 0.9791 | 0.5601 | 0.3187 | 0.7130 | 0.7370 |

Table A-10: P-values for Shapiro-Wilk (top) and Kolmogorov-Smirnov (bottom) tests for the time to resolve conflicts with small maneuvering space.

| ρ | MVP | RS1 | RS2 | RS3 | RS4 | RS5 | RS6 | RS7 | RS8 |
|--------|---------------|---------------|---------------|---------------|---------------|--------|---------------|---------------|--------|
| 2.5 | <u>0.0000</u> | <u>0.0005</u> | <u>0.0305</u> | <u>0.0000</u> | 0.1590 | 0.5855 | <u>0.0005</u> | <u>0.0006</u> | 0.8241 |
| 5.0 | 0.1152 | <u>0.0426</u> | 0.5661 | 0.4880 | 0.7492 | 0.2510 | 0.2078 | 0.1475 | 0.7818 |
| 7.5 | 0.8343 | 0.7130 | 0.0675 | 0.9403 | <u>0.0436</u> | 0.3251 | 0.7604 | 0.9853 | 0.2518 |
| 2.5 | 0.0890 | 0.1496 | 0.8057 | 0.2200 | 0.8811 | 0.9999 | 0.6098 | 0.2967 | 0.9239 |
| 5.0 | 0.3503 | 0.4038 | 0.5629 | 0.8766 | 0.9207 | 0.9176 | 0.6265 | 0.8715 | 0.9600 |
| 7.5 | 0.9804 | 0.8390 | 0.8172 | 0.9839 | 0.6951 | 0.9383 | 0.9789 | 0.9875 | 0.6508 |

Table A-11: P-values for Shapiro-Wilk (top) and Kolmogorov-Smirnov (bottom) tests for the time to resolve conflicts with large maneuvering space.

| ρ | MVP | RS1 | RS2 | RS3 | RS4 | RS5 | RS6 | RS7 | RS8 |
|--------|---------------|---------------|---------------|---------------|---------------|--------|--------|--------|--------|
| 2.5 | <u>0.0000</u> | <u>0.0027</u> | <u>0.0180</u> | <u>0.0001</u> | 0.4703 | 0.3122 | 0.4882 | 0.5923 | 0.4994 |
| 5.0 | 0.0591 | 0.1242 | 0.3046 | 0.2337 | 0.5522 | 0.2453 | 0.4383 | 0.9225 | 0.4528 |
| 7.5 | 0.7923 | <u>0.0480</u> | 0.2097 | 0.6013 | <u>0.0374</u> | 0.5491 | 0.6137 | 0.1728 | 0.8428 |
| 2.5 | 0.0748 | 0.3627 | 0.4085 | 0.4276 | 0.9167 | 0.8797 | 0.8606 | 0.7211 | 0.9172 |
| 5.0 | 0.9188 | 0.6168 | 0.5192 | 0.7331 | 0.7515 | 0.8438 | 0.7952 | 0.8513 | 0.9777 |
| 7.5 | 0.8375 | 0.4440 | 0.5595 | 0.9746 | 0.2349 | 0.9382 | 0.8709 | 0.7875 | 0.9243 |

Table A-12: P-values for Shapiro-Wilk (top) and Kolmogorov-Smirnov (bottom) tests for the time to resolve intrusions with small maneuvering space.

| ρ | MVP | RS1 | RS2 | RS3 | RS4 | RS5 | RS6 | RS7 | RS8 |
|--------|---------------|---------------|---------------|---------------|---------------|--------|---------------|---------------|--------|
| 2.5 | <u>0.0000</u> | <u>0.0000</u> | <u>0.0058</u> | <u>0.0000</u> | <u>0.0134</u> | 0.2386 | 0.8532 | <u>0.0000</u> | 0.9838 |
| 5.0 | 0.2061 | 0.7653 | 0.3517 | 0.4527 | <u>0.0007</u> | 0.6432 | <u>0.0000</u> | <u>0.0000</u> | 0.6810 |
| 7.5 | <u>0.0002</u> | 0.6904 | 0.4356 | 0.1735 | 0.4528 | 0.8763 | 0.5654 | <u>0.0001</u> | 0.8859 |
| 2.5 | 0.1065 | 0.0910 | 0.2580 | <u>0.0000</u> | 0.8681 | 0.7659 | 0.9680 | <u>0.0126</u> | 0.8414 |
| 5.0 | 0.5335 | 0.9771 | 0.8948 | 0.9568 | 0.5420 | 0.9667 | 0.1414 | 0.0665 | 0.9546 |
| 7.5 | 0.0690 | 0.9294 | 0.9010 | 0.6857 | 0.9492 | 0.9843 | 0.9368 | 0.3884 | 0.7901 |

Table A-13: P-values for Shapiro-Wilk (top) and Kolmogorov-Smirnov (bottom) tests for the time to resolve intrusions with large maneuvering space.

| ρ | MVP | RS1 | RS2 | RS3 | RS4 | RS5 | RS6 | RS7 | RS8 |
|--------|---------------|---------------|---------------|---------------|---------------|---------------|--------|---------------|--------|
| 2.5 | <u>0.0000</u> | <u>0.0000</u> | <u>0.0240</u> | <u>0.0000</u> | <u>0.0000</u> | 0.2649 | 0.0950 | <u>0.0000</u> | 0.2543 |
| 5.0 | <u>0.0000</u> | <u>0.0205</u> | 0.7744 | 0.4038 | 0.3203 | <u>0.0018</u> | 0.6155 | <u>0.0076</u> | 0.9025 |
| 7.5 | <u>0.0001</u> | 0.1692 | 0.8637 | <u>0.0009</u> | 0.7741 | 0.4087 | 0.3691 | 0.6939 | 0.2115 |
| 2.5 | 0.0884 | <u>0.0241</u> | 0.6564 | <u>0.0000</u> | 0.1316 | 0.9230 | 0.9830 | <u>0.0457</u> | 0.8617 |
| 5.0 | <u>0.0464</u> | 0.3093 | 0.5741 | 0.8864 | 0.4849 | 0.2748 | 0.9275 | 0.8595 | 0.9961 |
| 7.5 | 0.1643 | 0.7891 | 0.9858 | 0.1543 | 0.9889 | 0.7095 | 0.8528 | 0.9070 | 0.9347 |

Table A-14: P-values for Shapiro-Wilk (top) and Kolmogorov-Smirnov (bottom) tests for the time spent in conflict with small maneuvering space.

| ρ | MVP | RS1 | RS2 | RS3 | RS4 | RS5 | RS6 | RS7 | RS8 |
|--------|---------------|---------------|--------|---------------|--------|--------|--------|---------------|---------------|
| 2.5 | <u>0.0000</u> | <u>0.0384</u> | 0.3623 | <u>0.0001</u> | 0.2606 | 0.4767 | 0.4282 | <u>0.0056</u> | 0.6552 |
| 5.0 | 0.3743 | 0.2329 | 0.4022 | 0.6249 | 0.6165 | 0.4799 | 0.3273 | 0.0585 | 0.6610 |
| 7.5 | 0.5394 | 0.1955 | 0.9219 | 0.7624 | 0.9775 | 0.0759 | 0.0708 | 0.4172 | <u>0.0221</u> |
| 2.5 | <u>0.0312</u> | 0.1627 | 0.9726 | 0.1519 | 0.2918 | 0.8979 | 0.6563 | 0.3896 | 0.9426 |
| 5.0 | 0.8359 | 0.7115 | 0.9292 | 0.7990 | 0.9955 | 0.7732 | 0.9880 | 0.7407 | 0.7706 |
| 7.5 | 0.9072 | 0.9974 | 0.9979 | 0.9645 | 0.9999 | 0.3575 | 0.9158 | 0.8743 | 0.4499 |

Table A-15: P-values for Shapiro-Wilk (top) and Kolmogorov-Smirnov (bottom) tests for the time spent in conflict with large maneuvering space.

| ρ | MVP | RS1 | RS2 | RS3 | RS4 | RS5 | RS6 | RS7 | RS8 |
|--------|---------------|---------------|--------|---------------|--------|---------------|--------|--------|--------|
| 2.5 | <u>0.0001</u> | <u>0.0002</u> | 0.7441 | <u>0.0022</u> | 0.5928 | 0.0861 | 0.9391 | 0.5334 | 0.9269 |
| 5.0 | 0.0974 | 0.5707 | 0.7914 | 0.3764 | 0.3024 | 0.1202 | 0.9748 | 0.7658 | 0.9086 |
| 7.5 | 0.5929 | 0.2832 | 0.8951 | 0.4115 | 0.0587 | <u>0.0380</u> | 0.6925 | 0.8116 | 0.1524 |
| 2.5 | 0.0660 | 0.0993 | 0.9381 | 0.2248 | 0.9275 | 0.7799 | 0.9917 | 0.9853 | 0.9936 |
| 5.0 | 0.3512 | 0.9834 | 0.5943 | 0.9650 | 0.5777 | 0.7259 | 0.9883 | 0.8791 | 0.8036 |
| 7.5 | 0.7470 | 0.8886 | 0.6950 | 0.3808 | 0.6124 | 0.5391 | 0.8812 | 0.9965 | 0.5987 |

Table A-16: P-values for Shapiro-Wilk (top) and Kolmogorov-Smirnov (bottom) tests for the time spent in LoS with small maneuvering space.

| ρ | MVP | RS1 | RS2 | RS3 | RS4 | RS5 | RS6 | RS7 | RS8 |
|--------|---------------|---------------|--------|---------------|---------------|---------------|--------|---------------|---------------|
| 2.5 | <u>0.0000</u> | <u>0.0000</u> | 0.2430 | <u>0.0000</u> | <u>0.0000</u> | <u>0.0465</u> | 0.3426 | <u>0.0003</u> | <u>0.0059</u> |
| 5.0 | <u>0.0003</u> | 0.9436 | 0.0595 | 0.4429 | <u>0.0000</u> | 0.2196 | 0.0527 | <u>0.0069</u> | 0.2807 |
| 7.5 | <u>0.0389</u> | 0.0826 | 0.1702 | 0.4607 | 0.4046 | 0.2894 | 0.1038 | 0.8699 | 0.1454 |
| 2.5 | <u>0.0465</u> | 0.1584 | 0.8439 | <u>0.0112</u> | 0.1261 | 0.5805 | 0.7535 | 0.2500 | 0.5992 |
| 5.0 | 0.2085 | 0.9530 | 0.1221 | 0.7860 | 0.3195 | 0.7201 | 0.7795 | 0.1898 | 0.7299 |
| 7.5 | 0.6397 | 0.4572 | 0.9417 | 0.6245 | 0.8586 | 0.8988 | 0.8103 | 0.8908 | 0.3529 |

Table A-17: P-values for Shapiro-Wilk (top) and Kolmogorov-Smirnov (bottom) tests for the time spent in LoS with large maneuvering space.

| ρ | MVP | RS1 | RS2 | RS3 | RS4 | RS5 | RS6 | RS7 | RS8 |
|--------|---------------|---------------|---------------|---------------|---------------|--------|---------------|---------------|---------------|
| 2.5 | <u>0.0000</u> | <u>0.0003</u> | <u>0.0466</u> | <u>0.0000</u> | <u>0.0023</u> | 0.0636 | <u>0.0481</u> | <u>0.0007</u> | <u>0.0172</u> |
| 5.0 | <u>0.0071</u> | 0.8459 | 0.1834 | <u>0.0049</u> | 0.8523 | 0.7455 | 0.6259 | 0.9026 | 0.2465 |
| 7.5 | <u>0.0000</u> | 0.1403 | 0.8476 | 0.4106 | 0.3084 | 0.5673 | 0.6361 | 0.4379 | 0.9918 |
| 2.5 | <u>0.0426</u> | 0.1485 | 0.6909 | <u>0.0087</u> | 0.4343 | 0.5883 | 0.4414 | 0.2482 | 0.1504 |
| 5.0 | 0.7058 | 0.7574 | 0.6825 | 0.3480 | 0.9420 | 0.9672 | 0.7517 | 0.8942 | 0.7914 |
| 7.5 | 0.1494 | 0.7266 | 0.6592 | 0.7860 | 0.7878 | 0.9737 | 0.7856 | 0.8299 | 0.9835 |

A-5 Stability Metrics Normality Test

Table A-18: P-values for Shapiro-Wilk (top) and Kolmogorov-Smirnov (bottom) tests for the DEP with small maneuvering space.

| ρ | MVP | RS1 | RS2 | RS3 | RS4 | RS5 | RS6 | RS7 | RS8 |
|--------|--------|--------|---------------|---------------|--------|--------|--------|---------------|---------------|
| 2.5 | 0.8538 | 0.2899 | 0.2724 | 0.5201 | 0.8589 | 0.3180 | 0.3568 | 0.4876 | 0.8278 |
| 5.0 | 0.7931 | 0.5920 | <u>0.0486</u> | <u>0.0486</u> | 0.3326 | 0.8572 | 0.4021 | 0.0792 | 0.6414 |
| 7.5 | 0.5567 | 0.6671 | 0.9969 | 0.9001 | 0.9413 | 0.2548 | 0.0756 | <u>0.0419</u> | <u>0.0279</u> |
| 2.5 | 0.8528 | 0.6838 | 0.8822 | 0.7961 | 0.9869 | 0.9494 | 0.9486 | 0.7815 | 0.9957 |
| 5.0 | 0.9975 | 0.9317 | 0.7717 | 0.3123 | 0.9679 | 0.9386 | 0.8474 | 0.8013 | 0.6902 |
| 7.5 | 0.8906 | 0.8901 | 0.9991 | 0.9719 | 0.9997 | 0.5865 | 0.7564 | 0.3579 | 0.4088 |

Table A-19: P-values for Shapiro-Wilk (top) and Kolmogorov-Smirnov (bottom) tests for the DEP with large maneuvering space.

| ρ | MVP | RS1 | RS2 | RS3 | RS4 | RS5 | RS6 | RS7 | RS8 |
|--------|--------|--------|--------|---------------|---------------|--------|--------|--------|--------|
| 2.5 | 0.8922 | 0.2442 | 0.6226 | 0.9779 | 0.1631 | 0.4414 | 0.4666 | 0.6568 | 0.2727 |
| 5.0 | 0.8348 | 0.9126 | 0.9970 | <u>0.0013</u> | 0.1069 | 0.6790 | 0.4900 | 0.6352 | 0.3898 |
| 7.5 | 0.1434 | 0.8926 | 0.7531 | 0.4120 | <u>0.0463</u> | 0.0518 | 0.6944 | 0.6685 | 0.0692 |
| 2.5 | 0.9764 | 0.5884 | 0.9374 | 0.9973 | 0.6031 | 0.6771 | 0.9598 | 0.7244 | 0.3931 |
| 5.0 | 0.9998 | 0.9978 | 0.9999 | 0.2917 | 0.6606 | 0.9312 | 0.9388 | 0.9577 | 0.7429 |
| 7.5 | 0.7494 | 0.9516 | 0.5493 | 0.7631 | 0.6244 | 0.5816 | 0.9109 | 0.7408 | 0.4335 |

Table A-20: P-values for Shapiro-Wilk (top) and Kolmogorov-Smirnov (bottom) tests for the multi-aircraft conflicts with small maneuvering space.

| ρ | MVP | RS1 | RS2 | RS3 | RS4 | RS5 | RS6 | RS7 | RS8 |
|--------|--------|---------------|---------------|---------------|--------|--------|--------|--------|--------|
| 2.5 | 0.2190 | <u>0.0020</u> | <u>0.0279</u> | 0.7778 | 0.1389 | 0.4830 | 0.6823 | 0.0623 | 0.2607 |
| 5.0 | 0.0757 | 0.7451 | 0.1963 | <u>0.0143</u> | 0.2774 | 0.2109 | 0.6515 | 0.7171 | 0.9394 |
| 7.5 | 0.2377 | 0.1356 | 0.8651 | 0.0610 | 0.1547 | 0.5681 | 0.8198 | 0.1600 | 0.7706 |
| 2.5 | 0.8890 | 0.3541 | 0.1492 | 0.8573 | 0.5522 | 0.5443 | 0.9876 | 0.2901 | 0.6998 |
| 5.0 | 0.5640 | 0.8991 | 0.8019 | 0.5387 | 0.6419 | 0.4889 | 0.9865 | 0.8437 | 0.9928 |
| 7.5 | 0.6277 | 0.3665 | 0.9049 | 0.8518 | 0.2128 | 0.7897 | 0.9858 | 0.7898 | 0.8803 |

Table A-21: P-values for Shapiro-Wilk (top) and Kolmogorov-Smirnov (bottom) tests for the multi-aircraft conflicts with large maneuvering space.

| ρ | MVP | RS1 | RS2 | RS3 | RS4 | RS5 | RS6 | RS7 | RS8 |
|--------|--------|--------|--------|--------|--------|--------|--------|--------|---------------|
| 2.5 | 0.3246 | 0.1512 | 0.0650 | 0.2743 | 0.1943 | 0.7743 | 0.1077 | 0.0882 | <u>0.0093</u> |
| 5.0 | 0.4496 | 0.1206 | 0.6119 | 0.0724 | 0.7686 | 0.2445 | 0.6470 | 0.4315 | 0.0645 |
| 7.5 | 0.9088 | 0.9569 | 0.3678 | 0.6607 | 0.8481 | 0.7881 | 0.3104 | 0.0949 | 0.2955 |
| 2.5 | 0.9774 | 0.7335 | 0.5553 | 0.6282 | 0.8321 | 0.8418 | 0.1993 | 0.3953 | 0.4885 |
| 5.0 | 0.8990 | 0.8862 | 0.8041 | 0.6841 | 0.8543 | 0.4216 | 0.9993 | 0.8410 | 0.6225 |
| 7.5 | 0.9640 | 0.9598 | 0.9633 | 0.9230 | 0.9638 | 0.9983 | 0.8809 | 0.4419 | 0.7370 |

A-6 Efficiency Metrics Normality Test

Table A-22: P-values for Shapiro-Wilk (top) and Kolmogorov-Smirnov (bottom) tests for the extra expended energy with small maneuvering space.

| ρ | MVP | RS1 | RS2 | RS3 | RS4 | RS5 | RS6 | RS7 | RS8 |
|--------|---------------|--------|---------------|---------------|--------|--------|--------|--------|--------|
| 2.5 | 0.3337 | 0.3613 | <u>0.0286</u> | <u>0.0060</u> | 0.7655 | 0.7505 | 0.1330 | 0.7200 | 0.7696 |
| 5.0 | 0.0929 | 0.0636 | <u>0.0067</u> | 0.6489 | 0.6332 | 0.9438 | 0.3306 | 0.2608 | 0.8053 |
| 7.5 | <u>0.0186</u> | 0.7953 | 0.7471 | 0.8406 | 0.9406 | 0.6071 | 0.6676 | 0.2413 | 0.0824 |
| 2.5 | 0.7456 | 0.7894 | 0.6183 | 0.4544 | 0.9855 | 0.9083 | 0.3803 | 0.5478 | 0.9381 |
| 5.0 | 0.4634 | 0.2309 | 0.5415 | 0.8016 | 0.8823 | 0.9830 | 0.6995 | 0.7148 | 0.9649 |
| 7.5 | 0.4212 | 0.9054 | 0.9639 | 0.9178 | 0.9998 | 0.8232 | 0.9566 | 0.5291 | 0.5876 |

Table A-23: P-values for Shapiro-Wilk (top) and Kolmogorov-Smirnov (bottom) tests for the extra expended energy with large maneuvering space.

| ρ | MVP | RS1 | RS2 | RS3 | RS4 | RS5 | RS6 | RS7 | RS8 |
|--------|--------|--------|---------------|---------------|--------|---------------|--------|---------------|--------|
| 2.5 | 0.3568 | 0.1779 | <u>0.0054</u> | <u>0.0001</u> | 0.3954 | <u>0.0412</u> | 0.1135 | <u>0.0218</u> | 0.8046 |
| 5.0 | 0.0968 | 0.7290 | 0.9022 | <u>0.0228</u> | 0.2840 | 0.2357 | 0.9042 | 0.3665 | 0.4170 |
| 7.5 | 0.5948 | 0.4729 | 0.5042 | 0.4322 | 0.1362 | 0.2214 | 0.5132 | 0.9791 | 0.1079 |
| 2.5 | 0.9466 | 0.7183 | 0.5771 | 0.2031 | 0.8980 | 0.8244 | 0.7864 | 0.3115 | 0.9748 |
| 5.0 | 0.2990 | 0.9575 | 0.9858 | 0.1154 | 0.6974 | 0.7748 | 0.9634 | 0.6330 | 0.9751 |
| 7.5 | 0.7872 | 0.5837 | 0.8476 | 0.3980 | 0.5186 | 0.3890 | 0.9873 | 0.9797 | 0.4563 |

Table A-24: P-values for Shapiro-Wilk (top) and Kolmogorov-Smirnov (bottom) tests for the extra travel time with small maneuvering space.

| ρ | MVP | RS1 | RS2 | RS3 | RS4 | RS5 | RS6 | RS7 | RS8 |
|--------|---------------|---------------|---------------|--------|--------|--------|--------|--------|--------|
| 2.5 | 0.3140 | 0.6464 | <u>0.0092</u> | 0.0625 | 0.9035 | 0.9256 | 0.2764 | 0.9614 | 0.9007 |
| 5.0 | 0.2007 | <u>0.0480</u> | <u>0.0065</u> | 0.6635 | 0.5106 | 0.8393 | 0.4087 | 0.2711 | 0.7411 |
| 7.5 | <u>0.0319</u> | 0.7882 | 0.7485 | 0.8377 | 0.9544 | 0.6346 | 0.6910 | 0.2753 | 0.0744 |
| 2.5 | 0.9642 | 0.9904 | 0.1621 | 0.7808 | 0.9989 | 0.9019 | 0.4413 | 0.8443 | 0.9776 |
| 5.0 | 0.6369 | 0.1979 | 0.5621 | 0.7465 | 0.9791 | 0.9920 | 0.8846 | 0.9024 | 0.9532 |
| 7.5 | 0.5635 | 0.8442 | 0.9712 | 0.8870 | 0.9993 | 0.8756 | 0.9586 | 0.3661 | 0.4228 |

Table A-25: P-values for Shapiro-Wilk (top) and Kolmogorov-Smirnov (bottom) tests for the extra travel time with large maneuvering space.

| ρ | MVP | RS1 | RS2 | RS3 | RS4 | RS5 | RS6 | RS7 | RS8 |
|--------|--------|--------|---------------|---------------|--------|--------|--------|--------|--------|
| 2.5 | 0.6161 | 0.1453 | <u>0.0151</u> | <u>0.0014</u> | 0.3558 | 0.2592 | 0.2605 | 0.1673 | 0.9247 |
| 5.0 | 0.3050 | 0.6566 | 0.8719 | <u>0.0193</u> | 0.3506 | 0.1737 | 0.9318 | 0.4366 | 0.5450 |
| 7.5 | 0.4839 | 0.4183 | 0.5666 | 0.4318 | 0.0912 | 0.2257 | 0.6737 | 0.9837 | 0.1140 |
| 2.5 | 0.8930 | 0.7767 | 0.5857 | 0.2805 | 0.7893 | 0.7246 | 0.6282 | 0.5983 | 0.9618 |
| 5.0 | 0.8788 | 0.8150 | 0.9957 | 0.1069 | 0.8218 | 0.8156 | 0.9923 | 0.7253 | 0.9881 |
| 7.5 | 0.7022 | 0.5681 | 0.8692 | 0.4285 | 0.3913 | 0.3857 | 0.9797 | 0.9658 | 0.4245 |

Table A-26: P-values for Shapiro-Wilk (top) and Kolmogorov-Smirnov (bottom) tests for the extra travel distance with small maneuvering space.

| ρ | MVP | RS1 | RS2 | RS3 | RS4 | RS5 | RS6 | RS7 | RS8 |
|--------|---------------|--------|---------------|---------------|--------|--------|--------|--------|--------|
| 2.5 | 0.3337 | 0.3613 | <u>0.0286</u> | <u>0.0060</u> | 0.7655 | 0.7505 | 0.1330 | 0.7200 | 0.7696 |
| 5.0 | 0.0929 | 0.0636 | <u>0.0067</u> | 0.6489 | 0.6332 | 0.9438 | 0.3306 | 0.2608 | 0.8053 |
| 7.5 | <u>0.0186</u> | 0.7953 | 0.7471 | 0.8406 | 0.9406 | 0.6071 | 0.6676 | 0.2413 | 0.0824 |
| 2.5 | 0.7456 | 0.7894 | 0.6183 | 0.4544 | 0.9855 | 0.9083 | 0.3803 | 0.5478 | 0.9381 |
| 5.0 | 0.4634 | 0.2309 | 0.5415 | 0.8016 | 0.8823 | 0.9830 | 0.6995 | 0.7148 | 0.9649 |
| 7.5 | 0.4212 | 0.9054 | 0.9639 | 0.9178 | 0.9998 | 0.8232 | 0.9566 | 0.5291 | 0.5876 |

Table A-27: P-values for Shapiro-Wilk (top) and Kolmogorov-Smirnov (bottom) tests for the extra travel distance with large maneuvering space.

| ρ | MVP | RS1 | RS2 | RS3 | RS4 | RS5 | RS6 | RS7 | RS8 |
|--------|--------|--------|---------------|---------------|--------|---------------|--------|---------------|--------|
| 2.5 | 0.3568 | 0.1779 | <u>0.0054</u> | <u>0.0001</u> | 0.3954 | <u>0.0412</u> | 0.1135 | <u>0.0218</u> | 0.8046 |
| 5.0 | 0.0968 | 0.7290 | 0.9022 | <u>0.0228</u> | 0.2840 | 0.2357 | 0.9042 | 0.3665 | 0.4170 |
| 7.5 | 0.5948 | 0.4729 | 0.5042 | 0.4322 | 0.1362 | 0.2214 | 0.5132 | 0.9791 | 0.1079 |
| 2.5 | 0.9466 | 0.7183 | 0.5771 | 0.2031 | 0.8980 | 0.8244 | 0.7864 | 0.3115 | 0.9748 |
| 5.0 | 0.2990 | 0.9575 | 0.9858 | 0.1154 | 0.6974 | 0.7748 | 0.9634 | 0.6330 | 0.9751 |
| 7.5 | 0.7872 | 0.5837 | 0.8476 | 0.3980 | 0.5186 | 0.3890 | 0.9873 | 0.9797 | 0.4563 |

Table A-28: P-values for Shapiro-Wilk (top) and Kolmogorov-Smirnov (bottom) tests for the density with small maneuvering space.

| ρ | MVP | RS1 | RS2 | RS3 | RS4 | RS5 | RS6 | RS7 | RS8 | NO CR |
|--------|--------|--------|---------------|--------|--------|--------|--------|---------------|--------|--------|
| 2.5 | 0.6053 | 0.0975 | <u>0.0350</u> | 0.5412 | 0.8501 | 0.5171 | 0.2790 | 0.8794 | 0.7341 | 0.5965 |
| 5.0 | 0.1003 | 0.2051 | 0.6547 | 0.6147 | 0.6626 | 0.6569 | 0.2850 | <u>0.0394</u> | 0.3790 | 0.9136 |
| 7.5 | 0.2657 | 0.7786 | 0.8694 | 0.4952 | 0.2660 | 0.7996 | 0.9427 | 0.7653 | 0.3435 | 0.5038 |
| 2.5 | 0.7905 | 0.9660 | 0.6216 | 0.8966 | 0.9004 | 0.8355 | 0.4364 | 0.8246 | 0.8599 | 0.9207 |
| 5.0 | 0.5971 | 0.9793 | 0.9388 | 0.9912 | 0.8092 | 0.9919 | 0.9710 | 0.4909 | 0.6360 | 0.8911 |
| 7.5 | 0.5766 | 0.9740 | 0.8826 | 0.9149 | 0.7508 | 0.9169 | 0.9708 | 0.9022 | 0.9219 | 0.9810 |

Table A-29: P-values for Shapiro-Wilk (top) and Kolmogorov-Smirnov (bottom) tests for the density with large maneuvering space.

| ρ | MVP | RS1 | RS2 | RS3 | RS4 | RS5 | RS6 | RS7 | RS8 |
|--------|--------|--------|---------------|--------|--------|--------|--------|--------|--------|
| 2.5 | 0.6527 | 0.3736 | <u>0.0053</u> | 0.4871 | 0.6440 | 0.3654 | 0.5629 | 0.6850 | 0.9752 |
| 5.0 | 0.3858 | 0.5272 | 0.1992 | 0.3382 | 0.0698 | 0.1501 | 0.2911 | 0.4646 | 0.8526 |
| 7.5 | 0.1037 | 0.3017 | 0.9931 | 0.3572 | 0.8860 | 0.2387 | 0.5256 | 0.8549 | 0.6088 |
| 2.5 | 0.9624 | 0.7714 | 0.2254 | 0.9118 | 0.6751 | 0.9618 | 0.9753 | 0.9434 | 0.9837 |
| 5.0 | 0.9340 | 0.6945 | 0.8605 | 0.8826 | 0.2044 | 0.1429 | 0.7602 | 0.8953 | 0.9574 |
| 7.5 | 0.4362 | 0.9601 | 0.9996 | 0.5828 | 0.8627 | 0.8602 | 0.8529 | 0.9421 | 0.5645 |

Table A-30: P-values for Shapiro-Wilk (top) and Kolmogorov-Smirnov (bottom) tests for the magnitude of the resolution vector with small maneuvering space.

| ρ | MVP | RS1 | RS2 | RS3 | RS4 | RS5 | RS6 | RS7 | RS8 | NO CR |
|--------|--------|--------|---------------|--------|--------|--------|--------|---------------|--------|--------|
| 2.5 | 0.6053 | 0.0975 | <u>0.0350</u> | 0.5412 | 0.8501 | 0.5171 | 0.2790 | 0.8794 | 0.7341 | 0.5965 |
| 5.0 | 0.1003 | 0.2051 | 0.6547 | 0.6147 | 0.6626 | 0.6569 | 0.2850 | <u>0.0394</u> | 0.3790 | 0.9136 |
| 7.5 | 0.2657 | 0.7786 | 0.8694 | 0.4952 | 0.2660 | 0.7996 | 0.9427 | 0.7653 | 0.3435 | 0.5038 |
| 2.5 | 0.7905 | 0.9660 | 0.6216 | 0.8966 | 0.9004 | 0.8355 | 0.4364 | 0.8246 | 0.8599 | 0.9207 |
| 5.0 | 0.5971 | 0.9793 | 0.9388 | 0.9912 | 0.8092 | 0.9919 | 0.9710 | 0.4909 | 0.6360 | 0.8911 |
| 7.5 | 0.5766 | 0.9740 | 0.8826 | 0.9149 | 0.7508 | 0.9169 | 0.9708 | 0.9022 | 0.9219 | 0.9810 |

Table A-31: P-values for Shapiro-Wilk (top) and Kolmogorov-Smirnov (bottom) tests for the magnitude of the resolution vector with large maneuvering space.

| ρ | MVP | RS1 | RS2 | RS3 | RS4 | RS5 | RS6 | RS7 | RS8 |
|--------|--------|--------|---------------|--------|--------|--------|--------|--------|--------|
| 2.5 | 0.6527 | 0.3736 | <u>0.0053</u> | 0.4871 | 0.6440 | 0.3654 | 0.5629 | 0.6850 | 0.9752 |
| 5.0 | 0.3858 | 0.5272 | 0.1992 | 0.3382 | 0.0698 | 0.1501 | 0.2911 | 0.4646 | 0.8526 |
| 7.5 | 0.1037 | 0.3017 | 0.9931 | 0.3572 | 0.8860 | 0.2387 | 0.5256 | 0.8549 | 0.6088 |
| 2.5 | 0.9624 | 0.7714 | 0.2254 | 0.9118 | 0.6751 | 0.9618 | 0.9753 | 0.9434 | 0.9837 |
| 5.0 | 0.9340 | 0.6945 | 0.8605 | 0.8826 | 0.2044 | 0.1429 | 0.7602 | 0.8953 | 0.9574 |
| 7.5 | 0.4362 | 0.9601 | 0.9996 | 0.5828 | 0.8627 | 0.8602 | 0.8529 | 0.9421 | 0.5645 |

A-7 Safety Metrics Wilcoxon Signed-Rank Test

Table A-32: Test statistic (top) and p-values (bottom) for Wilcoxon signed-rank test for number of conflicts with small maneuvering space.

| ρ | RS1 | RS2 | RS3 | RS4 | RS5 | RS6 | RS7 | RS8 |
|--------|----------------|----------------|----------------|----------------|----------------|----------------|----------------|----------------|
| 2.5 | -5.476 | -6.154 | -5.613 | -3.741 | -3.692 | -6.154 | -5.138 | -4.765 |
| 5.0 | -6.154 | -6.154 | -6.154 | -6.154 | -6.154 | -6.154 | -6.154 | -6.154 |
| 7.5 | -6.154 | -6.154 | -6.154 | -6.154 | -6.154 | -6.154 | -6.154 | -6.154 |
| 2.5 | <u>4.3e-08</u> | <u>7.5e-10</u> | <u>2.0e-08</u> | <u>0.0002</u> | <u>0.0002</u> | <u>7.5e-10</u> | <u>2.8e-07</u> | <u>1.9e-06</u> |
| 5.0 | <u>7.6e-10</u> | <u>7.6e-10</u> | <u>7.6e-10</u> | <u>7.6e-10</u> | <u>7.5e-10</u> | <u>7.6e-10</u> | <u>7.6e-10</u> | <u>7.6e-10</u> |
| 7.5 | <u>7.6e-10</u> |

Table A-33: Test statistic (top) and p-values (bottom) for Wilcoxon signed-rank test for number of conflicts with large maneuvering space.

| ρ | RS1 | RS2 | RS3 | RS4 | RS5 | RS6 | RS7 | RS8 |
|--------|----------------|----------------|----------------|----------------|----------------|----------------|----------------|----------------|
| 2.5 | -4.810 | -6.154 | -5.690 | -2.626 | -3.032 | -6.096 | -5.492 | -4.489 |
| 5.0 | -6.154 | -6.154 | -6.154 | -6.154 | -6.154 | -6.154 | -6.154 | -6.154 |
| 7.5 | -6.154 | -6.154 | -6.154 | -6.154 | -6.154 | -6.154 | -6.154 | -6.154 |
| 2.5 | <u>1.5e-06</u> | <u>7.5e-10</u> | <u>1.3e-08</u> | 0.0086 | <u>0.0024</u> | <u>1.1e-09</u> | <u>4.0e-08</u> | <u>7.1e-06</u> |
| 5.0 | <u>7.6e-10</u> |
| 7.5 | <u>7.6e-10</u> |

Table A-34: Test statistic (top) and p-values (bottom) for Wilcoxon signed-rank test for number of intrusions with small maneuvering space.

| ρ | RS1 | RS2 | RS3 | RS4 | RS5 | RS6 | RS7 | RS8 |
|--------|----------------|----------------|----------------|----------------|----------------|----------------|----------------|----------------|
| 2.5 | -4.190 | -6.093 | -3.378 | -4.814 | -5.267 | -6.154 | -4.124 | -4.975 |
| 5.0 | -5.973 | -6.154 | -6.130 | -6.154 | -6.154 | -6.154 | -6.115 | -6.154 |
| 7.5 | -6.154 | -6.154 | -6.154 | -6.154 | -6.154 | -6.154 | -6.154 | -6.154 |
| 2.5 | <u>2.2e-05</u> | <u>1.0e-09</u> | <u>0.0005</u> | <u>1.0e-06</u> | <u>1.2e-07</u> | <u>7.4e-10</u> | <u>2.9e-05</u> | <u>5.8e-07</u> |
| 5.0 | <u>2.2e-09</u> | <u>7.5e-10</u> | <u>8.4e-10</u> | <u>7.3e-10</u> | <u>7.3e-10</u> | <u>7.5e-10</u> | <u>9.3e-10</u> | <u>7.4e-10</u> |
| 7.5 | <u>7.5e-10</u> | <u>7.6e-10</u> | <u>7.5e-10</u> | <u>7.5e-10</u> | <u>7.5e-10</u> | <u>7.6e-10</u> | <u>7.5e-10</u> | <u>7.5e-10</u> |

Table A-35: Test statistic (top) and p-values (bottom) for Wilcoxon signed-rank test for number of intrusions with large maneuvering space.

| ρ | RS1 | RS2 | RS3 | RS4 | RS5 | RS6 | RS7 | RS8 |
|--------|----------------|----------------|----------------|----------------|----------------|----------------|----------------|----------------|
| 2.5 | -3.907 | -6.003 | -3.243 | -4.247 | -5.619 | -6.154 | -4.504 | -5.640 |
| 5.0 | -6.067 | -6.154 | -6.093 | -6.072 | -6.154 | -6.154 | -5.968 | -6.154 |
| 7.5 | -6.154 | -6.154 | -6.154 | -6.154 | -6.154 | -6.154 | -6.154 | -6.154 |
| 2.5 | <u>7.9e-05</u> | <u>1.8e-09</u> | <u>0.0009</u> | <u>1.7e-05</u> | <u>1.7e-08</u> | <u>7.2e-10</u> | <u>5.4e-06</u> | <u>1.4e-08</u> |
| 5.0 | <u>1.3e-09</u> | <u>7.5e-10</u> | <u>1.1e-09</u> | <u>1.2e-09</u> | <u>7.4e-10</u> | <u>7.5e-10</u> | <u>2.3e-09</u> | <u>7.4e-10</u> |
| 7.5 | <u>7.5e-10</u> | <u>7.6e-10</u> | <u>7.5e-10</u> | <u>7.5e-10</u> | <u>7.5e-10</u> | <u>7.5e-10</u> | <u>7.5e-10</u> | <u>7.5e-10</u> |

Table A-36: Test statistic (top) and p-values (bottom) for Wilcoxon signed-rank test for the IPR with small maneuvering space.

| ρ | RS1 | RS2 | RS3 | RS4 | RS5 | RS6 | RS7 | RS8 |
|--------|----------------|----------------|----------------|----------------|----------------|----------------|----------------|----------------|
| 2.5 | -3.884 | -6.144 | -2.963 | -4.774 | -5.102 | -6.154 | -3.959 | -5.008 |
| 5.0 | -5.691 | -6.154 | -5.893 | -6.154 | -6.154 | -6.154 | -5.980 | -6.154 |
| 7.5 | -6.154 | -6.154 | -6.144 | -6.154 | -6.154 | -6.154 | -6.154 | -6.154 |
| 2.5 | <u>0.0001</u> | <u>8.0e-10</u> | <u>0.0030</u> | <u>1.8e-06</u> | <u>3.4e-07</u> | <u>7.6e-10</u> | <u>7.5e-05</u> | <u>5.5e-07</u> |
| 5.0 | <u>1.3e-08</u> | <u>7.6e-10</u> | <u>3.8e-09</u> | <u>7.6e-10</u> | <u>7.6e-10</u> | <u>7.6e-10</u> | <u>2.2e-09</u> | <u>7.6e-10</u> |
| 7.5 | <u>7.6e-10</u> | <u>7.6e-10</u> | <u>8.0e-10</u> | <u>7.6e-10</u> | <u>7.6e-10</u> | <u>7.6e-10</u> | <u>7.6e-10</u> | <u>7.6e-10</u> |

Table A-37: Test statistic (top) and p-values (bottom) for Wilcoxon signed-rank test for the IPR with large maneuvering space.

| ρ | RS1 | RS2 | RS3 | RS4 | RS5 | RS6 | RS7 | RS8 |
|--------|----------------|----------------|----------------|----------------|----------------|----------------|----------------|----------------|
| 2.5 | -3.672 | -6.009 | -2.349 | -4.133 | -5.735 | -6.154 | -4.287 | -5.613 |
| 5.0 | -5.990 | -6.154 | -6.106 | -5.749 | -6.154 | -6.154 | -5.971 | -6.154 |
| 7.5 | -6.154 | -6.154 | -6.154 | -6.154 | -6.154 | -6.154 | -6.144 | -6.154 |
| 2.5 | <u>0.0002</u> | <u>1.9e-09</u> | 0.0188 | <u>3.6e-05</u> | <u>9.8e-09</u> | <u>7.6e-10</u> | <u>1.8e-05</u> | <u>2.0e-08</u> |
| 5.0 | <u>2.1e-09</u> | <u>7.6e-10</u> | <u>1.0e-09</u> | <u>9.0e-09</u> | <u>7.6e-10</u> | <u>7.6e-10</u> | <u>2.4e-09</u> | <u>7.6e-10</u> |
| 7.5 | <u>7.6e-10</u> | <u>7.6e-10</u> | <u>7.6e-10</u> | <u>7.6e-10</u> | <u>7.6e-10</u> | <u>7.6e-10</u> | <u>8.0e-10</u> | <u>7.6e-10</u> |

Table A-38: Test statistic (top) and p-values (bottom) for Wilcoxon signed-rank test for the intrusion severity with small maneuvering space.

| ρ | RS1 | RS2 | RS3 | RS4 | RS5 | RS6 | RS7 | RS8 |
|--------|--------|---------------|----------------|----------------|----------------|----------------|--------|---------------|
| 2.5 | -1.429 | -0.507 | -1.545 | -0.024 | -0.420 | -3.509 | -1.436 | -0.363 |
| 5.0 | -1.569 | -2.592 | -3.837 | -2.495 | -1.057 | -5.025 | -2.244 | -2.351 |
| 7.5 | -1.501 | -3.586 | -5.034 | -3.905 | -4.107 | -6.154 | -1.771 | -3.856 |
| 2.5 | 0.1531 | 0.6123 | 0.1223 | 0.9807 | 0.6745 | <u>0.0004</u> | 0.1510 | 0.7165 |
| 5.0 | 0.1167 | 0.0095 | <u>0.0001</u> | 0.0126 | 0.2905 | <u>5.0e-07</u> | 0.0248 | 0.0187 |
| 7.5 | 0.1333 | <u>0.0003</u> | <u>4.8e-07</u> | <u>9.4e-05</u> | <u>4.0e-05</u> | <u>7.6e-10</u> | 0.0765 | <u>0.0001</u> |

Table A-39: Test statistic (top) and p-values (bottom) for Wilcoxon signed-rank test for the intrusion severity with large maneuvering space.

| ρ | RS1 | RS2 | RS3 | RS4 | RS5 | RS6 | RS7 | RS8 |
|--------|--------|--------|----------------|--------|--------|----------------|--------|--------|
| 2.5 | -0.287 | -1.868 | -1.249 | -0.985 | -0.767 | -3.171 | -0.932 | -0.208 |
| 5.0 | -0.372 | -2.061 | -3.355 | -0.854 | -0.719 | -2.631 | -0.304 | -0.420 |
| 7.5 | -0.188 | -0.970 | -4.175 | -0.864 | -0.101 | -5.034 | -0.285 | -0.796 |
| 2.5 | 0.7740 | 0.0618 | 0.2118 | 0.3248 | 0.4428 | <u>0.0015</u> | 0.3516 | 0.8356 |
| 5.0 | 0.7102 | 0.0393 | <u>0.0008</u> | 0.3929 | 0.4720 | 0.0085 | 0.7611 | 0.6745 |
| 7.5 | 0.8507 | 0.3320 | <u>3.0e-05</u> | 0.3876 | 0.9193 | <u>4.8e-07</u> | 0.7758 | 0.4258 |

Table A-40: Test statistic (top) and p-values (bottom) for Wilcoxon signed-rank test for the time to resolve conflicts with small maneuvering space.

| ρ | RS1 | RS2 | RS3 | RS4 | RS5 | RS6 | RS7 | RS8 |
|--------|----------------|----------------|----------------|----------------|----------------|----------------|----------------|----------------|
| 2.5 | -6.154 | -6.154 | -6.154 | -6.154 | -6.154 | -6.154 | -6.154 | -6.154 |
| 5.0 | -6.154 | -6.154 | -6.154 | -6.154 | -6.154 | -6.154 | -6.154 | -6.154 |
| 7.5 | -6.154 | -6.154 | -6.154 | -6.154 | -6.154 | -6.154 | -6.154 | -6.154 |
| 2.5 | <u>7.6e-10</u> |
| 5.0 | <u>7.6e-10</u> |
| 7.5 | <u>7.6e-10</u> |

Table A-41: Test statistic (top) and p-values (bottom) for Wilcoxon signed-rank test for the time to resolve conflicts with large maneuvering space.

| ρ | RS1 | RS2 | RS3 | RS4 | RS5 | RS6 | RS7 | RS8 |
|--------|----------------|----------------|----------------|----------------|----------------|----------------|----------------|----------------|
| 2.5 | -6.154 | -6.154 | -6.154 | -6.154 | -6.154 | -6.154 | -6.154 | -6.154 |
| 5.0 | -6.154 | -6.154 | -6.154 | -6.154 | -6.154 | -6.154 | -6.154 | -6.154 |
| 7.5 | -6.154 | -6.154 | -6.154 | -6.154 | -6.154 | -6.154 | -6.154 | -6.154 |
| 2.5 | <u>7.6e-10</u> |
| 5.0 | <u>7.6e-10</u> |
| 7.5 | <u>7.6e-10</u> |

Table A-42: Test statistic (top) and p-values (bottom) for Wilcoxon signed-rank test for the time to resolve intrusions with small maneuvering space.

| ρ | RS1 | RS2 | RS3 | RS4 | RS5 | RS6 | RS7 | RS8 |
|--------|---------------|---------------|---------------|--------|----------------|----------------|---------------|----------------|
| 2.5 | -0.595 | -2.061 | -2.148 | -2.188 | -4.339 | -4.643 | -0.076 | -4.347 |
| 5.0 | -1.038 | -3.046 | -3.007 | -2.650 | -4.979 | -5.498 | -1.752 | -5.333 |
| 7.5 | -2.949 | -1.926 | -0.874 | -0.632 | -2.959 | -5.613 | -3.046 | -2.505 |
| 2.5 | 0.5515 | 0.0393 | 0.0317 | 0.0286 | <u>1.4e-05</u> | <u>3.4e-06</u> | 0.9390 | <u>1.4e-05</u> |
| 5.0 | 0.2994 | <i>0.0023</i> | <i>0.0026</i> | 0.0081 | <u>6.4e-07</u> | <u>3.9e-08</u> | 0.0798 | <u>9.6e-08</u> |
| 7.5 | <i>0.0032</i> | 0.0541 | 0.3823 | 0.5272 | <i>0.0031</i> | <u>2.0e-08</u> | <i>0.0023</i> | 0.0122 |

Table A-43: Test statistic (top) and p-values (bottom) for Wilcoxon signed-rank test for the time to resolve intrusions with large maneuvering space.

| ρ | RS1 | RS2 | RS3 | RS4 | RS5 | RS6 | RS7 | RS8 |
|--------|--------|---------------|--------|--------|----------------|----------------|---------------|----------------|
| 2.5 | -0.969 | -3.528 | -2.243 | -2.774 | -4.148 | -4.136 | -1.900 | -3.953 |
| 5.0 | -1.221 | -2.650 | -1.405 | -0.874 | -4.011 | -3.577 | -0.893 | -3.914 |
| 7.5 | -2.853 | -2.466 | -0.681 | -1.501 | -3.605 | -4.928 | -2.978 | -3.615 |
| 2.5 | 0.3324 | <u>0.0004</u> | 0.0248 | 0.0055 | <u>3.4e-05</u> | <u>3.5e-05</u> | 0.0574 | <u>7.7e-05</u> |
| 5.0 | 0.2220 | 0.0081 | 0.1602 | 0.3823 | <u>6.0e-05</u> | <u>0.0003</u> | 0.3719 | <u>9.1e-05</u> |
| 7.5 | 0.0043 | 0.0136 | 0.4962 | 0.1333 | <u>0.0003</u> | <u>8.3e-07</u> | <i>0.0029</i> | <u>0.0003</u> |

Table A-44: Test statistic (top) and p-values (bottom) for Wilcoxon signed-rank test for the time spent in conflict with small maneuvering space.

| ρ | RS1 | RS2 | RS3 | RS4 | RS5 | RS6 | RS7 | RS8 |
|--------|----------------|----------------|----------------|----------------|----------------|----------------|----------------|----------------|
| 2.5 | -6.154 | -6.154 | -6.154 | -6.154 | -6.154 | -6.154 | -6.154 | -6.154 |
| 5.0 | -6.154 | -6.154 | -6.154 | -6.154 | -6.154 | -6.154 | -6.154 | -6.154 |
| 7.5 | -6.154 | -6.154 | -6.154 | -6.154 | -6.154 | -6.154 | -6.154 | -6.154 |
| 2.5 | <u>7.6e-10</u> |
| 5.0 | <u>7.6e-10</u> |
| 7.5 | <u>7.6e-10</u> |

Table A-45: Test statistic (top) and p-values (bottom) for Wilcoxon signed-rank test for the time spent in conflict with large maneuvering space.

| ρ | RS1 | RS2 | RS3 | RS4 | RS5 | RS6 | RS7 | RS8 |
|--------|----------------|----------------|----------------|----------------|----------------|----------------|----------------|----------------|
| 2.5 | -6.154 | -6.154 | -6.154 | -6.154 | -6.154 | -6.154 | -6.154 | -6.154 |
| 5.0 | -6.154 | -6.154 | -6.154 | -6.154 | -6.154 | -6.154 | -6.154 | -6.154 |
| 7.5 | -6.154 | -6.154 | -6.154 | -6.154 | -6.154 | -6.154 | -6.154 | -6.154 |
| 2.5 | <u>7.6e-10</u> |
| 5.0 | <u>7.6e-10</u> |
| 7.5 | <u>7.6e-10</u> |

Table A-46: Test statistic (top) and p-values (bottom) for Wilcoxon signed-rank test for the time spent in LoS with small maneuvering space.

| ρ | RS1 | RS2 | RS3 | RS4 | RS5 | RS6 | RS7 | RS8 |
|--------|----------------|----------------|----------------|----------------|----------------|----------------|----------------|----------------|
| 2.5 | -2.486 | -6.096 | -4.042 | -4.477 | -5.575 | -6.154 | -2.407 | -5.471 |
| 5.0 | -5.594 | -6.154 | -5.990 | -6.125 | -6.154 | -6.154 | -5.517 | -6.154 |
| 7.5 | -6.125 | -6.154 | -6.154 | -6.154 | -6.154 | -6.154 | -6.125 | -6.154 |
| 2.5 | 0.0129 | <u>1.1e-09</u> | <u>5.3e-05</u> | <u>7.6e-06</u> | <u>2.5e-08</u> | <u>7.6e-10</u> | 0.0161 | <u>4.5e-08</u> |
| 5.0 | <u>2.2e-08</u> | <u>7.6e-10</u> | <u>2.1e-09</u> | <u>9.1e-10</u> | <u>7.6e-10</u> | <u>7.6e-10</u> | <u>3.5e-08</u> | <u>7.6e-10</u> |
| 7.5 | <u>9.1e-10</u> | <u>7.6e-10</u> | <u>7.6e-10</u> | <u>7.6e-10</u> | <u>7.6e-10</u> | <u>7.6e-10</u> | <u>9.1e-10</u> | <u>7.6e-10</u> |

Table A-47: Test statistic (top) and p-values (bottom) for Wilcoxon signed-rank test for the time spent in LoS with large maneuvering space.

| ρ | RS1 | RS2 | RS3 | RS4 | RS5 | RS6 | RS7 | RS8 |
|--------|----------------|----------------|----------------|----------------|----------------|----------------|----------------|----------------|
| 2.5 | -3.056 | -5.951 | -3.810 | -4.482 | -5.715 | -6.154 | -3.919 | -5.551 |
| 5.0 | -5.710 | -6.154 | -5.932 | -5.797 | -6.154 | -6.154 | -5.834 | -6.154 |
| 7.5 | -5.864 | -6.154 | -6.154 | -6.125 | -6.154 | -6.154 | -5.864 | -6.154 |
| 2.5 | <u>0.0022</u> | <u>2.7e-09</u> | <u>0.0001</u> | <u>7.4e-06</u> | <u>1.1e-08</u> | <u>7.6e-10</u> | <u>8.9e-05</u> | <u>2.8e-08</u> |
| 5.0 | <u>1.1e-08</u> | <u>7.6e-10</u> | <u>3.0e-09</u> | <u>6.8e-09</u> | <u>7.6e-10</u> | <u>7.6e-10</u> | <u>5.4e-09</u> | <u>7.6e-10</u> |
| 7.5 | <u>4.5e-09</u> | <u>7.6e-10</u> | <u>7.6e-10</u> | <u>9.1e-10</u> | <u>7.6e-10</u> | <u>7.6e-10</u> | <u>4.5e-09</u> | <u>7.6e-10</u> |

A-8 Stability Metrics Wilcoxon Signed-Rank Test

Table A-48: Test statistic (top) and p-values (bottom) for Wilcoxon signed-rank test for the DEP with small maneuvering space.

| ρ | RS1 | RS2 | RS3 | RS4 | RS5 | RS6 | RS7 | RS8 |
|--------|----------------|----------------|----------------|----------------|----------------|----------------|----------------|----------------|
| 2.5 | -5.471 | -6.154 | -5.609 | -3.779 | -3.656 | -6.154 | -5.143 | -4.720 |
| 5.0 | -6.154 | -6.154 | -6.154 | -6.154 | -6.154 | -6.154 | -6.154 | -6.154 |
| 7.5 | -6.154 | -6.154 | -6.154 | -6.154 | -6.154 | -6.154 | -6.154 | -6.154 |
| 2.5 | <u>4.5e-08</u> | <u>7.6e-10</u> | <u>2.0e-08</u> | <u>0.0002</u> | <u>0.0003</u> | <u>7.5e-10</u> | <u>2.7e-07</u> | <u>2.4e-06</u> |
| 5.0 | <u>7.6e-10</u> | <u>7.5e-10</u> |
| 7.5 | <u>7.6e-10</u> |

Table A-49: Test statistic (top) and p-values (bottom) for Wilcoxon signed-rank test for the DEP with large maneuvering space.

| ρ | RS1 | RS2 | RS3 | RS4 | RS5 | RS6 | RS7 | RS8 |
|--------|----------------|----------------|----------------|----------------|----------------|----------------|----------------|----------------|
| 2.5 | -4.872 | -6.154 | -5.685 | -2.600 | -3.016 | -6.096 | -5.497 | -4.436 |
| 5.0 | -6.154 | -6.154 | -6.154 | -6.154 | -6.154 | -6.154 | -6.154 | -6.154 |
| 7.5 | -6.154 | -6.154 | -6.154 | -6.154 | -6.154 | -6.154 | -6.154 | -6.154 |
| 2.5 | <u>1.1e-06</u> | <u>7.5e-10</u> | <u>1.3e-08</u> | <u>0.0093</u> | <u>0.0026</u> | <u>1.1e-09</u> | <u>3.8e-08</u> | <u>9.2e-06</u> |
| 5.0 | <u>7.6e-10</u> |
| 7.5 | <u>7.6e-10</u> |

Table A-50: Test statistic (top) and p-values (bottom) for Wilcoxon signed-rank test for the multi-aircraft conflicts with small maneuvering space.

| ρ | RS1 | RS2 | RS3 | RS4 | RS5 | RS6 | RS7 | RS8 |
|--------|----------------|----------------|----------------|----------------|----------------|----------------|----------------|----------------|
| 2.5 | -6.144 | -4.532 | -6.154 | -6.139 | -6.019 | -3.845 | -6.154 | -4.870 |
| 5.0 | -6.154 | -5.068 | -6.135 | -4.083 | -1.687 | -3.866 | -6.154 | -4.067 |
| 7.5 | -3.084 | -6.154 | -4.894 | -6.144 | -6.154 | -6.154 | -4.148 | -6.154 |
| 2.5 | <u>8.0e-10</u> | <u>5.8e-06</u> | <u>7.5e-10</u> | <u>8.3e-10</u> | <u>1.7e-09</u> | <u>0.0001</u> | <u>7.5e-10</u> | <u>1.1e-06</u> |
| 5.0 | <u>7.6e-10</u> | <u>4.0e-07</u> | <u>8.5e-10</u> | <u>4.4e-05</u> | 0.0915 | <u>0.0001</u> | <u>7.5e-10</u> | <u>4.8e-05</u> |
| 7.5 | <u>0.0020</u> | <u>7.6e-10</u> | <u>9.9e-07</u> | <u>8.0e-10</u> | <u>7.6e-10</u> | <u>7.6e-10</u> | <u>3.3e-05</u> | <u>7.6e-10</u> |

Table A-51: Test statistic (top) and p-values (bottom) for Wilcoxon signed-rank test for the multi-aircraft conflicts with large maneuvering space.

| ρ | RS1 | RS2 | RS3 | RS4 | RS5 | RS6 | RS7 | RS8 |
|--------|----------------|----------------|----------------|----------------|----------------|----------------|----------------|----------------|
| 2.5 | -6.139 | -4.677 | -6.154 | -4.824 | -3.942 | -4.984 | -6.154 | -2.737 |
| 5.0 | -6.154 | -3.277 | -6.154 | -2.631 | -5.262 | -1.154 | -6.154 | -5.415 |
| 7.5 | -2.433 | -6.154 | -4.329 | -6.154 | -6.154 | -6.154 | -4.402 | -6.154 |
| 2.5 | <u>8.2e-10</u> | <u>2.9e-06</u> | <u>7.5e-10</u> | <u>1.4e-06</u> | <u>8.0e-05</u> | <u>6.2e-07</u> | <u>7.5e-10</u> | 0.0062 |
| 5.0 | <u>7.6e-10</u> | <u>0.0010</u> | <u>7.5e-10</u> | 0.0085 | <u>1.4e-07</u> | 0.2485 | <u>7.5e-10</u> | <u>6.1e-08</u> |
| 7.5 | 0.0150 | <u>7.6e-10</u> | <u>1.5e-05</u> | <u>7.6e-10</u> | <u>7.6e-10</u> | <u>7.6e-10</u> | <u>1.1e-05</u> | <u>7.5e-10</u> |

A-9 Efficiency Metrics Wilcoxon Signed-Rank Test

Table A-52: Test statistic (top) and p-values (bottom) for Wilcoxon signed-rank test for the extra expended energy with small maneuvering space.

| ρ | RS1 | RS2 | RS3 | RS4 | RS5 | RS6 | RS7 | RS8 |
|--------|----------------|----------------|----------------|----------------|----------------|----------------|----------------|----------------|
| 2.5 | -6.154 | -6.154 | -6.154 | -6.154 | -6.154 | -6.154 | -6.154 | -6.144 |
| 5.0 | -6.154 | -6.154 | -6.154 | -6.154 | -6.154 | -6.154 | -6.154 | -6.154 |
| 7.5 | -6.154 | -6.154 | -6.154 | -6.154 | -6.154 | -6.154 | -6.154 | -6.154 |
| 2.5 | <u>7.6e-10</u> | <u>8.0e-10</u> |
| 5.0 | <u>7.6e-10</u> |
| 7.5 | <u>7.6e-10</u> |

Table A-53: Test statistic (top) and p-values (bottom) for Wilcoxon signed-rank test for the extra expended energy with large maneuvering space.

| ρ | RS1 | RS2 | RS3 | RS4 | RS5 | RS6 | RS7 | RS8 |
|--------|----------------|----------------|----------------|----------------|----------------|----------------|----------------|----------------|
| 2.5 | -6.154 | -6.154 | -6.154 | -6.154 | -6.154 | -6.154 | -6.154 | -6.154 |
| 5.0 | -6.154 | -6.154 | -6.154 | -6.154 | -6.154 | -6.154 | -6.154 | -6.154 |
| 7.5 | -6.154 | -6.154 | -6.154 | -6.154 | -6.154 | -6.154 | -6.154 | -6.154 |
| 2.5 | <u>7.6e-10</u> |
| 5.0 | <u>7.6e-10</u> |
| 7.5 | <u>7.6e-10</u> |

Table A-54: Test statistic (top) and p-values (bottom) for Wilcoxon signed-rank test for the extra travel time with small maneuvering space.

| ρ | RS1 | RS2 | RS3 | RS4 | RS5 | RS6 | RS7 | RS8 |
|--------|----------------|----------------|----------------|----------------|----------------|----------------|----------------|----------------|
| 2.5 | -6.154 | -6.154 | -6.154 | -6.154 | -6.154 | -6.154 | -6.154 | -6.144 |
| 5.0 | -6.154 | -6.154 | -6.154 | -6.154 | -6.154 | -6.154 | -6.154 | -6.154 |
| 7.5 | -6.154 | -6.154 | -6.154 | -6.154 | -6.154 | -6.154 | -6.154 | -6.154 |
| 2.5 | <u>7.6e-10</u> | <u>8.0e-10</u> |
| 5.0 | <u>7.6e-10</u> |
| 7.5 | <u>7.6e-10</u> |

Table A-55: Test statistic (top) and p-values (bottom) for Wilcoxon signed-rank test for the extra travel time with large maneuvering space.

| ρ | RS1 | RS2 | RS3 | RS4 | RS5 | RS6 | RS7 | RS8 |
|--------|----------------|----------------|----------------|----------------|----------------|----------------|----------------|----------------|
| 2.5 | -6.154 | -6.154 | -6.154 | -6.154 | -6.154 | -6.154 | -6.154 | -6.154 |
| 5.0 | -6.154 | -6.154 | -6.154 | -6.154 | -6.154 | -6.154 | -6.154 | -6.154 |
| 7.5 | -6.154 | -6.154 | -6.154 | -6.154 | -6.154 | -6.154 | -6.154 | -6.154 |
| 2.5 | <u>7.6e-10</u> |
| 5.0 | <u>7.6e-10</u> |
| 7.5 | <u>7.6e-10</u> |

Table A-56: Test statistic (top) and p-values (bottom) for Wilcoxon signed-rank test for the extra travel distance with small maneuvering space.

| ρ | RS1 | RS2 | RS3 | RS4 | RS5 | RS6 | RS7 | RS8 |
|--------|----------------|----------------|----------------|----------------|----------------|----------------|----------------|----------------|
| 2.5 | -6.154 | -6.154 | -6.154 | -6.154 | -6.154 | -6.154 | -6.154 | -6.144 |
| 5.0 | -6.154 | -6.154 | -6.154 | -6.154 | -6.154 | -6.154 | -6.154 | -6.154 |
| 7.5 | -6.154 | -6.154 | -6.154 | -6.154 | -6.154 | -6.154 | -6.154 | -6.154 |
| 2.5 | <u>7.6e-10</u> | <u>8.0e-10</u> |
| 5.0 | <u>7.6e-10</u> |
| 7.5 | <u>7.6e-10</u> |

Table A-57: Test statistic (top) and p-values (bottom) for Wilcoxon signed-rank test for the extra travel distance with large maneuvering space.

| ρ | RS1 | RS2 | RS3 | RS4 | RS5 | RS6 | RS7 | RS8 |
|--------|----------------|----------------|----------------|----------------|----------------|----------------|----------------|----------------|
| 2.5 | -6.154 | -6.154 | -6.154 | -6.154 | -6.154 | -6.154 | -6.154 | -6.154 |
| 5.0 | -6.154 | -6.154 | -6.154 | -6.154 | -6.154 | -6.154 | -6.154 | -6.154 |
| 7.5 | -6.154 | -6.154 | -6.154 | -6.154 | -6.154 | -6.154 | -6.154 | -6.154 |
| 2.5 | <u>7.6e-10</u> |
| 5.0 | <u>7.6e-10</u> |
| 7.5 | <u>7.6e-10</u> |

Table A-58: Test statistic (top) and p-values (bottom) for Wilcoxon signed-rank test for the density with small maneuvering space.

| ρ | RS1 | RS2 | RS3 | RS4 | RS5 | RS6 | RS7 | RS8 |
|--------|----------------|----------------|----------------|----------------|----------------|----------------|----------------|----------------|
| 2.5 | -6.154 | -6.154 | -6.154 | -6.154 | -6.154 | -6.154 | -6.154 | -6.135 |
| 5.0 | -6.154 | -6.154 | -6.154 | -6.154 | -6.154 | -6.154 | -6.154 | -6.154 |
| 7.5 | -6.154 | -6.154 | -6.154 | -6.154 | -6.154 | -6.154 | -6.154 | -6.154 |
| 2.5 | <u>7.6e-10</u> | <u>8.5e-10</u> |
| 5.0 | <u>7.6e-10</u> |
| 7.5 | <u>7.6e-10</u> |

Table A-59: Test statistic (top) and p-values (bottom) for Wilcoxon signed-rank test for the density with large maneuvering space.

| ρ | RS1 | RS2 | RS3 | RS4 | RS5 | RS6 | RS7 | RS8 |
|--------|----------------|----------------|----------------|----------------|----------------|----------------|----------------|----------------|
| 2.5 | -6.154 | -6.086 | -6.144 | -4.088 | -2.457 | -6.154 | -6.154 | -1.530 |
| 5.0 | -6.154 | -3.345 | -3.750 | -6.154 | -6.154 | -6.154 | -6.154 | -6.154 |
| 7.5 | -6.154 | -6.154 | -6.154 | -6.154 | -6.154 | -6.154 | -6.154 | -6.154 |
| 2.5 | <u>7.6e-10</u> | <u>1.2e-09</u> | <u>8.0e-10</u> | <u>4.3e-05</u> | 0.0140 | <u>7.6e-10</u> | <u>7.6e-10</u> | 0.1260 |
| 5.0 | <u>7.6e-10</u> | <u>0.0008</u> | <u>0.0002</u> | <u>7.6e-10</u> | <u>7.6e-10</u> | <u>7.6e-10</u> | <u>7.6e-10</u> | <u>7.6e-10</u> |
| 7.5 | <u>7.6e-10</u> |

Table A-60: Test statistic (top) and p-values (bottom) for Wilcoxon signed-rank test for the magnitude of the resolution vector with small maneuvering space.

| ρ | RS1 | RS2 | RS3 | RS4 | RS5 | RS6 | RS7 | RS8 |
|--------|----------------|----------------|----------------|----------------|----------------|----------------|----------------|----------------|
| 2.5 | -6.154 | -6.154 | -6.154 | -6.154 | -6.154 | -6.154 | -6.154 | -6.135 |
| 5.0 | -6.154 | -6.154 | -6.154 | -6.154 | -6.154 | -6.154 | -6.154 | -6.154 |
| 7.5 | -6.154 | -6.154 | -6.154 | -6.154 | -6.154 | -6.154 | -6.154 | -6.154 |
| 2.5 | <u>7.6e-10</u> | <u>8.5e-10</u> |
| 5.0 | <u>7.6e-10</u> |
| 7.5 | <u>7.6e-10</u> |

Table A-61: Test statistic (top) and p-values (bottom) for Wilcoxon signed-rank test for the magnitude of the resolution vector with large maneuvering space.

| ρ | RS1 | RS2 | RS3 | RS4 | RS5 | RS6 | RS7 | RS8 |
|--------|----------------|----------------|----------------|----------------|----------------|----------------|----------------|----------------|
| 2.5 | -6.154 | -6.086 | -6.144 | -4.088 | -2.457 | -6.154 | -6.154 | -1.530 |
| 5.0 | -6.154 | -3.345 | -3.750 | -6.154 | -6.154 | -6.154 | -6.154 | -6.154 |
| 7.5 | -6.154 | -6.154 | -6.154 | -6.154 | -6.154 | -6.154 | -6.154 | -6.154 |
| 2.5 | <u>7.6e-10</u> | <u>1.2e-09</u> | <u>8.0e-10</u> | <u>4.3e-05</u> | 0.0140 | <u>7.6e-10</u> | <u>7.6e-10</u> | 0.1260 |
| 5.0 | <u>7.6e-10</u> | <u>0.0008</u> | <u>0.0002</u> | <u>7.6e-10</u> | <u>7.6e-10</u> | <u>7.6e-10</u> | <u>7.6e-10</u> | <u>7.6e-10</u> |
| 7.5 | <u>7.6e-10</u> |

Appendix B

Unit Tests of the SSD in BlueSky

This appendix serves as a verification of the implementation of the Solution Space Diagram (SSD) in BlueSky. The traffic situation used for the verification is identical to the traffic situation illustrated in Figure 4 of the scientific paper in Part I. The SSD for this traffic situation is illustrated in Figures B-1 and B-2. Figure B-1 depicts the basic coordination rulesets and has a larger velocity vector than Figure B-2, which depicts the coordination rulesets that incorporate priority. Figures B-3 to B-12 show that the SSD and its rulesets are correctly implemented in BlueSky.

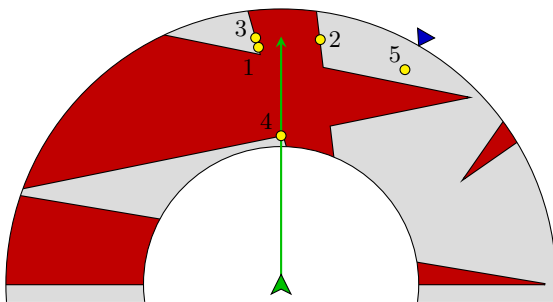


Figure B-1: Resolution points for basic coordination rulesets.

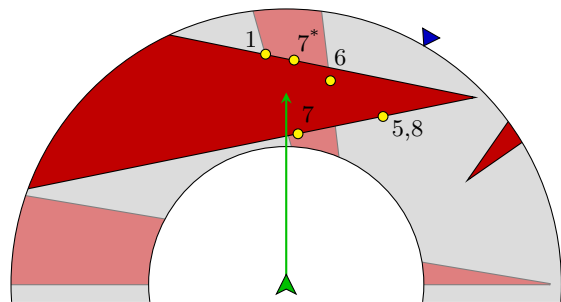


Figure B-2: Resolution points for coordination rulesets incorporating priority rules

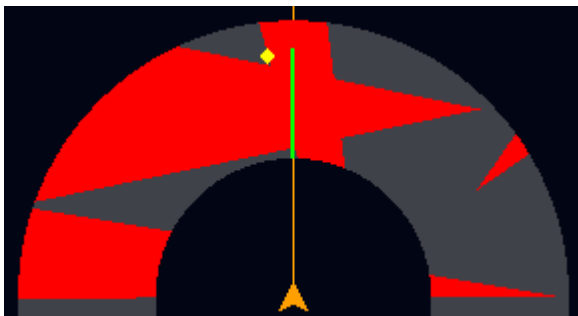


Figure B-3: Resolution point for OPT or RS1 corresponding to Figure B-1.

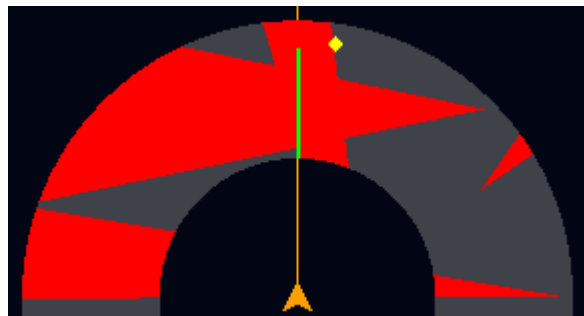


Figure B-4: Resolution point for RIGHT or RS2 corresponding to Figure B-1.

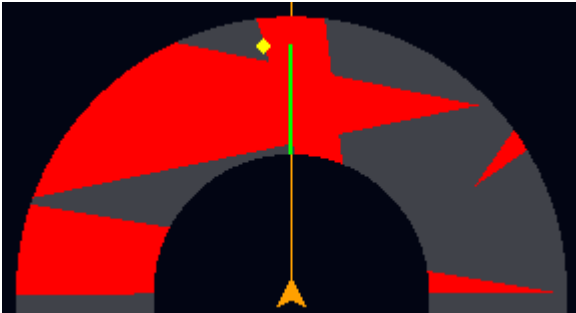


Figure B-5: Resolution point for HDG or RS3 corresponding to Figure B-1.

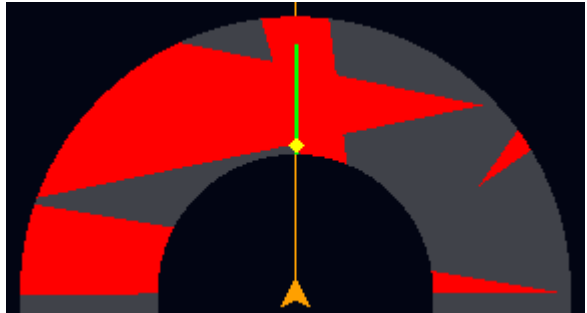


Figure B-6: Resolution point for SPD or RS4 corresponding to Figure B-1.

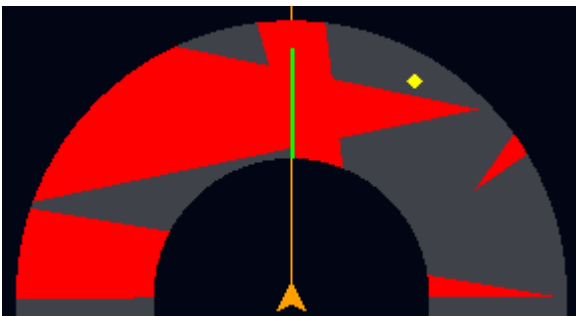


Figure B-7: Resolution point for DEST or RS5 corresponding to Figure B-1.

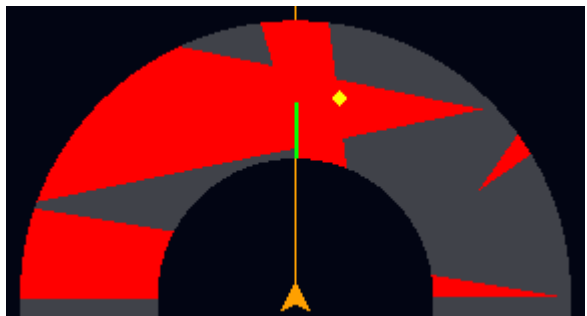


Figure B-8: Resolution point for ROTA or RS6 corresponding to Figure B-2.

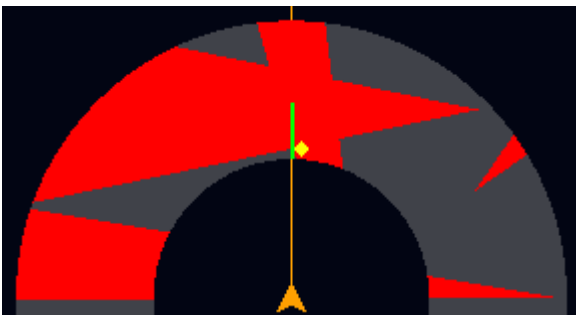


Figure B-9: Resolution point for OPT+ or RS7 corresponding to Figure B-2.

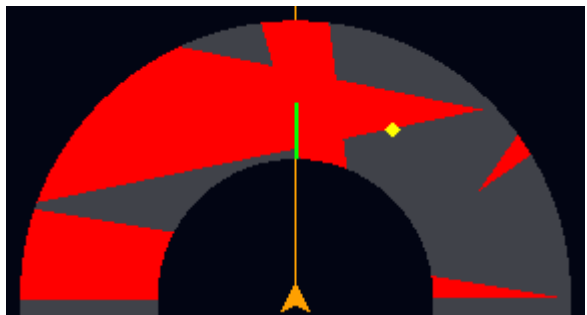


Figure B-10: Resolution point for DEST+ or RS8 corresponding to Figure B-2.

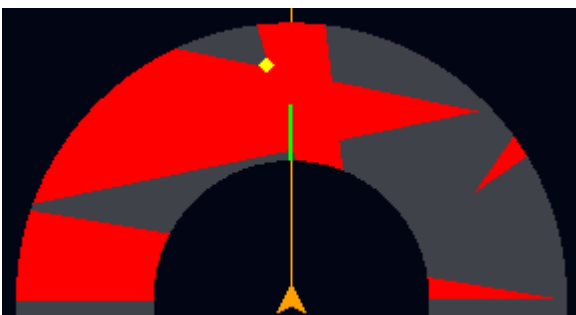


Figure B-11: Resolution point for OPT or RS1 corresponding to Figure B-2.

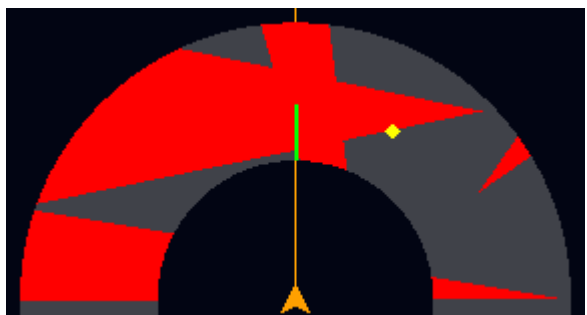


Figure B-12: Resolution point for DEST or RS5 corresponding to Figure B-2.

Part III

Preliminary Report [already graded]

Chapter 1

Introduction

Air travel has grown tremendously in the last decades as a result of technological advancements and further globalization. With parts of the world, such as Asia and the Middle East, also widely adopting flying as means of travel, the airspace is reaching its maximum in terms of capacity [1]. The emergence of Unmanned Aerial Vehicles (UAVs) and the recovering growth of the economy after the economic crisis further aggravate this limited capacity [2,3]. To facilitate the unceasing growth of air traffic in the crowded airspace, new Air Traffic Management (ATM) concepts are continuously being developed. This is in line with the goals of the Single European Sky ATM Research (SESAR) concept [4]. This concept and similarly ambitious initiatives, such as the Free Flight concept proposed in 1995, delegate the responsibility of separation between aircraft from the Air Traffic Controller (ATCo) on the ground towards the crew in the air [5,6]. In essence, this implies that the current centralized approach will be replaced by a decentralized approach. Within this delegation of responsibility towards airborne self-separation, insufficiently solved problems are the interactions between three or more aircraft, each having different targets and capabilities.

An important interaction that is subject of a lot of research within ATM are aircraft conflicts. By propagating state information, such as speed, direction and altitude, an aircraft is said to be in conflict when a Loss of Separation (LoS) is expected in the future. Automatic Dependent Surveillance - Broadcast (ADS-B) is the used technology that allows for the derivation of the required state information. In general, these aircraft conflicts are dealt with in three main components: Conflict Detection (CD), Conflict Prevention (CP) and Conflict Resolution (CR) [7]. Research on these conflicts treats one or more of the aforementioned components. As the title already suggests, a method for CR is proposed in this MSc thesis.

In the context of conflicts and airborne separation in ATM a lot of research has already been conducted. The research scope can vary greatly, which is the reason that this thesis will focus on earlier work that has been conducted at Delft University of Technology (TU Delft). The goal is to improve the use of the SSD or the set of Velocity Obstacles (VOs) in the airborne self-separation task and investigate its performance in conflicts involving three or more aircraft. Note that the SSD and the set of VOs can be used interchangeably in the context of this thesis. However, these two concepts are not exactly the same and their key

difference is visualized in Figures 1-1b and 1-1c. The SSD also accounts for the performance limits of the aircraft, which means it consists of a ring-shaped subset of the union set of VOs.

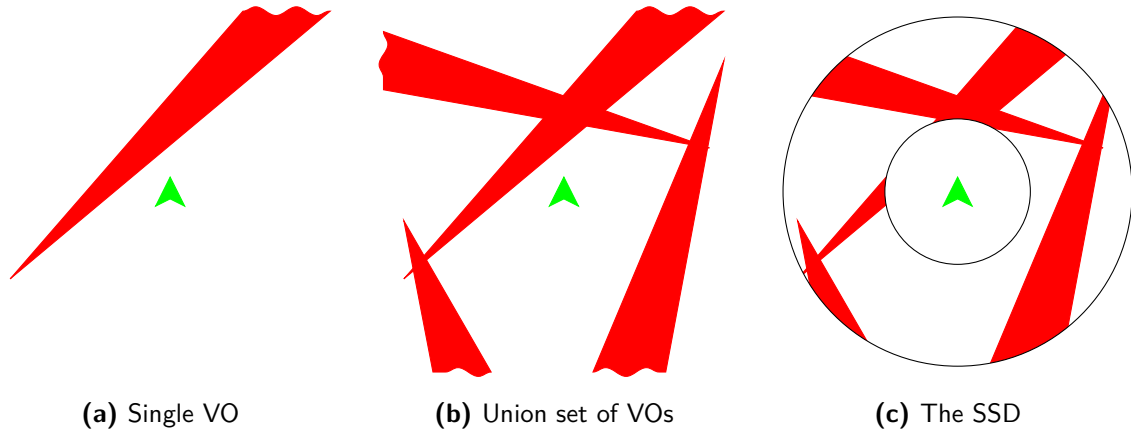


Figure 1-1: Differences in the set of VOs and the SSD

The usage of VOs, that originate from robotics [8], is certainly not new. For example, the principles of a VO are used by the Modified Voltage Potential (MVP), a method that has components of CD, CP and CR [9]. A VO is defined in the velocity space of an aircraft and represents another aircraft in the vicinity. When the velocity vector of the aircraft lies inside the VO, it is said to be in conflict. This can be observed in Figure 1-1a as the red cone-shaped area. Velocity vectors inside the white area are therefore conflict-free. The advantage of this obstacle approach is that VOs can be joined to visualize the complete conflict situation surrounding an aircraft. An obvious application would be for pilots to see the visualization of the SSD, or the combined set of VOs including the performance limits, on their navigational display and choose a resolution point [10, 11]. However, this research focuses on the use of a numerical representation of the SSD in combination with a set of coordination rules to propose a promising automated resolution method comprising both CP and CR.

In the following sections of this introductory chapter the MSc thesis assignment is defined, demarcated and structured within the ongoing research in ATM, such that it is manageable for a MSc graduate research project.

1-1 Thesis Objective and Research Questions

As stated before a part of the research on separation in ATM must be isolated, such that it can be used as a feasible objective of research for this MSc thesis. Therefore, the research objective is defined as follows:

The research objective is to further develop previous work on the SSD for use as a conflict resolution method, dealing with the issues that arise when more than two aircraft are involved in a conflict at the same time by analyzing, categorizing and solving coordination issues in a simulation study.

The research objective is divided into six activities, or sub-goals, with associated research questions. Performing these activities and answering these questions will ensure that the

research objective will be attained at the end of the research. The sub-goals are stated in the remainder of this section. It has already been chosen that any simulation will be performed with the help of BlueSky, an Air Traffic Control (ATC) simulator project mainly developed by students and staff of TU Delft [12]. BlueSky is a well-functioning, easy-to-use, open-source simulator, which allows for more efficiency in setting up simulations.

Research Activity 1

Further develop the implementation of the SSD in BlueSky, making it suitable for use as a CR-method.

Before the start of the thesis the SSD has not been used in CR-algorithms [10, 13–15]. For example, it is only implemented as a graphical overlay in BlueSky. Serving purely as a visualization of the conflict situation for individual aircraft, the overlay cannot be used in CR-algorithms. In the overlay each VO, which can be seen as a triangular polygon, is printed on screen, which results visually in the correct SSD. For purposes in CR-methods, a numerical representation is needed that can be used for calculations. Therefore, all the VOs must be merged into one polygon in an efficient manner. The accompanying research question is therefore phrased:

- (a) *How must the SSD be implemented numerically in BlueSky for CR-purposes?*

Research Activity 2

Develop promising coordination rulesets that can be used in combination with the SSD.

CR using the SSD is considered to be a resolution method. Within this method different resolution algorithms or coordination rulesets can be employed. The two terms are used interchangeably in this thesis, since they both represent the same sequence of actions according to a predefined set of rules to resolve a conflict. The difference can be seen in the way of representing. The coordination ruleset is less mathematical and can be depicted with a simple flowchart. The resolution algorithm is a broader concept that entails the coordination ruleset, but also includes more mathematical representations such as pseudocode. Developing at least one set of rules that uses the SSD to resolve conflicts is the purpose of this sub-goal. For each set of rules the following question can be asked:

- (a) *Do conflict geometries exist that are inherently not resolvable by the developed ruleset?*
(b) *In case the geometries of (a) exist, what characterizes them?*

Research Activity 3

Define small-scale conflict scenarios involving three or more aircraft.

Conflicts between two aircraft have already been subject of many studies, which is one of the reasons it is interesting to research conflicts involving three or more aircraft, of which some can be referred to as multi-aircraft conflicts. In this sub-goal different types of conflict scenarios or conflict geometries are categorized, which will be used as a starting point for the simulations. Small-scale conflict scenarios and conflict geometries can be used interchangeably and represent at maximum ten aircraft. Since it is challenging to define all relevant scenarios, some simulations will have to be run first. This effectively creates an interaction between this and the next activity. Research questions related to this sub-goal are:

- (a) *What properties can characterize a conflict scenario?*
- (b) *How can a conflict scenario be represented?*

Research Activity 4

Simulate the defined conflict scenarios using the developed coordination rulesets.

The conflict scenarios defined in Research Activity 3 will be resolved by simulation using the coordination rulesets developed in Research Activity 2. By evaluating these simulations, more interesting conflict scenarios can be defined, indeed showing the interaction between this and the previous activity. Interesting conflict scenarios in this case are scenarios that show the strengths or weaknesses of the coordination rulesets. The strengths or weaknesses follow from evaluating the simulations, which explains the research question:

- (a) *On what basis can the performance of a resolution method in a small-scale conflict scenario be evaluated?*

Research Activity 5

Develop an improved coordination ruleset.

The developed coordination rulesets in Research Activity 2 can very likely be improved using the knowledge gained from Research Activities 3 and 4. This can be done by altering or possibly adding coordination rules such as priority rules.

Research Activity 6

Evaluate the performance of the improved coordination ruleset and compare it with the performance of MVP in large-scale scenarios.

Evaluating the performance of the new CR-method is also essential. It is decided that its performance will be compared with an already existing force field CR-method in BlueSky, the MVP. Similar to the previous simulations, for this comparison it should be known on what characteristics or parameters the CR-methods will be evaluated after simulating the large-scale scenarios. This activity will consider high density large-scale airspaces, contrary to the previous simulations, where small-scale conflict scenarios with at maximum ten aircraft were considered. This will probably require other metrics, which explains the last questions:

- (a) *On what basis can the performance of a resolution method in a large-scale conflict scenario be evaluated?*
- (b) *What are the strengths and weaknesses of the SSD-based method compared with the MVP?*

Briefly summarizing the research activities, first the SSD is implemented in BlueSky. This is followed by the development of coordination rulesets that use the SSD. Subsequently, conflict scenarios with limited numbers of aircraft are categorized which will serve as starting points for the simulations in the next step. This will lead to more interesting conflict scenarios, creating an iterative process of defining conflict scenarios and simulations. This is followed by the development of an improved coordination ruleset, which is essentially the new CR-method. Lastly, the performance of the new CR-method is evaluated and compared with the already existing MVP in high density airspaces.

1-2 Research Approach

As explained in the previous section the research objective will be met when the research activities are performed and the research questions are answered adequately. In this section the necessary sequence of steps during the thesis will be explained.

Reiterating what was presented before, the research is divided into six activities, each accompanied by one or more research questions. The framework containing the activities and corresponding phases within the thesis is illustrated in Figure 1-2.

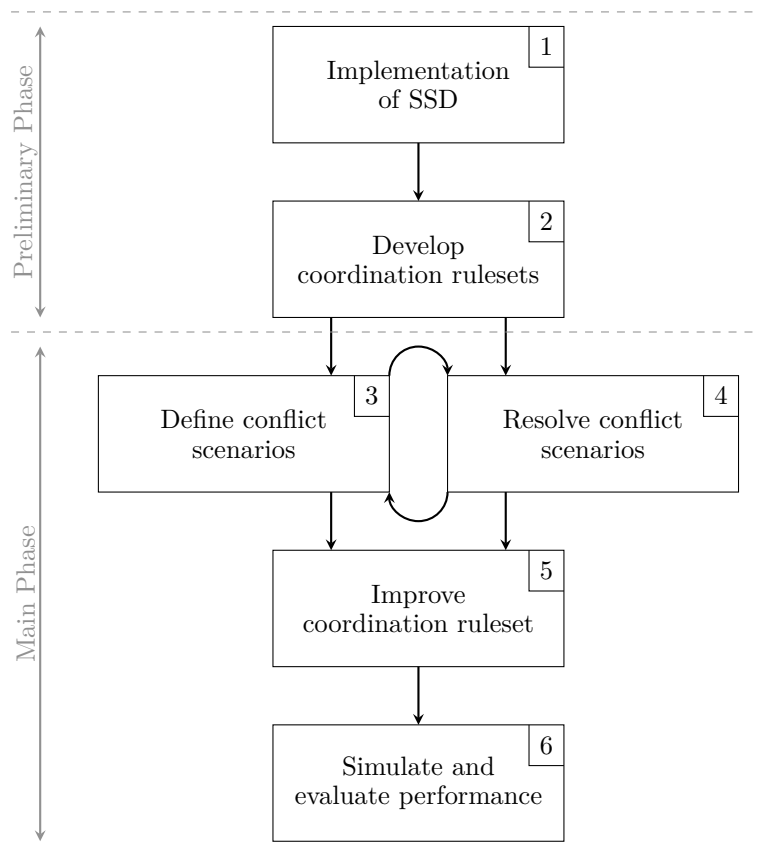


Figure 1-2: Research framework

The research activities listed in Section 1-1 are indicated with their corresponding number in the framework. It already shows a distinction for work expected to be completed during the preliminary and main phase respectively.

The first and second activity, implementing the SSD in BlueSky such that it can be used for CR-purposes and the development of the initial coordination rulesets are expected to be completed in the preliminary phase. Research Activities 3 and 4 will be performed simultaneously as the result of the simulations can be used to define more interesting small-scale conflict scenarios. From the knowledge obtained from this iterative process, a possible improved ruleset can be developed in the fifth activity. The last activity is focused on evaluating the performance of the new CR-method using the SSD in large-scale scenarios. This is ac-

completed by comparing it with the already implemented MVP without CP and is expected to be completed at the end of the main phase.

1-3 Research Scope

Besides clearly defining the research objective and activities, further demarcation can take place by limiting the research scope. This section is divided into a list of assumptions that will limit the scope and a list of further considerations that might be looked into when time allows at the end of the research.

1-3-1 Assumptions

The following assumptions disassociate the results from reality. This will be important to realize when discussing the application of the results. These assumptions can also be the starting points for further studies on this subject.

Assumption 1

Only en-route air traffic is considered under Instrument Flight Rules (IFR).

The aircraft will be in their cruise phase in the simulated scenarios. This ensures that the aircraft have enough Maneuvering Space (MS). In addition, the involved aircraft will have to rely solely on the instruments in the cockpit as a consequence of using IFR.

Assumption 2

The airspace is considered to be unmanaged.

This is not necessarily an assumption, but rather a consequence of using the Free Flight concept as guideline. This assumption effectively implies airborne self-separation.

Assumption 3

The CR-method will use a horizontal resolution strategy.

This will limit the MS of the aircraft. In terms of available speed vectors, the speed will be limited by a minimum and maximum speed that depends on aircraft type and altitude. Naturally, three-dimensional resolution maneuvers will be more efficient. Besides limiting the research scope, other reasons to not consider the three-dimensional case are cases where it is not possible to maneuver vertically and pilots actually preferring single-axis maneuvering [16].

Assumption 4

The CR-method will use implicit coordination.

Conflicts are preferably solved by implicit coordination since it is more robust than explicit coordination where preferred resolution maneuvers must be communicated. The additional layer of communication in explicit coordination might impose more requirements on the equipment of involved aircraft. Furthermore, there is a risk of timeout in communication, which leads to a pair of conflicting aircraft unable to resolve an emerging conflict. The drawback of implicit coordination is that it must be designed in such a way, that it will be able to resolve all possible conflicts. An example of implicit coordination under Visual Flight Rules (VFR)

are the *rules of the air* [17]. For IFR there is no standardized form of implicit coordination. This research aims to find a feasible implicit coordination ruleset under IFR.

Assumption 5

The CR-method will use perfect, current ADS-B information.

It is expected that the technological possibilities of ADS-B will advance in the future years. However, for this thesis only the currently available information is considered, implying that the relative speed vector and altitude of other aircraft can be used. Moreover, it is assumed that the information is perfect, meaning phenomena such as data loss, latency and other uncertainties are neglected. This implies that state information of other aircraft, such as speed and altitude are continuously available. Section 2-4 elaborates upon the validity of this assumption.

Assumption 6

The CR-method will not use intent information.

The current state information will be propagated through the look-ahead time to detect potential conflicts. The disadvantage is that the CR-method will advise resolution maneuvers, even if one or both of the aircraft intend to turn away within the look-ahead time. The advantage is that it is not possible to end up with urgent conflicts due to aircraft not following their intended route. The thesis will therefore focus more on tactical maneuvering rather than strategic maneuvering as can be seen in research on for example four-dimensional trajectories [18, 19].

Assumption 7

The CR-method will use a look-ahead time of five minutes.

Closely tied with the previous assumption, the choice for five minutes is in line with the focus on tactical maneuvering. A longer look-ahead time would lead to unnecessary maneuvering as there is no intent information. A much shorter look-ahead time would require sharper maneuvering as it limits the MS. This is detrimental for passenger comfort [20]. Furthermore, the minimum coverage of ADS-B shows that five minutes is the maximum possible look-ahead time.

Assumption 8

The rule-complexity of the CR-method will not be too high.

Another property of CR-methods is the complexity of its coordination ruleset. In general it can be assumed that the simpler and more intuitive the ruleset is, the better. Especially pilots, who eventually have to follow the advised resolutions, are benefited by this, as they generally tend to distrust illogical or complex Resolution Advisories (RAs) [21, 22].

1-3-2 Further considerations

The list of assumptions is continued with the following assumptions. However, it is expected that these assumptions can be reassessed without much effort due to the possibilities of BlueSky or the intended implementation of the SSD. It is difficult to judge whether there is enough time to reconsider these assumptions. Therefore, it is decided that initially it will serve as a continuation of the aforementioned list of assumptions. Should there be ample time

left, they might be reconsidered. Otherwise, they can also serve as convenient starting points for further research.

Assumption 9

Wind and turbulence are not considered.

It is acknowledged that presence of wind and turbulence can be disruptive for estimating velocities from ADS-B data [23]. For the initial investigation wind and turbulence are considered to be absent. However, due to BlueSky allowing for relatively simple inclusion of wind, it does not take much effort to take wind into account.

Assumption 10

Aircraft will be of the same type during simulation.

Initially, all simulations will be performed using one aircraft type, being the Boeing 747-400. As a consequence, all aircraft have the same performance limits. In BlueSky the aircraft types can be varied effortlessly, signifying that this assumption can be reconsidered.

Assumption 11

Maneuver dynamics are not considered when constructing VOs.

The VOs will be constructed as triangles which will be explained in Section 2-3. Including maneuver dynamics, which is the same as including the time to turn, will increase the size of a VO without needing further alterations [24]. It should be noted that the more imminent the conflict, the bigger the error will be when neglecting maneuver dynamics. Implementing maneuver dynamics only requires the constructed VOs to be altered.

1-4 Outline of the Preliminary Thesis Report

The purpose of this report is to give an overview of the result of the preliminary phase of the thesis. The next chapter presents the Literature Review aimed to indicate the knowledge gap in the usage of the SSD that this research tries to fill. Simultaneously, it will explain fundamental concepts and the terminology used throughout the thesis. Chapter 3 concerns the setup of the simulations and introduces the independent and dependent variables. The last chapter will conclude this preliminary thesis report and summarizes the expectations of the main phase of this research.

Chapter 2

Literature Review

An overview of existing literature, elaboration on key concepts and explanation of used terminology are incorporated in this chapter. The first section will be on the differences between CD, CP and CR. A broad analysis of different types of CR-methods is given in Section 2-2. Some of these methods rely on VOs, which are described in the following section. In this section the relation between the set VOs and the SSD is also further clarified. This chapter concludes with Section 2-4, where the enabling technology for the intended CR-method, ADS-B is detailed.

2-1 Detecting, Preventing and Resolving Conflicts

One of the responsibilities of ATC is to ensure separation of air traffic that fly under IFR. Advancements in radar technologies assisted immensely in determining the location of aircraft within the controlled airspace from ground-based stations [25]. Nowadays, two types of radar systems are combined for this purpose, namely the Primary Radar (PR) and Secondary Surveillance Radar (SSR). The PR works independently and is able to measure the slant range towards an aircraft. Combining the slant range with the altitude and an identification code provided by the SSR allows for fairly accurate measurements of the position and altitude of an aircraft. However, the SSR is not independent and requires the aircraft to be equipped with a Mode C transponder. Nowadays, an ATCo uses these systems to ensure separation and thus prevent conflicts. How conflicts are defined and how they are used within ATM research relevant to this thesis is discussed in this section.

2-1-1 The Definition of Conflicts

Aircraft cannot fly in very close proximity to each other due to uncertainties in tracking with radar systems and turbulence effects such as wake vortices. For radar controlled en-route airspace, separation minima are often set at 5NM horizontally and 1,000ft vertically [26]. In the remainder of the thesis this separation standard is adhered to, in line with similar

studies on conflicts within the field of ATM [9, 20]. These separation minima create a very flat cylinder around an aircraft, the *ownship*, into which another aircraft, the *intruder* is not allowed to enter. This cylinder is called the Protected Zone (PZ) and is visualized in Figure 2-1.

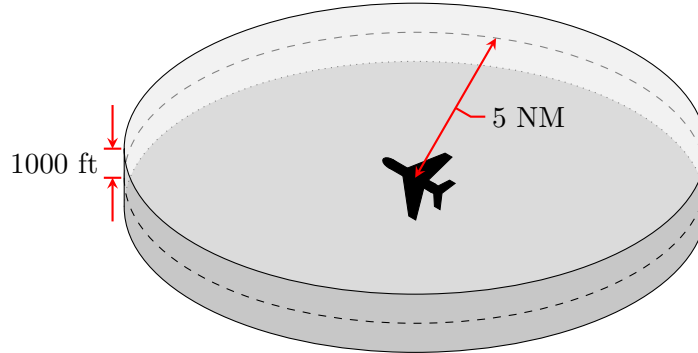


Figure 2-1: The PZ and protection minima [20]

Closely related to the PZ in the previous paragraph is a LoS, which is an event that occurs when an intruder enters the PZ of the ownship. Obviously, an ATCo and other separation methods aim to avoid a LoS. Note that there is another definition of the PZ where a LoS occurs when the PZs of the ownship and intruder touch [5]. However, the PZ in this definition uses half of the separation minima, which effectively means that the LoS occurs under the same circumstances in both definitions of the PZ [27].

A conflict arises when the trajectories of two or more aircraft are bound to cause a LoS in the near future. The near future in this case depends on the context, but is interchangeable with the concept of look-ahead time. Repeating Assumption 7 from Section 1-3, this thesis uses a look-ahead time of five minutes which orientates it in a more tactical setting. Additionally, Assumption 6 states that no intent information is used, which leads to the following definition for a conflict used in this thesis:

Definition 1

A conflict between two or more aircraft occurs when a LoS is predicted as the current aircraft states are linearly extrapolated over the specified look-ahead time of five minutes.

In a simple conflict with only two aircraft, the Closest Point of Approach (CPA) is the instance when the involved aircraft will not approach any closer. This can be used in combination with other parameters to completely define the geometry of the conflict. The parameters are the distance at CPA (d_{CPA}), the time to LoS (t_{LoS}) and the ground speed vectors of the ownship and (\mathbf{V}_{own} , \mathbf{V}_{int}). The geometry defined with these parameters is illustrated in Figure 2-2. The t_{LoS} is the time left until the intruder makes an intrusion to the PZ of the ownship. It occurs earlier than the time until it reaches CPA (t_{CPA}) and is not drawn in the figure. Using solely the magnitude of the ground speed vectors without direction, additionally requires two of the following three angles: the heading angle of the ownship (χ_{own}), the heading angle of the intruder (χ_{int}) or the conflict angle (χ_{CA}) [23]. Due to Assumption 9, the influence of wind can be neglected. Otherwise the track angle has to be used instead of the heading angle.

Figure 2-2 illustrates the most simplistic type of conflict involving only two aircraft. Involving more aircraft might result in multi-aircraft conflicts as defined in Definition 2. The probability

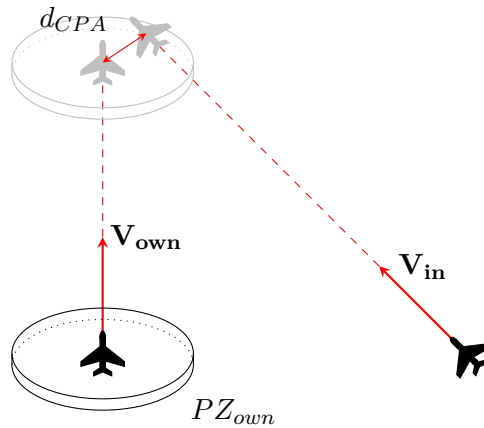


Figure 2-2: The conflict geometry for a conflict involving two aircraft

of multi-aircraft conflicts is very low [28, 29]. However, the increasing air traffic will make it more likely to encounter multi-aircraft conflicts [2, 3].

Definition 2

A multi-aircraft conflict is a conflict (Definition 1) where one aircraft is in conflict with at least two other aircraft.

Formally not a multi-aircraft conflict, but another subtype of conflicts involving three or more aircraft are two conflicting aircraft and at least one intruder in the vicinity. The presence of intruders can cause secondary conflicts which is often referred to as the *domino effect*. This effect, measured by the Domino Effect Parameter (DEP), is also regarded in this thesis [30].

Categorizing conflict geometries for multi-aircraft conflicts becomes more difficult as each conflict pair results in the set of parameters visualized in Figure 2-2. A multi-aircraft conflict with three aircraft already has three possible conflict pairs and six possible conflict pairs emerge with four involved aircraft. This grows as the sequence of triangular numbers, giving $\frac{n(n-1)}{2}$ or $\binom{n}{2}$ conflict pairs for n aircraft. Clearly, it is worthwhile to investigate other parameters that can describe conflict geometries for multi-aircraft conflicts adequately, which is done in Sections 3-2 and 3-3.

2-1-2 Conflict Detection, Prevention and Resolution

Reiterating what has been stated before, research into conflicts within the field of ATM can be divided into three main categories, being Conflict Detection (CD), Conflict Prevention (CP) and Conflict Resolution (CR). Many methods that handle conflicts have been developed over the years, not necessarily constrained to airborne separation, but also for maritime, robotic and autonomous vehicle applications [22, 31]. The methods are not restricted to one category. In fact, many methods fall under two or three of the categories. Note that CP is often left unmentioned in literature, leading to the more common term of CD&R. However, due the significant difference between methods with and without CP, it will be acknowledged in the remainder of this thesis. For the definition of the conflict methods, the work of Rand and Eby has been used as reference [7].

Definition 3

Conflict Detection is the process of propagating expected trajectories of the ownship and intruders into the near future in order to find possible conflicts.

Definition 4

Conflict Prevention is the process of propagating expected trajectories of intruders into the near future to find the maneuvers of the ownship that would lead to conflicts.

Definition 5

Conflict Resolution is the process of propagating expected trajectories of intruders into the near future to find the maneuvers of the ownship that would resolve conflicts.

Similar to the definition of a conflict in Section 2-1-1, phrasing the near future in the definitions is the same as using the specified look-ahead time of five minutes. The process of CD will not necessarily result into conflicts and CP can be performed regardless of the existence of conflicts. On the other hand, CR is only to be performed when there are existing conflicts.

2-2 Conflict Resolution Methods

A logical result of the extensive research on aircraft conflicts in ATM is that many different types of methods and algorithms have been developed over the years. This section focuses on the different types of conflict resolution methods. Note that these CR-methods might also encompass CD and CP. The classification in these different types of resolution methods is based on early work from Kuchar and Yang [22]. The taxonomy of CD&R methods by Jenie et al. is used to provide a more recent insight [32]. Although the second taxonomy is aimed at UAVs, it is still very applicable for the application of the airborne separation task of manned aircraft. The last part of this section assesses some methods in particular, the Traffic Collision Avoidance System (TCAS) and the MVP.

2-2-1 Kuchar and Yang's Taxonomy

In the year 2000 an effort was made by Kuchar and Yang to make a proper survey of existing CD&R-methods [22]. However, they did not acknowledge CP as a separate function. A total of 68 methods were investigated and categorized using six different criteria.

The first criterion was on the propagation of the current state into the future. Three types were distinguished as illustrated in Figure 2-3, being nominal, worst-case and probabilistic. The methods predict future states using current information on location, speed, rate of climb or descend, direction and altitude. The simplest way is to assume that an aircraft keeps on following its current velocity vector or following its nominal trajectory as shown in Figure 2-3a. In the next figure a more thorough approach is depicted that considers all possible trajectories and subsequently evaluates the worst-case variants. However, this requires some knowledge of the performance limits of the other aircraft, such as turning rates and climb- or descend rates. These two approaches offer a deterministic view on the existence of conflicts. The probabilistic approach combines the two, by assuming that some maneuvers, such as worst-case maneuvers, are less probable than others, which results into a probability of conflict.

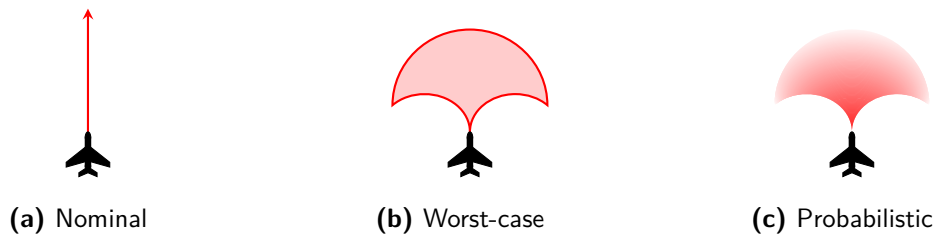


Figure 2-3: Different types of state propagation methods [22]

The second criterion is regarding the dimensions of the used state information of an aircraft. The dimensions can be seen as planes that can be purely horizontal, purely vertical or a combination of both. In literature, horizontal information is sometimes described as two-dimensional and the combination of horizontal and vertical as three-dimensional. Methods that use purely vertical state information are uncommon [33].

Whether a method explicitly mentions a threshold to detect conflicts is examined in the third criterion. Some methods heavily focus on CR, disregarding the CD. Generally, the threshold is set using separation minima or look-ahead times.

The fourth criterion concerns the type of resolution method, which is categorized into the following five types: prescribed, optimized, force field, manual and no proposed resolution. In prescribed resolution methods maneuvers are the same regardless of the conflict. An obvious example given by Kuchar and Yang is the Ground Proximity Warning System (GPWS), for which the resolution maneuver should always be to pitch up in case of an imminent conflict [33]. Optimized resolution methods consider possible resolution maneuvers and select the most optimal by evaluating some cost function. The third type essentially uses charged particles as an analogy for aircraft. These aircraft will be equally charged, which results in repulsive forces between them, effectively maintaining separation [34]. The fourth type of resolution methods expects the user to provide a resolution maneuver, after which the user is notified whether the maneuvers is acceptable or not. The last type is for the methods that do not provide a resolution, which are actually not CR-methods.

The fifth criterion looks at the dimensions of the proposed resolution, similar to the second criterion that regards the used state information. Possible maneuvers fall within at least one of the following maneuvers: turns, vertical maneuvers and speed changes.

Kuchar and Yang have assessed how resolution methods handle multi-aircraft conflicts for the last criterion. It is dealt with in two possible ways, pairwise resolution or a global resolution. If multi-aircraft conflicts are not mentioned in literature on conflict resolution methods, it can be assumed that the multi-aircraft conflicts are solved pairwise.

The categorization into these six criteria is summarized in Figure 2-4. It is important to realize these six criteria cannot be combined without restrictions as certain combinations are impossible.

2-2-2 Jenie's Taxonomy

Similar to Kuchar and Yang's taxonomy in the previous section, Jenie et al. have proposed a taxonomy for CD&R-methods for UAVs [32]. Even though it is specifically proposed for

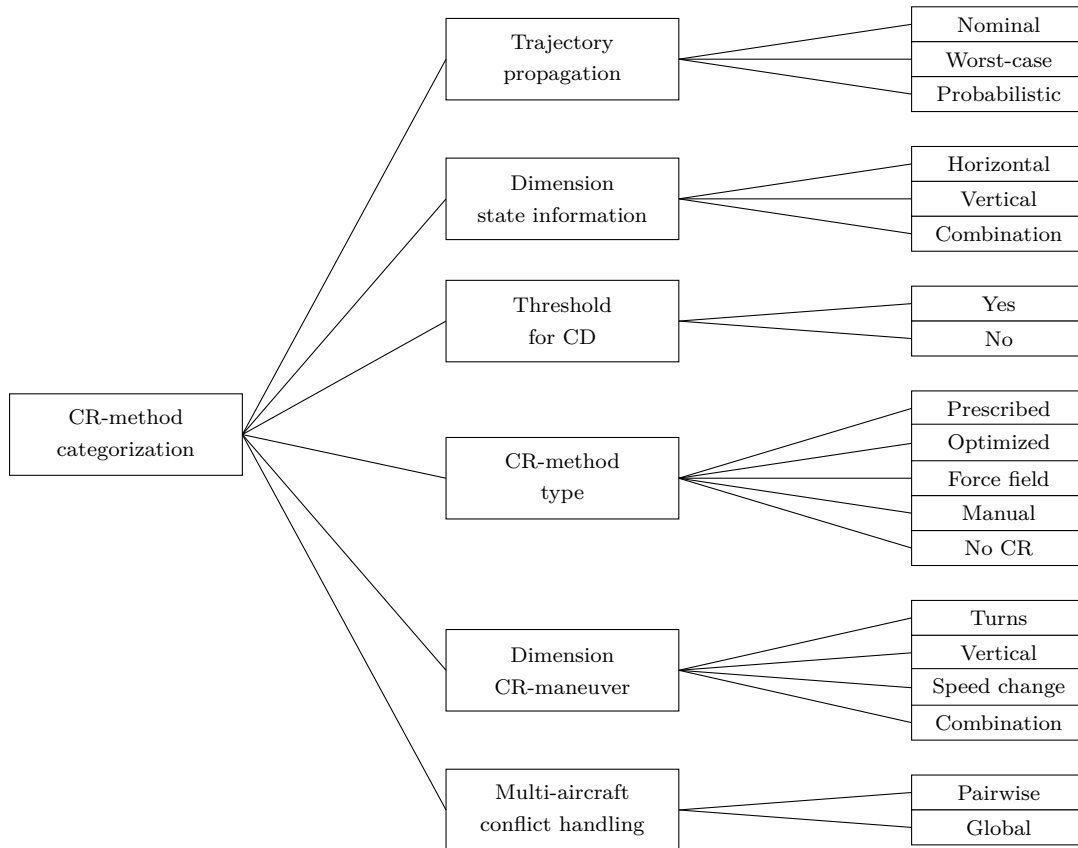


Figure 2-4: Overview of categorization criteria in Kuchar and Yang's taxonomy

UAVs, it is still heavily linked to manned flight. Another reason it is worth to mention in this literature study is that it provides a fundamentally different point of view compared to the criteria used in Kuchar and Yang's taxonomy. Jenie et al. propose to categorize methods using four different criteria.

The first criterion is on the airspace surveillance, divided into three types. In the first type, centralized-dependent surveillance, a ground-based system has access to all information in the controlled airspace and utilizes this to make decisions. The most obvious example for this is how ATC provides surveillance nowadays. Distributed-dependent surveillance is strongly advocated in the Free Flight concept [5,6]. This type of surveillance depends on aircraft providing their own surveillance, thus ensuring airborne self-separation, using data transmitted by other aircraft. The enabling technology for this is ADS-B which is elaborated upon in Section 2-4. The last type of surveillance is independent, but is not very applicable anymore for manned aircraft. An aircraft in independent surveillance relies completely on on-board sensors to detect and avoid other aircraft. As a result, ADS-B cannot be used as it uses data broadcast by other traffic. Due to cruising speeds and separation minima for manned aircraft this type of surveillance is generally not researched into for application in manned flight.

Three types of coordination are used for avoidance according to the next criterion, being explicitly coordinated, implicitly coordinated and uncoordinated. In explicitly coordinated avoidance, the avoidance maneuver is conveyed between conflicting aircraft [7,27]. In implicit

coordination predefined rules are followed, similar to how the *rules of the air* are used under VFR [17]. The predefined rules for implicit coordination are often referred to as a coordination ruleset in this thesis. As was also the case in the first criterion, the third type is again only suitable for UAVs as uncoordinated maneuvering introduces unacceptable high risks for manned aircraft.

The third criterion is on the type of maneuvering, which seems similar to the fifth criterion in Kuchar and Yang’s taxonomy where the dimensions of the resolution maneuver were determined. However, it is not characterized by the dimension of the maneuver, but rather by the range at which the maneuver is performed. A long-range maneuver is called strategic and often includes the flight plan of aircraft. A tactical maneuver is said to be at mid-range and typically does not include a flight plan. The short-range maneuver is called an escape maneuver. In manned flight this last type is to be avoided as it is an aggressive maneuver at the performance limits of an aircraft, which is detrimental for passenger comfort. However, methods in this maneuvering range are essential as they act as a last resort safety mechanism when longer range methods have failed. The maneuvering range of resolution methods is strongly related to its look-ahead time as listed in Table 2-1. Note that the rows should be considered with some margin as it depends on the (relative) speed of conflicting aircraft, which makes the table unsuitable for UAVs whose range and look-ahead times are generally much lower.

Table 2-1: Relationship between the range and look-ahead time of maneuvers

| Maneuver | Range | Look-ahead time |
|-----------|-------|-----------------|
| Strategic | Long | 10–20 min |
| Tactical | Mid | 3–20 min |
| Escape | Short | <2 min |

The last criterion involves the type of autonomy of the method. The avoidance maneuvers are conducted either manually or autonomously. The aim within ATM is to keep a human operator in the loop in manned aircraft, where humans decide on the maneuvers assisted by conflict avoidance systems [4, 5]. Therefore, fully autonomous resolution methods are not applicable to manned flight.

Again a summary of the categorization into the stated criteria is shown in Figure 2-5. Jenie et al. have additionally made an extensive specification of combinations of these four criteria that are infeasible or even impossible. In Sections 2-2-3 and 2-2-4 different CR-methods will be characterized by the explained taxonomies serving as a brief description of the respective methods.

2-2-3 TCAS

The taxonomies presented in Sections 2-2-1 and 2-2-2 are accompanied with many examples. One method that is used extensively as example in both taxonomies is the Traffic Collision Avoidance System (TCAS), a system that is used as a last safety mechanism in avoiding collisions by issuing commands to climb or descend. It can be used to illustrate the difference in the categorization for both taxonomies quite well. TCAS is in fact a method that is already implemented and operational in current aircraft [35]. As such, it is also part of the Airborne

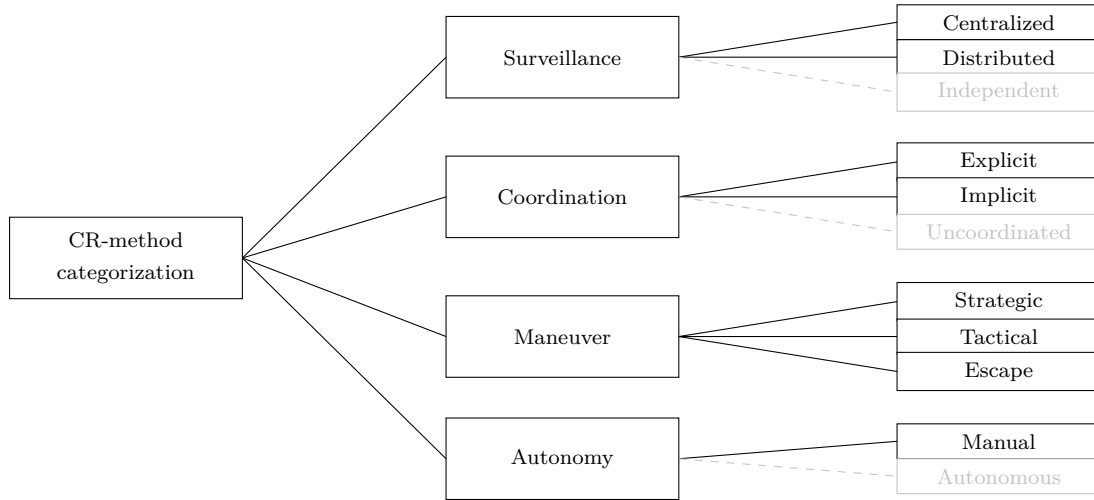


Figure 2-5: Overview of categorization criteria in Jenie's taxonomy. Elements for UAVs are grayed out

Collision Avoidance System (ACAS) of an aircraft. Another system that is part of ACAS is the GPWS, mentioned in Section 2-2-1. Note that in this thesis the widely implemented version, TCAS II, is referred to as simply TCAS.

As is customary for implementations of systems in ACAS, TCAS can issue Traffic Advisories (TAs) and RAs [35]. TAs are used to notify the pilots that other traffic is nearby, whereas RAs are used to avoid imminent collisions. In light of the definitions in Section 2-1, TCAS can be said to provide both CD and CR. It does not prevent future conflicts and thus lacks CP.

According to the taxonomy by Kuchar and Yang, TCAS propagates trajectories nominally. It detects intruder aircraft within a horizontal range of 14NM and within a vertical range of 10,000 ft [35], which is clearly a combination of horizontal and vertical planes. Obviously, the threshold for CD is given. Since TCAS chooses the least aggressive resolution maneuver from a list of potential maneuvers it can be seen as an optimized approach. The current implementation only issues vertical RAs and resolves conflict pairwise.

After the categorization of TCAS using Kuchar and Yang's taxonomy, the taxonomy by Jenie et al. can be used to accomplish another categorization. TCAS is a distributed system as it is equipped on every aircraft and makes these aircraft responsible for their own surveillance in this conflict regime. When issuing RAs, conflicting aircraft must agree upon whether to climb or descend. This agreement, or *handshaking*, is achieved by means of explicit coordination. Maneuvers due to RAs issued by TCAS are required to avoid very short-range conflicts, effectively making it an escape maneuver. And even though RAs notify pilots what action needs to be performed, the pilots are still in control and have to manually operate the aircraft to follow this command.

The requirement of the pilot manually complying with the RA is a drawback that all manual controlled resolution methods exhibit. In the case of TCAS, it has even led to fatal accidents [36]. The Überlingen mid-air collision happened as a Russian airliner descended, following the instructions from ATC, whereas the TCAS issued the RA to climb. The other conflicting

aircraft mimicked the descent of the Russian airliner as it correctly followed its RA. This resulted into a mid-air collision with 71 casualties and led to improvements in the current TCAS implementation [35,37]. The principle of this improvement is that the RA is reversed for the complying aircraft, when the other conflicting aircraft is not complying.

2-2-4 The Modified Voltage Potential

Force field, or voltage potential methods are often introduced as an analogy where aircraft are related to charged particles. However, this analogy is not very practical and accordingly Eby has developed this original voltage potential method into a feasible conflict resolution method in 1994 [34]. This was slightly modified by Hoekstra et al. and subsequently called the Modified Voltage Potential (MVP) [27,38]. A notable difference with the previously discussed TCAS is that the MVP not only has CD and CR, but also CP. The MVP can be seen as part of the Airborne Separation Assurance System (ASAS) and not as part of the ACAS. The difference between the two is that ASAS is intended for strategic and tactical maneuvering, whereas ACAS is more of a short-range escape maneuvering system.

Placing MVP in the previously detailed taxonomies, it has a nominal trajectory propagation and uses horizontal and vertical state information. The threshold it uses for CD is five minutes. As introduced earlier, it is a force field method and the resolution maneuvers are a combination of turns, speed changes and vertical maneuvers. The MVP solves multi-aircraft pairwise, which wraps up Kuchar and Yang's taxonomy. Looking from the perspective of the taxonomy by Jenie et al., the method has distributed surveillance and implicit coordination. The look-ahead time is five minutes, making it mid-range and thus a tactical maneuvering method. To conclude, the MVP provides advisories that pilots still have to follow manually.

The CD of MVP is achieved by nominally propagating trajectories of surrounding aircraft using state information obtained from ADS-B. The algorithm developed for the CR is more complicated. The essence is that intruder aircraft will be pushed away from the PZ, as explained in Section 2-1-1, of the ownship. The reverse is also true, the ownship will be pushed away from the PZ of intruders, retaining the analogy of the force field methods. Figure 2-6 is used to illustrate the start of the algorithm. In this figure only the one-sided case is depicted, with an intruder moving towards the PZ of the ownship. Also the velocity vector of the ownship is subtracted from both agents, making the PZ of the ownship a static obstacle and making the velocity of the intruder relative towards the ownship.

The aircraft are in conflict since the CPA lies within the PZ. In order to avoid conflicts, Eby stated that an avoidance maneuver has to be performed such that the CPA moves outside the PZ [34]. Hoekstra argued that this avoidance vector could be perpendicular to the initial relative path. In Figure 2-6 this new point is depicted as P_G . However, following this updated relative path, the dashed line in the figure, demonstrates that the new CPA still lies within the PZ. Hoekstra has corrected this by computing point P_H in such a way that the final relative path is tangent to the PZ, which means that the CPA is on the boundary of the PZ [27]. In fact, this final relative path is a significant aspect of the VOs, which are explained in Section 2-3. This final relative path can be used to construct the avoidance vector, which will be perpendicular to the initial relative path. Note that a shorter avoidance vector is also available, which is perpendicular to the final relative path instead [23]. This optimal avoidance vector is denoted in Figure 2-6 with \mathbf{V}_{opt} . In similar fashion the vertical avoidance maneuver

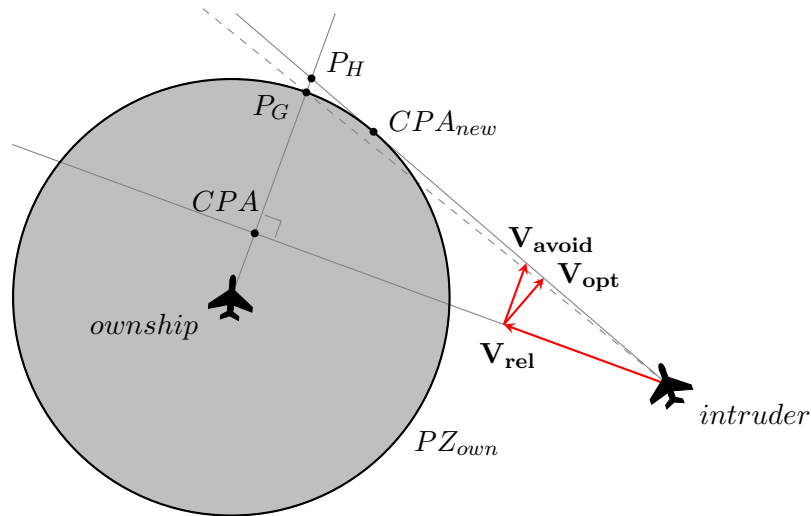


Figure 2-6: Construction of the avoidance vector in the MVP [27, 39]

can also be computed [27]. Another advantage is that MVP can handle multi-aircraft conflicts, since resolution maneuvers can be summed for each conflict pair, thus solving multi-aircraft conflicts pairwise.

After the CPA is passed, the aircraft can start a recovery maneuver to return to its initial heading and velocity [27, 39]. The CP added to the MVP is useful while returning to the initial heading of the aircraft as it shall not trigger the same conflict again. The CP-component of MVP is called Predictive ASAS (PASAS) and essentially visualizes the areas that the pilot should not turn into on displays in the cockpit [40]. Thus, it can be concluded that the MVP indeed entails CD, CP and CR.

2-3 Velocity Obstacles

Part of the objective of the thesis project is to further develop a conflict resolution method, which was the topic of Section 2-2. The intention is to achieve this by using Velocity Obstacles (VOs), which will be the topic of this section. First the basics and origin of the VOs is explained. After which a two-dimensional VO-method by Jenie et al. is presented. After this, a formal mathematical representation is given using set theory. This section is concluded with a discussion on the SSD.

2-3-1 Basics of a Velocity Obstacle

Research aiming at the concept of VOs originated from robotics [41]. *Collision Cones (CCs)* and *Avoidance Cones* were terminology used to indicate the same or very similar concepts, until Fiorini and Shiller gave the concept its definitive name [8, 42]. Figure 2-7 is used to explain the construction of a VO.

CCs and VOs are represented in the velocity space of a conflict geometry. Similar to the intruder in the MVP, obstacles have a PZ around them. Subtracting the velocity of the

obstacle (\mathbf{V}_{obs}) from the complete velocity space yields the relative velocity space as shown in Figure 2-7a. Since the obstacle is not moving in this relative space, the ownship is in conflict with the obstacle and without intervention a LoS will occur. To avoid this conflict, the relative velocity vector must be moved outside the CC. The CC is an infinitely extending area bounded by two lines tangent to the PZ.

To reiterate, this CC is defined in the relative velocity space. However, it is desirable to translate this back to the absolute velocity space. This is achieved by adding \mathbf{V}_{obs} to every object in Figure 2-7a, which results in Figure 2-7b. Instead of avoiding the CC, now the ownship must move its velocity vector outside of what is now called the VO, which is more intuitive than moving a relative velocity vector. In essence, the VO is simply the translated CC. Another advantage of the VOs is that they can be summed since they share the same reference frame, whereas CCs have different reference frames depending on the movement of the obstacles [8]. As a consequence, the VOs are suitable for use in multi-aircraft conflicts.

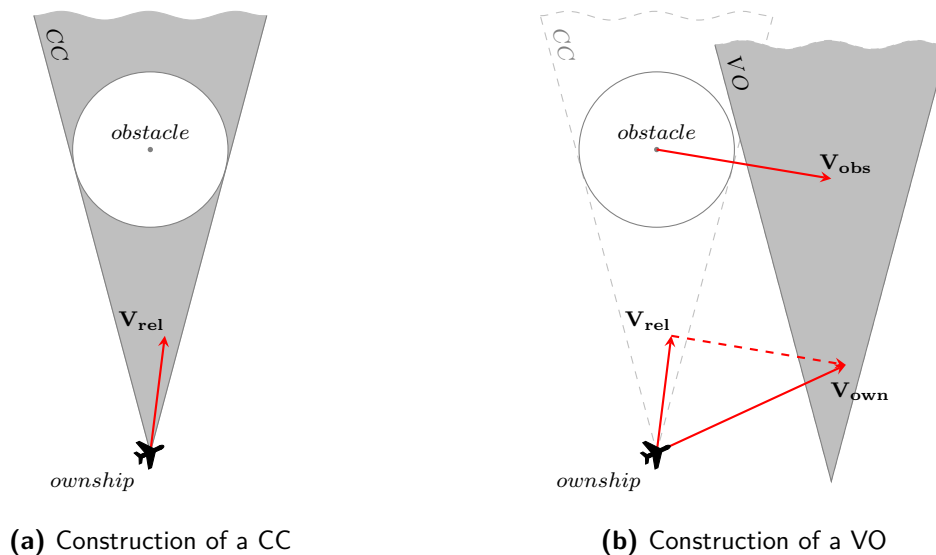


Figure 2-7: The CC and VO in the different velocity spaces of the conflict geometry

2-3-2 Methods using Velocity Obstacles

Research into aircraft conflicts have previously used a single VO to provide the resolution maneuvers [43, 44]. The method by Jenie et al. called the Selective Velocity Obstacle (SVO) method is implicitly coordinated and is aimed at UAVs, but the ruleset used in the method is still applicable to manned flight. Interestingly, the implicit coordination ruleset used by the SVO method is based on an already existing ruleset currently used under VFR, the *rules of the air* [17].

To incorporate the *rules of the air* of the air, the resolution algorithm distinguishes five encounter types: right converging, left converging, head on, taking over and being taken over. Departing from these encounter types, four sectors have been defined in the velocity space of the ownship. These sectors are subsequently used to determine the resolution vector by obeying to the *rules of the air*.

In order to resolve the conflicts, the SVO method uses three modes to generate the maneuvers. The turn mode lets an aircraft turn while obeying the ruleset. The maintain mode keeps an aircraft flying at its current velocity and heading. The mission mode allows the aircraft to fly towards its target. Before the initial analysis both aircraft start in the mission mode as they are flying towards their target. When the conflict is detected, the algorithm resolves by putting the aircraft with priority into the maintain mode. The other aircraft is put into the turn mode, which will eventually clear the conflict. Once the conflict is cleared, both aircraft will return to the mission mode.

A Monte Carlo simulation has been performed using random initial conditions to prove the validity of the SVO method. The method proved to be very successful in pairwise resolving conflicts involving two aircraft. Multi-aircraft conflicts might be resolved in a pairwise manner using the SVO method, but this has not been simulated enough to draw substantiated conclusions [44]. Ellerbroek et al. also performed Monte Carlo simulations on resolutions using a single VO [43]. This study investigated not only the *rules of the air* as coordination ruleset, but also the more optimal *shortest way out* principle. Besides the different coordination rulesets, it also assessed the influence of conflict geometry parameters and system delay.

2-3-3 Set theory representation

In this subsection more formal descriptions are given of terminology that will eventually lead to the SSD. Note that the terminology for the remainder of the thesis is not always consistent with terminology used in literature. Beginning with the Forbidden Velocities (FV) and the Reachable Velocities (RV).

Definition 6

The FV are the union of the VOs of all intruders for a single ownship.

Definition 7

The RV are the reachable velocities for a single ownship limited by its minimum and maximum speed.

The FV are an area that extends infinitely in mathematical sense, whereas the RV are bounded by the performance limits of the corresponding aircraft being V_{min} and V_{max} . Definitions 6 and 7 can also be expressed mathematically on \mathbb{R}^2 with N intruders and VO_i corresponding to each intruder i as shown in Eqs. 2-1 and 2-2 respectively.

$$FV = \bigcup_{i=1}^N VO_i \quad (2-1)$$

$$RV = \{(x, y) \in \mathbb{R}^2 \mid x^2 + y^2 \geq V_{min}^2, x^2 + y^2 \leq V_{max}^2\} \quad (2-2)$$

The same definitions can also be illustrated, which is done in Figures 2-8 and 2-9 respectively.

From the definitions it is evident that the *Allowed Velocities* are the complement of the FV and the *Unreachable Velocities* are logically the complement of the RV. Combining these

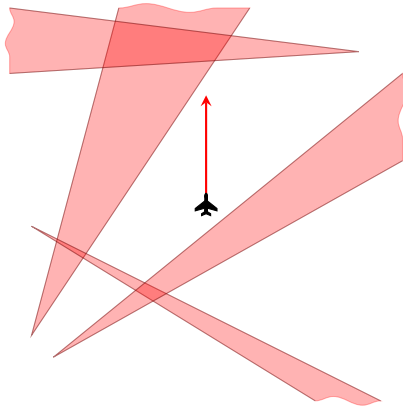


Figure 2-8: The FV

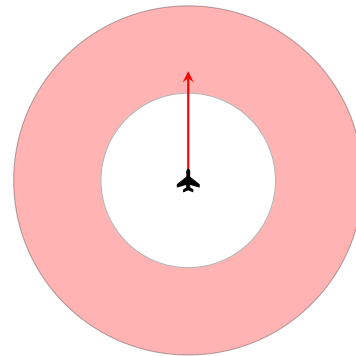


Figure 2-9: The RV

definitions, one can get the Forbidden Reachable Velocities (FRV) and Allowed Reachable Velocities (ARV), which are shown in Eqs. 2-3 and 2-4.

$$FRV = RV \cap FV \tag{2-3}$$

$$ARV = RV \cap FV^C \tag{2-4}$$

Mathematically speaking, the ownship is in conflict when $\mathbf{V}_{\text{own}} \in FRV$ and is not in conflict when $\mathbf{V}_{\text{own}} \in ARV$. The FRV and ARV together form the components of the SSD, which is ring-shaped due to the ring-shaped RV. This combination of sets is depicted in Figure 2-10.

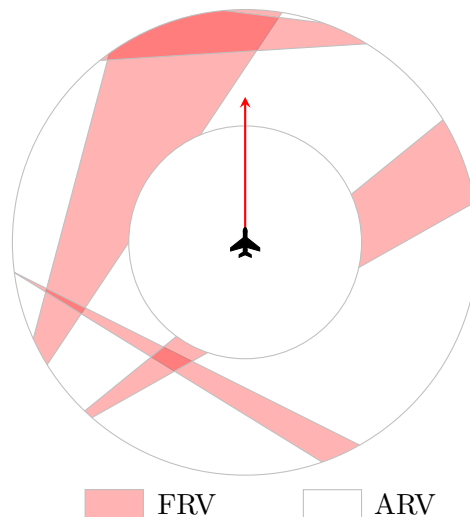


Figure 2-10: Combining the FRV and the ARV into the SSD

It can also be concluded that the SSD provides CD, CP and CR. Having the current speed vector in the set of FRV implies that the aircraft is in conflict (CD). Also, the same set of

FRV indicates what velocity vectors should not be used when navigating (CP). And finally, the set of ARV indicates which velocity vectors would resolve conflicts (CR).

2-3-4 The Solution Space Diagram

In the previous subsection the SSD was derived, which is essentially joining the VOs and including the performance limits of the corresponding aircraft. The SSD will assist in the research objective to develop a CR-method for multi-aircraft conflicts. As of yet, the SSD has not been used in CR-algorithms to provide resolution maneuvers. In this subsection a brief overview of the current applications of the SSD is given.

The Solution Space Diagram was first conceptualized by Hermes et al. who have proposed it as an alternative metric to predict workload for an ATCo [13]. Following this study, more research has been conducted into the usage of the SSD as a workload metric [45–47]. Other applications are decision-support tools based on the SSD. In principle, the SSD is a circular ring in the velocity space of an aircraft containing *go* and *no-go* areas (ARV and FRV). Moving the speed vector of the aircraft into the ARV ensures separation, making the SSD indeed suitable as a supporting tool in the separation task. Mercado Velasco et al. investigated the possibility of reducing ATCo-workload in separating air traffic by using a visualization of the SSD [15]. The acceptance of automated resolutions by ATCos using the SSD as supporting tool was studied by Borst et al. [48, 49].

Likewise, pilots can benefit from the capabilities of the SSD, which can be projected as a visual aid on the navigational display in the cockpit [10, 11]. Having visual supporting tools such as the SSD available in the cockpit allows the pilots to ensure separation without the assistance of an ATCo. This is in line with ambitious initiatives that delegate the airborne separation task from the ground towards the air [5].

Experiments with conflicts involving two aircraft being resolved with VOs have shown promising results [43, 44]. These type of conflicts introduce only a single VO, making the corresponding SSD fairly straightforward. Multi-aircraft conflicts, where the VOs must be merged first to acquire the SSD, have not been experimented with in research within ATM. This explains the objective of this thesis to develop a method that uses this merged set of VOs in CR to advise resolution maneuvers for multi-aircraft conflicts. However, in the field of robotics multi-agent collision avoidance using VOs has resulted in resolution algorithms [50, 51].

Resolution methods based on the SSD can also be categorized using the previously introduced taxonomies. Similar to the MVP, it has a nominal trajectory propagation and uses horizontal and vertical state information. The CD-threshold will also be set at five minutes. However, the resolution maneuvers are a combination of turns and speed changes in the horizontal plane. The SSD-based method is optimized and it resolves globally in conflicts involving multiple aircraft. Note that the term global in this case is considering only the aircraft within the CD-range of this decentralized approach. The taxonomy by Jenie et al. will consider this method to be distributed and implicitly coordinated. Due to the look-ahead time of five minutes the resolution maneuvers are tactical by nature. The SSD also provides resolution advisories that pilots will have to follow manually.

2-4 ADS-B characteristics

The Automatic Dependent Surveillance - Broadcast (ADS-B) described in this section is the underlying technology that will enable airborne self-separation. ADS-B can be used in resolving aircraft conflicts since it is a technology that periodically relays the state information of an aircraft. Contrary to the SSR, the ADS-B will periodically broadcast messages without being interrogated. These messages can contain information on the aircraft's identification, surface position, airborne position and airborne velocity [52]. This type of information is often referred to as the aircraft's state information. The messages can be received by ground stations, but also by other aircraft equipped with a compatible receiver. The received information can be displayed to pilots to improve situational awareness. In this thesis, it is assumed that all aircraft have the necessary equipment to transmit and receive the state information.

The broadcast messages are received by all aircraft within a range of 80 NM to 200 NM [27]. The range depends on atmospheric conditions, altitude and practical limits such as transmitter power and receiver sensitivity. A worst case scenario would be a head-on conflict with two aircraft flying at 500 kts with an ADS-B range of 80 NM. A simple calculation shows that the conflict will be detected at $t_{CPA} = 4.8$ min. A look-ahead time of five minutes as stated in Assumption 7 would indeed be the maximum for a conflict resolution method relying on ADS-B.

In Assumption 5 it is assumed that state information will be continuously available. It was already acknowledged that the state information will actually exhibit a system delay [43]. First of all, the ADS-B messages are transmitted with an interval of at least 0.5 s [53]. Messages can be transmitted at a lower interval. However, not every message will contain the desired ground velocity as it can also hold other information such as position and identification as was explained earlier. But the interval of 0.5 s for the desired state information is guaranteed. The range at which ADS-B operates makes any communication delay negligible at around 1 ms. Likewise, the ADS-B will have a negligible small processing delay. It can be concluded that the message interval is the main reason for the discrete availability of the state information. Since this interval is relatively small compared with the intended look-ahead time of five minutes, it is acceptable to treat the state information as continuously available.

Chapter 3

Experiment Design

In order to meet the research objective, it must be studied whether the SSD can indeed be used as a CR-method. Research Activities 4 and 6 in Section 1-1 stipulate to run simulations on respectively small-scale conflict scenarios and large-scale airspaces. These simulations basically form the experiments of this research and are designed using the obtained knowledge from the literature review in the previous chapter. The designed experiments to be conducted during the main phase of the thesis are discussed in this chapter. The experiments are performed by simulating the small- and large-scale conflict scenarios in BlueSky. This simulation environment is briefly described in Section 3-1. Sections 3-2 and 3-3 respectively present the independent and dependent variables. Note that due to the nature of the small- and large-scale scenarios, not all metrics described in these sections can be applied to both scenario-types. The experiment design is concluded by formulating hypotheses in the last section of this chapter.

3-1 Simulations in BlueSky

The environment in which the conflicts are simulated is provided by BlueSky, an open data and open source ATC simulator project developed by students and researchers of the Aerospace Engineering faculty at TU Delft [12]. The project is partly aimed at making the BlueSky program suitable for ATM research such as this thesis. The program is written in Python 2 and relies on either pygame or OpenGL in a Qt windows environment for its user interface. Furthermore, BlueSky offers many advantages, but due to the available documentation and a conference paper [12], only a few are highlighted that will be relevant for this research.

The simulator is capable of running simulations involving hundreds of aircraft using relatively limited computational resources. This allows BlueSky to be run on ordinary computers, which can be convenient when a multi-aircraft conflict resolution algorithm is to be developed and assessed. Furthermore, the modular structure of the program makes it easy to modify, which is advantageous when a new conflict resolution algorithm must be implemented.

In Section 1-3 the assumption was made to neglect the influence of wind and turbulence. This leads to the groundspeed being equal to the true airspeed in the simulations. Since BlueSky has models for both wind and turbulence, it is fairly straightforward to investigate the influence of wind in future research. Similarly, the aircraft model is based on the Boeing 747-400 for all simulated aircraft in this research. The program allows researchers to change the aircraft type without restrictions, making simulations with a variety of different aircraft possible.

Before this thesis started, BlueSky already had a functioning ASAS that utilized MVP as its resolution method. The CP-component of MVP explained in Section 2-2-4 is not present in this automated resolution. Furthermore, a visualization of the SSD for individual aircraft was available. However, this visualization is not suited for automated resolution, which motivated Research Activity 1 to implement the SSD in BlueSky. Details of this implementation are covered in Appendix A.

3-2 Independent Variables

This subsection describes the independent variables that will be varied during the simulations. First, the different coordination rules are discussed, followed by the possible conflict scenarios. The last independent variable is on the MS due to different altitudes.

3-2-1 Coordination rules

The objective of the thesis is to develop a CR-algorithm using the SSD. The SSD provides all resolution vectors by means of the set of ARV. The crux in the objective is to develop an appropriate ruleset that will choose a velocity vector in this set of ARV. Assuming that an aircraft is in conflict, thus has its own velocity vector in the set of FRV ($\mathbf{V}_{\text{own}} \in FRV$), the coordination rulesets propose a resolution vector. The possible coordination rules for the small-scale conflict scenarios are visualized in Figure 3-1.

The depicted aircraft in the figure is in conflict and has a target heading of 0° . The first listed rule is to resolve the conflict by taking the shortest way out of the conflict. Another possibility would be to choose the closest right turning, or clockwise turning, resolution vector. Since the conflicting aircraft is approaching from the left, the depicted aircraft has the right of way according to the *rules of the air* and is therefore not required to resolve the conflict. The fourth possibility is to choose the closest point on the target heading or the point closest to the target heading. This slight difference is captured in one rule. Conflicts can also be resolved by only changing the heading or only changing the speed, which make up the last two rules.

It is likely that some of the rules propose the same resolution point. For example, the shortest way out can be identical to the closest clockwise turning resolution. Furthermore, rules five and six should be used in conjuncture with another rule, since these rules do not always provide resolutions. This also explains the difference between coordination rules and rulesets. A coordination rule is a single prescribed solution, whereas a coordination ruleset will always consist of at least one coordination rule and can even contain logic functions. This leads to

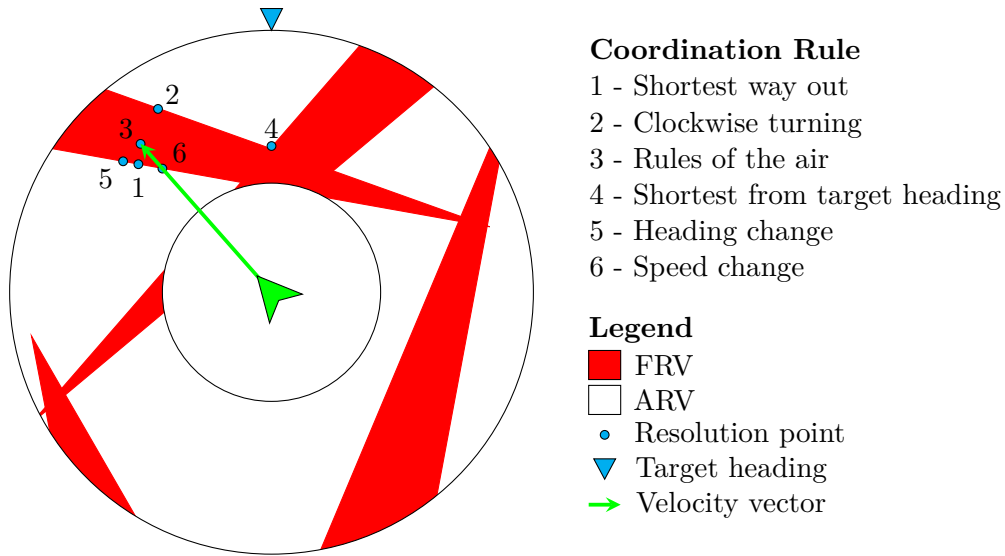


Figure 3-1: Resolution points under different coordination rules

the terminology of a resolution algorithm, which is used interchangeably with coordination rulesets in this thesis as explained in Section 1-1.

The intention is to use the simple coordination rules shown in Figure 3-1 for the small-scale scenarios in the simulations of Research Activity 4. The knowledge gained from the small-scale simulations will allow to develop an improved, but slightly more complicated, coordination ruleset. This improved ruleset will then be compared with the MVP in large-scale simulations.

3-2-2 Conflict Scenarios

The intention is to perform the experiment on two types of conflict scenarios. The first type is included in a set of small-scale scenarios, which will be simulated using the previously described coordination rules as imposed by Research Activity 4. And according to Research Activity 6, the second type will incorporate large-scale conflict scenarios.

These small-scale scenarios will incorporate at maximum ten aircraft and are aimed to showcase the strengths and weaknesses of different coordination rules. These strengths and weaknesses are not only compared within the coordination rules, but might also be compared with the MVP. Examples of such small-scale scenarios are shown in Appendix B. It is expected that these small-scale scenario simulations will offer enough knowledge to develop an improved coordination ruleset.

The improved coordination ruleset is evaluated in large-scale conflict scenario simulations. These large-scale simulations are much more suited to the performance metrics that will be discussed in the next section on the dependent variables.

3-2-3 Maneuvering Space

In Section 2-3 it is shown that the SSD is constructed by incorporating the minimum and maximum true airspeed. The minimum is due to the stall behavior, whereas the maximum due to structural constraints and thrust provided by the engine. The difference in the performance limits effectively determines the MS for the aircraft. The smaller the MS, the smaller the set of ARV and thus limiting the possibilities to resolve a conflict. Therefore, it is interesting to vary the range of these limits. Three ranges are chosen as true airspeeds and listed in Table 3-1. A factor that affects the MS is the altitude. At higher altitudes the stall speed increases, which decreases the MS.

Table 3-1: MS ranges used in the simulations

| Range [kts] | V_{\min} [kts] | V_{\max} [kts] |
|-------------|------------------|------------------|
| 100 | 400 | 500 |
| 200 | 350 | 550 |
| 300 | 250 | 550 |

3-3 Dependent Variables

This subsection describes the dependent variables that can be observed during the simulations. These variables can subsequently be used to assess the performance of different conflict resolution strategies under different conditions, as described in the previous section on the independent variables. The dependent variables are divided into multiple metrics on safety, efficiency and stability, similar to earlier studies [54–56].

3-3-1 Safety

Ideally, a proposed resolution method is safe. The method should be able to keep aircraft separated at a distance of at least their separation minimum. Four metrics are used to assess the safety. The number of conflicts (n_{cfl}) and the number of intrusions (n_{LoS}) are possible metrics. Conflicts, which were formally defined by Definition 1 in Section 2-1-1, occur when a LoS is predicted, whereas a LoS means that an aircraft has actually intruded another aircraft's PZ. From these numbers the Intrusion Prevention Rate (IPR) is derived [54]. The ability to resolve conflicts is measured by this first metric as shown in Eq. 3-1.

$$IPR = \frac{n_{cfl} - n_{LoS}}{n_{cfl}} \quad (3-1)$$

Every LoS can also be characterized. This leads to the second and third metric, the severity and duration of the intrusion. Since this thesis focuses on horizontal resolution maneuvers, the severity of intrusion can be computed with Eq. 3-2. Here, R is the minimum horizontal separation and d_{CPA} the closest distance between two aircraft.

$$LoS_{sev} = \frac{R - d_{CPA}}{R} \quad (3-2)$$

The duration of the intrusion is simply the duration for which the aircraft are in LoS (T_{LoS}). Another time-based metric would be time in conflict (T_{cfl}), which measures the time it takes to resolve conflicts. Since resolving conflicts can cause secondary conflicts due to the domino effect, it is considered less safe to take a relatively long time to resolve conflicts. The four safety metrics are summarized in Table 3-2.

Table 3-2: Safety metrics

| Symbol | Description |
|-------------|---------------------------|
| IPR | Intrusion prevention rate |
| LoS_{sev} | Severity of LoS |
| T_{LoS} | Duration of LoS |
| T_{cfl} | Time in conflict |

3-3-2 Efficiency

The performance of the resolution methods in economic, workload and environmental aspects can be measured by its efficiency. The efficiency can be viewed in two manners. First, the work done (W) by all aircraft in the scenario can be used as a global efficiency metric. Since the work done is strongly correlated with the fuel consumption, this can advocate the economic and environmental benefits of a certain resolution method. The metric for a single aircraft is calculated using Eq. 3-3, where \mathbf{T} is the thrust vector and \mathbf{s} the displacement vector along the path.

$$W = \int_{\text{path}} \mathbf{T} \cdot d\mathbf{s} \quad (3-3)$$

Another view on the efficiency can be in terms of the combined workload for pilots. Suppose a scenario where more than two aircraft are in conflict, which can be resolved with only one aircraft performing a resolution maneuver. It is favorable if only this aircraft maneuvers, since the pilots of the other aircraft do not have to maneuver, leading to a reduced combined workload. This is summarized in the Maneuver Efficiency Rate (MER). This second metric for efficiency is computed by Eq. 3-4. Contrary to the calculation of IPR, where the number of conflict pairs is used, the MER uses the number of aircraft in conflict (N_{cfl}) and the number of aircraft that have performed a resolution maneuver (N_{res}). Ideally, a resolution strategy is found with a low W as well as a high MER . The two efficiency metrics are summarized in Table 3-3.

$$MER = \frac{N_{cfl} - N_{res}}{N_{cfl}} \quad (3-4)$$

3-3-3 Stability

Any resolution method in multi-aircraft conflicts can potentially lead to new conflicts when performing resolution maneuvers. The stability of the method depends on the amount of new

Table 3-3: Efficiency metrics

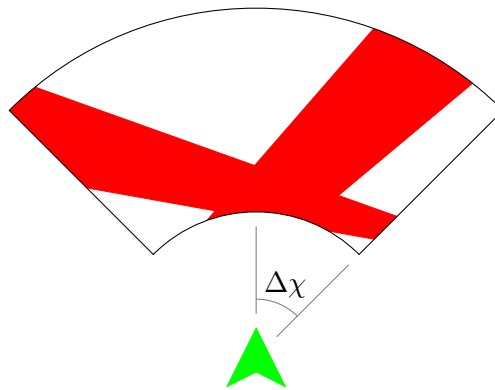
| Symbol | Description |
|--------|--------------------------|
| W | Work done |
| MER | Maneuver efficiency rate |

conflicts. An often used term to describe the instability of a method is the *domino effect* [27,57]. Bilimoria et al. devised a metric to measure this effect, the Domino Effect Parameter (DEP) [30].

Where Bilimoria et al. used the number of aircraft in conflict (N_{cfl}), this thesis will follow the approach of Sunil et al. and use the number of conflict pairs (n_{cfl}) [54]. This subtle difference describes multi-aircraft conflict scenarios more accurately as aircraft with multiple conflicts are included multiple times. The DEP is computed in Eq. 3-5. The number of encountered conflicts without CR (n_{cfl}^{OFF}) is found by simulating without any resolution. Subsequently the number of encountered conflicts with CR (n_{cfl}^{ON}) allows the calculation of the DEP. Generally, the lower the DEP, the more stable the resolution method is. It should be noted that the DEP is less significant in scenarios with a relatively low number of aircraft. Thus, this metric should only be considered in the large-scale scenarios.

$$DEP = \frac{n_{cfl}^{ON}}{n_{cfl}^{OFF}} - 1 \quad (3-5)$$

The SSD also provides insight into the stability of a resolution method by comparing the set of ARV with the set of FRV. This is similar to the explanation in Section 2-3-4, where the SSD has been used to measure ATCo workload and traffic complexity. In more complex traffic scenarios it is often still possible to resolve conflicts by performing substantial heading changes. However, it is undesired to only have a small set of ARV which would lead to these substantial heading changes. To some extent it can be interesting to observe the effect of a resolution method on the set of ARV within a relatively small heading change over time. This MS within a limited heading change ($\Delta\chi$) is visualized in Figure 3-2 and calculated with Eq. 3-6. Similar to DEP, this metric is more suited for the large-scale scenarios.

**Figure 3-2:** The MS within a given heading change ($\Delta\chi$)

$$MS_{\Delta\chi} = \frac{ARV_{\Delta\chi}}{ARV_{\Delta\chi} + FRV_{\Delta\chi}}$$

$$MS_{\Delta\chi} = \frac{ARV_{\Delta\chi}}{\frac{\chi}{180^\circ} \pi (V_{max}^2 - V_{min}^2)} \quad (3-6)$$

It is chosen to observe the MS within $\Delta\chi = \{30^\circ, 60^\circ, 90^\circ\}$. Evaluating these metrics over time allow to draw conclusions on the stability of the resolution method. The four stability metrics are summarized in Table 3-4.

Table 3-4: Stability metrics

| Symbol | Description |
|-------------------------|--|
| <i>DEP</i> | Domino effect parameter |
| <i>MS</i> ₃₀ | Ratio of ARV within a 30° heading change |
| <i>MS</i> ₆₀ | Ratio of ARV within a 60° heading change |
| <i>MS</i> ₉₀ | Ratio of ARV within a 90° heading change |

3-4 Hypothesis

The last activity of this thesis entails the comparison of the new proposed resolution method that uses the SSD with the MVP. Reviewing the nature of the resolution methods can prompt hypotheses on the performance of these methods, which will be discussed in this section.

Hypothesis 1

The metrics on stability (*DEP*) and efficiency (*MER*), are negatively correlated.

A method can create many secondary conflicts while resolving conflicts. In other words, such methods exhibit a significant domino effect, which implies that the *DEP* will be high. This can be confirmed by observing Eq. 3-5, where the number of conflict pairs (n_{cfl}^{ON}) shall be relatively high. Likewise, the number of aircraft performing resolution maneuvers (N_{res}) in Eq. 3-4 shall be relatively high, leading to a low *MER*. Similarly, the opposite case also holds, which explains the negative correlation between the two dependent variables.

Hypothesis 2

The metrics on efficiency (*W* and *MER*), are positively correlated.

It is expected that the performed work is lower when many aircraft have to perform small resolution maneuvers. Opposed to the case where less aircraft resolve, but make significant resolution maneuvers. In terms of the dependent variables, a high *MER* is expected to have a high *W* and vice versa.

Hypothesis 3

Resolution methods based on the SSD have a high *W*, a high *MER* and a low *DEP* compared with the MVP.

The MVP is a decentralized force field method, whereas a method based on the SSD can

be considered a decentralized global optimized method. A property of force field methods is that new conflicts are created as individual aircraft push their way through towards the target. Whereas SSD-based methods will have a less significant domino effect as it searches for a resolution with no conflicts. This explains the expectation of resolution methods based on the SSD having a relatively low DEP. Combining this with Hypotheses 1 and 2 clarifies the higher W and MER compared with the MVP.

Chapter 4

Conclusion

In order to cope with the continued growth of air traffic, the Free Flight concept proposes a decentralized separation approach. One of the early well-functioning separation methods is the MVP. This method resolves conflicts by calculating avoidance vectors for each conflicting pair of aircraft, effectively resolving in a pairwise manner. Pairwise resolving methods are capable of resolving conflicts involving more than two aircraft. However, the interactions between aircraft in these type of conflicts are still not fully known, unlike the intricacies of conflicts involving only two aircraft, which have been subject of a lot of research. A possible solution would be to use the SSD to provide a RA for the pilots to follow.

The SSD is constructed from VOs and the performance limits of the aircraft. It indicates the velocities an aircraft can reach that would lead to conflicting- or conflict-free trajectories. By using a coordination ruleset, a resolution point can be chosen on the SSD to resolve potential conflicts. The ruleset to generate this automated RA in the horizontal plane is one of the expected outcomes of this research. This is embedded in the research objective of further developing the SSD for use as a conflict resolution method. This method can subsequently be described as a decentralized, horizontal, implicitly coordinated, tactical resolution method that encompasses CD, CP and CR.

The research is divided into six activities that will lead to a successful completion of the research objective. The first two activities are the implementation of the SSD and the development of simple coordination rules in BlueSky, the used simulation environment. These two activities are part of the preliminary phase and covered in this preliminary report. The other four activities are planned during the main phase of the research. First, small-scale scenarios with at maximum ten aircraft are defined, followed by simulations of these small-scale scenarios using only simple coordination rules. The findings of these two activities are used to develop an improved coordination ruleset in the fifth activity. In the last activity, large-scale scenarios are to be simulated using the improved coordination ruleset.

The large-scale simulations using the SSD are compared with the MVP. It is expected that both methods will have their strengths and weaknesses in terms of efficiency and stability. For example, it is hypothesized that the SSD will be less efficient in terms of consumed energy, but

more efficient in the low amount of required resolution maneuvers. It should be noted that the findings of this research shall be valid within the defined research scope. The influence of wind, turbulence, transmission loss and noise are all neglected.

Appendix A

Deriving a Solution Space Diagram

The Solution Space Diagram (SSD) fulfills a significant role in the development of the conflict resolution algorithm. In this appendix the SSD is derived in more detail. The derivations are based on work by Ellerbroek [23] and Wu [58]. Furthermore, an initial and a well-functioning implementation of the derived equations in BlueSky are elaborated upon.

A-1 Deriving the legs of a Velocity Obstacle

Since the SSD is constructed from the Velocity Obstacles (VOs) and the performance limits, this first section will focus on the derivation for the VOs. In any conflict a VO should be constructed between the ownship and the obstacle in the absolute velocity space of the ownship. The derivation becomes less complicated when observing that a VO in the absolute velocity space is the same as a Collision Cone (CC) in the relative velocity space. This is also illustrated in Figure A-1. It is apparent that the absolute velocity space is mapped by addition of the obstacle velocity vector \mathbf{V}_{obs} to the relative velocity space. Naturally, the reverse mapping is achieved by subtracting \mathbf{V}_{obs} . This mapping explains Eq. A-1, where the relative velocity vector of the ownship towards the obstacle is derived.

$$\mathbf{V}_{\text{rel}} = \mathbf{V}_{\text{own}} - \mathbf{V}_{\text{obs}} \quad (\text{A-1})$$

Moving between velocity spaces does not influence the spatial domain, thus \mathbf{x}_{own} and \mathbf{x}_{obs} remain unaffected. In Figure A-2 a more detailed overview of the CC is shown. The distance d and relative bearing angle φ from the ownship towards the obstacle can be calculated in various ways. Relatively simple methods would employ flat or spherical earth approximations. A more accurate approximation, also used as navigation standard by ICAO [59], would be the World Geodetic System of 1984 (WGS-84). Conveniently, this standard is already implemented in BlueSky.

The half-angle of the CC is calculated in Eq. A-2, which will also be the half-angle of the corresponding VO. Reiterating the previous, the VO is obtained by adding \mathbf{V}_{obs} to the CC.

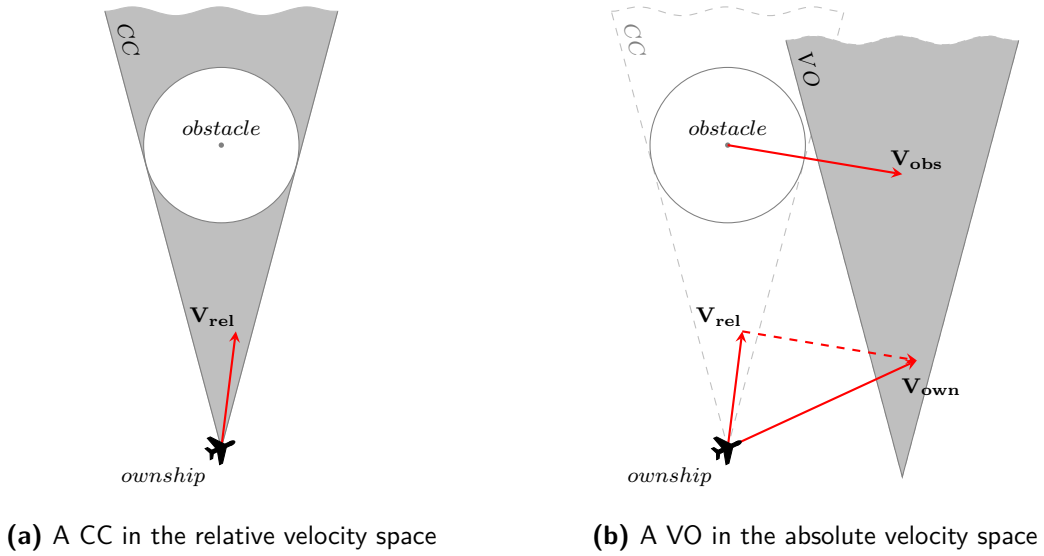


Figure A-1: The CC and VO in the different velocity spaces of the conflict geometry

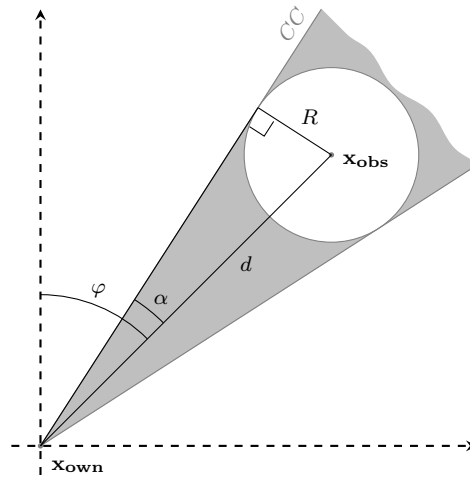


Figure A-2: Relevant angles and distances in the CC

$$\alpha = \arcsin\left(\frac{R}{d}\right) \quad (\text{A-2})$$

The VO can thus be defined using the bearing angle φ , the half-angle α and the obstacle velocity vector \mathbf{V}_{obs} , which results into an obstacle that has an unbounded area. For computational purposes it is useful to bound this area. For this purpose an extreme case of the VO is illustrated in Figure A-3. In this figure the obstacle is an intruder that is approaching from the northeast at the maximum velocity of any aircraft in the airspace ($V_{\text{max}}^{\text{sys}}$). Since this could be higher than the $V_{\text{max}}^{\text{own}}$ of the ownship, the tip of the extreme VO (\mathbf{V}_0) lies outside its performance limits. The remaining vertices of the VO, \mathbf{V}_1 and \mathbf{V}_2 , are chosen such that the base of the VO is tangent to the circle that represents the $V_{\text{max}}^{\text{own}}$ of the ownship.

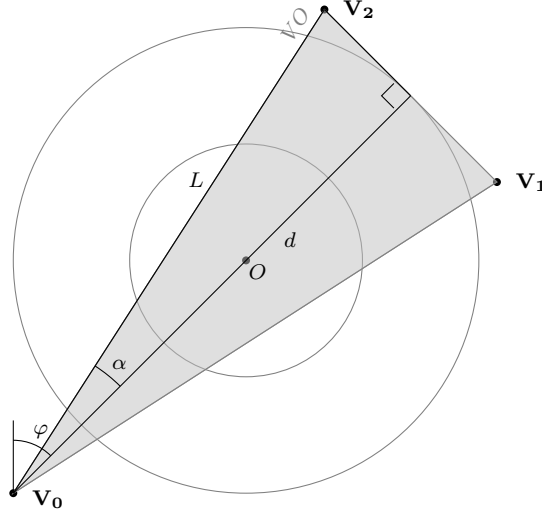


Figure A-3: Extreme VO case

In Eq. A-3 the distance d is formulated for this extreme VO case. The thesis will focus on a single aircraft type, which implies $n_d = 2$ since $V_{max}^{sys} = V_{max}^{own}$.

$$\begin{aligned}
 d &= V_{max}^{own} + V_{max}^{sys} \\
 d &= n_d \cdot V_{max}^{own} \quad \text{with} \quad n_d = \left(1 + \frac{V_{max}^{sys}}{V_{max}^{own}}\right)
 \end{aligned} \tag{A-3}$$

This result allows to calculate the length L of the obstacle legs as shown in Eq. A-4.

$$L = \frac{d}{\cos(\alpha)} \tag{A-4}$$

The first vertex of an arbitrary obstacle is easily found as it is the origin in the relative velocity space. Mapping towards the absolute velocity space needs the addition of the obstacle velocity vector \mathbf{V}_{obs} , which explains Eq. A-5.

$$\mathbf{V}_0 = \mathbf{V}_{obs} \tag{A-5}$$

Subsequently, the bearing angle φ and half-angle α can be used to calculate the remaining vertices of the arbitrary VO. To reduce the amount of trigonometric operations in the implementation, the addition and subtraction theorems for trigonometric functions are used in the derivation of Eq. A-6.

$$\mathbf{V}_2 = \begin{bmatrix} \sin(\varphi - \alpha) \\ \cos(\varphi - \alpha) \end{bmatrix} \cdot L + \mathbf{V}_{\text{obs}}$$

$$\mathbf{V}_2 = \begin{bmatrix} \sin(\varphi) \cos(\alpha) - \cos(\varphi) \sin(\alpha) \\ \cos(\varphi) \cos(\alpha) + \sin(\varphi) \sin(\alpha) \end{bmatrix} \cdot \frac{d}{\cos(\alpha)} + \mathbf{V}_{\text{obs}}$$

$$\mathbf{V}_2 = \begin{bmatrix} \sin(\varphi) - \cos(\varphi) \tan(\alpha) \\ \cos(\varphi) + \sin(\varphi) \tan(\alpha) \end{bmatrix} \cdot 2 \cdot V_{max}^{own} + \mathbf{V}_{\text{obs}} \quad (\text{A-6})$$

$$\mathbf{V}_1 = \begin{bmatrix} \sin(\varphi) + \cos(\varphi) \tan(\alpha) \\ \cos(\varphi) - \sin(\varphi) \tan(\alpha) \end{bmatrix} \cdot 2 \cdot V_{max}^{own} + \mathbf{V}_{\text{obs}} \quad (\text{A-7})$$

The last vertex is derived in similar fashion resulting in Eq. A-7. Note that the addition of \mathbf{V}_{obs} signifies that these vertices are formulated in the absolute velocity space. Having the vertices defined in this order ensures that a polygon with vertices $(\mathbf{V}_0, \mathbf{V}_1, \mathbf{V}_2)$ is always counterclockwise, which is a convention used in many applications. In these applications the exterior is defined using counterclockwise orientated polygons, whereas interiors are defined with clockwise orientated polygons.

A-2 Set operations on the Velocity Obstacle and Velocity Limits

In the construction of the SSD all the VOs are combined with the performance limits of the ownship. In the previous section of this appendix the vertices of an arbitrary VO were formulated. The next step is to take the union of all the VOs to obtain the set of Forbidden Velocities (FV) shown in Eq. A-8. These are the velocities that the ownship must avoid in order to prevent conflicts.

$$FV = \bigcup_{i=1}^N VO_i \quad (\text{A-8})$$

However, not all the velocities in this set can be reached, which can be seen in the set of Reachable Velocities (RV) shown in Eq. A-9. This ring-shaped set is bounded by the velocity limits of the ownship.

$$RV = \{(x, y) \in \mathbb{R}^2 \mid x^2 + y^2 \geq V_{min}^2, x^2 + y^2 \leq V_{max}^2\} \quad (\text{A-9})$$

Combining the FV and the RV by intersection yields the SSD, which consists of the Forbidden Reachable Velocities (FRV) and Allowed Reachable Velocities (ARV) as shown in Eqs. A-10 and A-11.

$$FRV = RV \cap FV \quad (\text{A-10})$$

$$ARV = RV \cap FV^C \quad (\text{A-11})$$

A-3 BlueSky implementation

While the SSD can be formulated in four relatively simple equations formulated in the previous section, the process behind the set operations is much more complex in computational sense. Performing boolean operations on polygons is commonly referred to as *clipping* in computer science and has been subject of multiple studies [60–63]. During the preliminary phase of the thesis the approach was to develop a clipping-module in Python that would perform the boolean operations on the polygons that represented the VOs. The performance in terms of accuracy and speed was poor compared to an existing external clipper-library, which led to decision to opt for the external clipper-library instead. Nevertheless, the initial module will be discussed in the first part of this section.

A-3-1 Initial module

This subsection explains the functioning of the initial developed clipper-module. Note that many exceptions, such as collinear vertices and edges, are excluded to ensure clarity of the explanation. The module distinguished two capabilities that had to be fulfilled. It should be able to return a union set of the VOs (Eq. A-8) and it should be able to intersect this union set with the ring-shaped RV (Eqs. A-10 and A-11).

Union set operation

The first capability to return the union of all VOs can be simplified. Instead of an algorithm that performs the set operation on all VOs simultaneously, the problem is subdivided into a repeating function where only two polygons are unified. This increases the amount of set operations, but reduces the complexity of the algorithm. The simplification is described in Algorithm A.1. Furthermore, it ensures that the algorithm only has to perform the set operation on a certain type of polygons. The unified polygon can possibly have multiple exteriors and interiors, which can be concave or convex. However, the second added polygon in line 4 of Algorithm A.1 is always convex with one exterior as it is a VO. Hence, the relatively simple second polygon further reduces the complexity of the algorithm.

Algorithm A.1 Taking the union set of all VOs

Precondition: *polygon* is a list of length n with the VOs

```

1: function UNION_MULTI(polygon)
2:    $p \leftarrow \text{UNION}(\text{polygon}[1], \text{polygon}[2])$            ▷ This function is described by Algorithm A.2
3:   for  $i \leftarrow 3$  to  $n$  do
4:      $p \leftarrow \text{UNION}(p, \text{polygon}[i])$                  ▷  $p$  will be the union set
5:   end for
6:   return  $p$ 
7: end function

```

The algorithm that performs the union set operation on the two polygons is outlined in Algorithm A.2. Initially an object is created that will hold all necessary information during the set operation. To assist in explaining the algorithm, the polygons shown in Figure A-4a are used. It is evident that the red polygon is the result of an earlier union of three VOs and the blue polygon is the VO that will be added. It should be clear that the red polygon is concave with an interior, whereas the blue polygon is convex with a single exterior.

Algorithm A.2 Perform the union set operation on two polygons

Precondition: $p1$ is the complex polygon, $p2$ is the simple polygon

```

1: function UNION( $p1, p2$ )
2:    $J \leftarrow$  class JOINER( $p1, p2$ )           ▷ An object that holds information during set operation
3:    $J \leftarrow$  MAKEVERTEXLIST( $J$ )
4:    $J \leftarrow$  MAKEEDGELIST( $J$ )
5:    $J \leftarrow$  INTERSECTEDGES( $J$ )
6:    $J \leftarrow$  CHAINEXTERIOR( $J$ )                 ▷ See Algorithm A.3
7:    $J \leftarrow$  CHAININTERIOR( $J$ )
8:    $p \leftarrow$  GETJOINEDPOLYGON( $J$ )
9:   return  $p$ 
10: end function

```

After defining the object, lists of all vertices and edges are made. Figure A-4a shows eighteen exterior vertices and three interior vertices for the red polygon and three exterior edges for the blue polygon. The amount of edges is exactly the same for both polygons. The next step is to check every edge of one polygon with every edge of another polygon for intersections. In the example this means $(18 + 3) \cdot 3 = 63$ operations, resulting in ten intersections. Each intersection results into a new vertex that should be updated in the object. Furthermore, the new intersections also affect the list of edges. For example, the edge $(2 - 7)$ changes to $(2 - 3)$, $(3 - 6)$, $(6 - 7)$. The result of the intersections is shown in Figure A-4b.

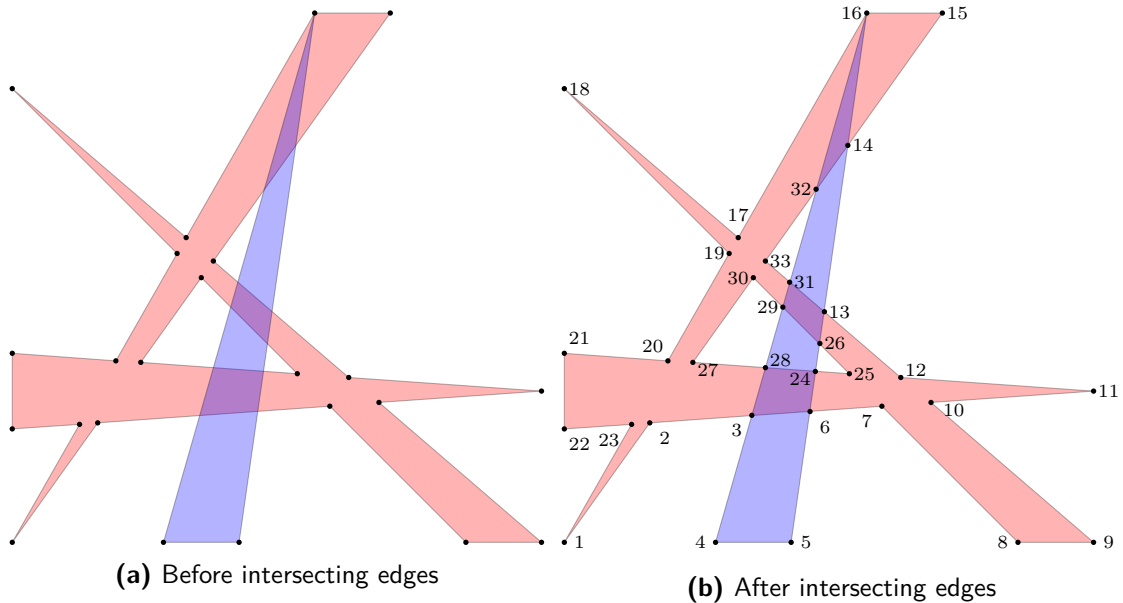


Figure A-4: Intersecting edges of the concave polygon (red) and the convex polygon (blue)

With the updated lists of vertices and edges the union set operation can be performed by a process that is called *chaining* here. This process is outlined in Algorithm A.3. First the exterior is chained, by starting from the most lower left point, vertex 1 in Figure A-4b. The basic idea of the process is to look in the list of edges for neighboring vertices. If only one valid neighbor remains, this vertex will be added to the chain. Otherwise, the next vertex of

the chain is chosen by taking the most clockwise vertex of all neighboring vertices. Herein clockwise is w.r.t. the previous edge in the chain. Taking the figure as example again, the exterior chain starts with 1, 2, 3. The list of edges will show its three neighbors, being 28, 6, 4. Vertex 4 is the most clockwise w.r.t. the edge (2–3) and will therefore be added to the chain. The chain is closed when the process reaches the first vertex again.

Algorithm A.3 Chaining process

Precondition: J is the object that holds information on the set operation

```

1: function CHAINEXTERIOR( $J$ )
2:    $chain \leftarrow$  FINDFIRSTVERTEX( $J$ )                                ▷ Lower left vertex
3:    $chaining \leftarrow$  True
4:   while  $chaining$  do
5:      $V \leftarrow$  FINDNEIGHBORVERTICES( $J, chain[last]$ )                ▷ Using list of edges
6:     if LENGTH( $V$ ) > 1 then
7:       SORTCLOCKWISE( $V$ )                                             ▷ W.r.t. previous edge
8:     end if
9:      $chain \leftarrow chain + V[first]$                                 ▷ Add neighbor vertex to chain
10:    if  $chain[first] = chain[last]$  then
11:       $chaining \leftarrow$  False
12:    end if
13:  end while
14:  UPDATEEDGES( $J, chain$ )                                             ▷ Added edges should not be used again
15:  return  $chain$ 
16: end function

```

In this example case one exterior can be found. The resulting vertices and edges are removed from the lists. A few extra conditions are imposed, which further shortens the lists. Now the interior chaining is processed in similar fashion, which results in three interiors. All resulting interiors and exteriors are saved in the object. The final step in the union set operation is to extract the interiors and exteriors and store them as a polygon.

Intersection set operation

The second capability the module had to fulfill is to intersect with the RV. It has been explained before that it is ring-shaped due to the two circles with radii V_{min} and V_{max} . The initial steps in the intersection set operation are similar to the union set operation. Again, an object is created that will hold the information during the set operation. Subsequently, lists of vertices and edges are stored in that object.

Similar to union set operations, intersections are found in the next step. Instead of edge-edge intersections, edge-circle intersections are calculated. The advantage is that the circles do not have to be discretized into edges and the calculation consists of only solving a quadratic equation. The result of these calculations is depicted with an example in Figure A-5a. This example shows an exterior, built from three VOs, and a single interior similar to the previous example. The figure indicates that some vertices are outside the ring-shaped RV. These vertices are removed in the next step and results in Figure A-5b. The single exterior has been split into three exteriors due to the presence of the circles.

The interior has been made into a smaller polygon with vertices 13, 16, 23. It is evident that five interiors are not included yet as they were not part of the initial polygon. Similar to union set operation, the chaining process (Algorithm A.3) is used to find these interiors. At

Algorithm A.4 Perform the section set operation on the joined polygon and RV

Precondition: p is the joined polygon, $V[\min]$ and $V[\max]$ are the velocity limits

```

1: function INTERSECTION( $p, V[\min], V[\max]$ )
2:    $l \leftarrow$  class INTER( $p, V[\min], V[\max]$ )      ▷ A class that holds information during set operation
3:    $l \leftarrow$  MAKEVERTEXLIST( $l$ )
4:    $l \leftarrow$  MAKEEDGELIST( $l$ )
5:    $l \leftarrow$  INTERSECTCIRCLES( $l$ )
6:    $l \leftarrow$  REMOVEVERTICES( $l$ )                  ▷ Vertices outside RV
7:    $l \leftarrow$  CHAININTERIOR( $l$ )                  ▷ Similar to Algorithm A.3
8:    $l \leftarrow$  CORRECTBOUNDARIES( $l$ )
9:    $p \leftarrow$  GETINTERSECTEDPOLYGON( $l$ )
10:  return  $p$ 
11: end function

```

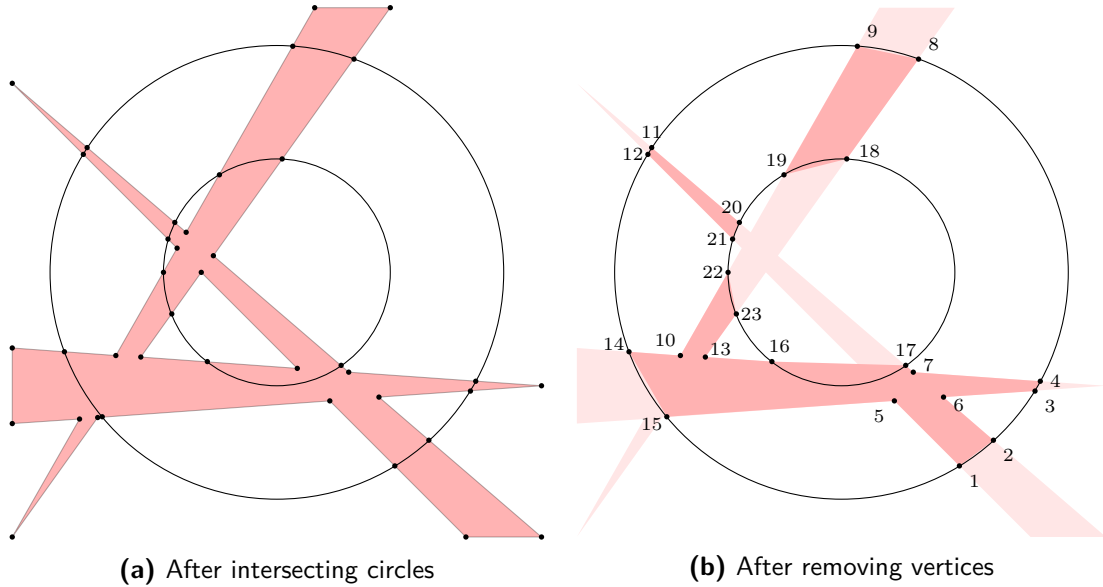


Figure A-5: Removing vertices outside the ring-shaped RV

this moment the correct amount of exteriors and interiors are stored in the object. Inspecting Figure A-5b indicates that one step is left. The vertices on the circles are connected with a single edge, see for example (14 – 15) and (16 – 17). These edges must be replaced by the arc of the circle along which the boundary of the SSD will run. In practice, this means that the single longer edge will be replaced by many shorter edges that follow the curvature of the circles more accurately. After saving the exteriors and interiors, the last function extracts them and saves them as a polygon. This polygon exactly represents the desired SSD after having performed the union and intersection set operations.

A-3-2 External module

Even though the initial module and its algorithms perform accurately in standard scenarios, it unfortunately was not free of inconsistencies. These inconsistencies required exception

handlers to be written into the module, which lowered the execution speed. The iterative nature of Algorithm A.1 further lowered the execution time of the module. Ultimately, this led to the decision to use an existing polygon clipper library. This library is written in Delphi, C# and C++ by Angus Johnson and is based on a clipping algorithm by Vatti [62]. For the implementation in BlueSky a wrapper for Python of the C++ version is used.

The capabilities of the library can be used to perform the union and intersection set operations in respectively Eqs. A-8 and A-10 to obtain the set of FRV. The set of ARV cannot be found using Eq. A-11 as the library is unable to perform operations on the complement of a set. For that reason Eq. A-12 is used to formulate an alternative method of clipping towards the set of ARV. Essentially this signifies taking the set difference of RV with FV. The obtained FRV and ARV complete the SSD.

$$ARV = RV \setminus FV \quad (\text{A-12})$$

Testing the external module against the initial module showed a significant increase in speed. For an example case with 10 aircraft, the initial clipper-module had an execution time of more than 120 ms, whereas the external clipper took only 3 ms to execute. This is mostly due to better optimized code, but also due to employing a lower level programming language. To conclude, the choice for the clipper library is justified since it has a faster execution time and remains to function correctly.

Examples of Simulated Conflict Scenarios

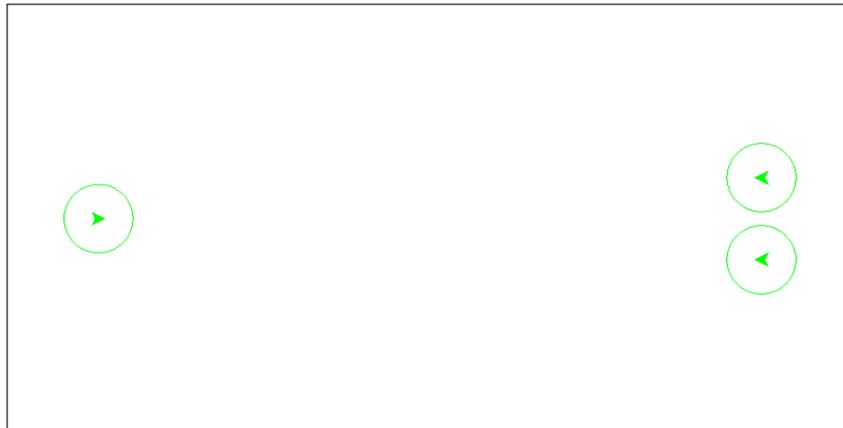


Figure B-1: A small-scale conflict scenario

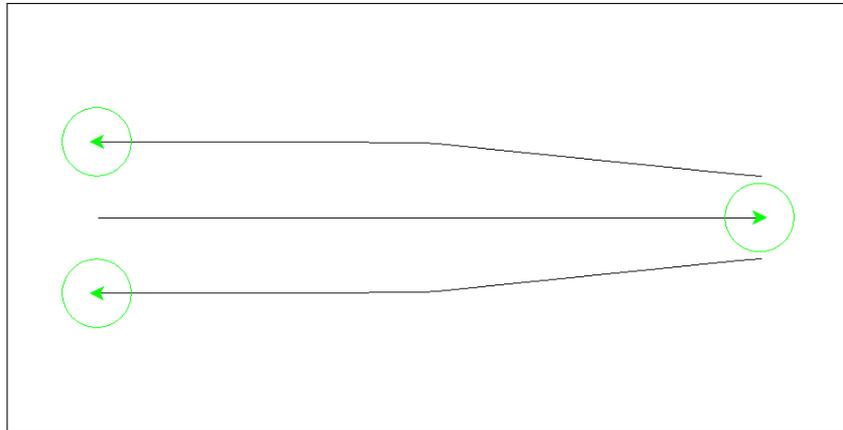


Figure B-2: Scenario of Figure B-1 simulated using the MVP

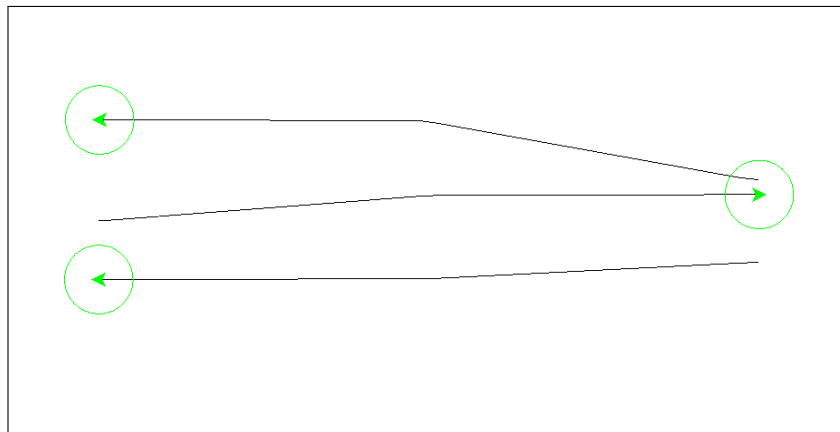


Figure B-3: Scenario of Figure B-1 simulated using the SSD with the shortest-way-out rule

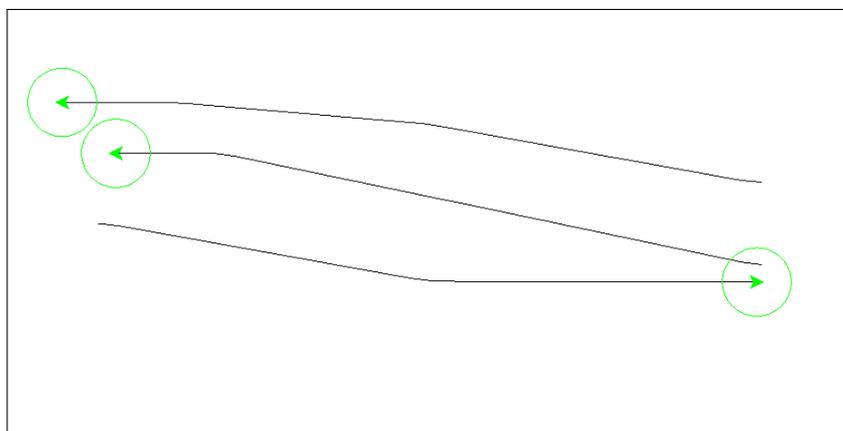


Figure B-4: Scenario of Figure B-1 simulated using the SSD with the clockwise-turning rule

Bibliography

- [1] ICAO, *Global Air Transport Outlook to 2030 and Trends to 2040*, vol. CIR 333. Montréal, Quebec: ICAO, 2013.
- [2] FAA, “FAA Aerospace Forecast: Fiscal Years 2016-2036,” tech. rep., FAA, Washington DC, March 2016.
- [3] EUROCONTROL, “Challenges of Growth 2013, Task 4: European Air Traffic in 2035,” tech. rep., EUROCONTROL, Brussels, June 2013.
- [4] SESAR, *European ATM Master Plan*. Brussels: SESAR, 2015.
- [5] RTCA, Inc., “Final Report of RTCA Task Force 3 on Free Flight Implementation,” tech. rep., RTCA, Inc., Washington DC, October 1995.
- [6] J. M. Hoekstra, R. C. J. Ruigrok, and R. N. H. W. Van Gent, “Free flight in a crowded airspace?,” *3rd USA/Europe Air Traffic Management R&D Seminar*, no. June, 2000.
- [7] T. W. Rand and M. S. Eby, “Algorithms for airborne conflict detection, prevention, and resolution,” *The 23rd Digital Avionics Systems Conference*, no. 3.B.1, pp. 1–17, 2004.
- [8] P. Fiorini and Z. Shiller, “Motion planning in dynamic environments using velocity obstacles,” *The International Journal of Robotics Research*, vol. 17, no. 7, pp. 760–772, 1998.
- [9] J. M. Hoekstra, R. N. H. W. van Gent, and R. C. J. Ruigrok, “Designing for safety: the ‘free flight’ air traffic management concept,” *Reliability Engineering & System Safety*, vol. 75, no. 2, pp. 215–232, 2002.
- [10] J. Ellerbroek, K. C. R. Brantegem, M. M. van Paassen, and M. Mulder, “Design of a coplanar airborne separation display,” *IEEE Transactions on Human-Machine Systems*, vol. 43, no. 3, pp. 277–289, 2013.
- [11] J. Ellerbroek, K. C. R. Brantegem, M. M. van Paassen, M. Mulder, and N. de Gelder, “Experimental evaluation of a co-planar airborne separation display,” *IEEE Transactions on Human-Machine Systems*, vol. 43, no. 3, pp. 290–301, 2013.

- [12] J. M. Hoekstra and J. Ellerbroek, "BlueSky ATC Simulator Project: an open Data and Open Source Approach," *Proceedings of the 7th International Conference on Research in Air Transportation*, no. June, 2016.
- [13] P. Hermes, M. Mulder, M. M. Van Paassen, J. H. L. Boering, and H. Huisman, "Solution-Space-Based Analysis of the Difficulty of Aircraft Merging Tasks," *Journal of Aircraft*, vol. 46, no. 6, pp. 1995–2015, 2009.
- [14] J. G. d'Engelbronner, M. Mulder, and M. M. van Paassen, "The Use of the Dynamic Solution Space to Assess Air Traffic Controller Workload," *AIAA Guidance, Navigation, and Control Conference*, no. August, pp. 1–21, 2010.
- [15] G. A. Mercado Velasco, M. Mulder, and M. M. Van Paassen, "Analysis of Air Traffic Controller Workload Reduction Based on the Solution Space for the Merging Task," *AIAA Guidance, Navigation, and Control Conference*, no. August, pp. 1–18, 2010.
- [16] E. M. Rantanen, J. Yang, and S. Yin, "Comparison of pilots' and controllers' conflict resolution maneuver preferences," *Proceedings of the Human Factors and Ergonomics Society 50th Annual Meeting*, pp. 16–19, 2006.
- [17] ICAO, "Annex 2: Rules of the Air," July 2005.
- [18] C. L. Tallec and A. Joulia, "IFATS: an Innovative Future Air Transport System concept," *4th Eurocontrol Innovative Research Workshop*, 2005.
- [19] S. Chaimatanan, D. Delahaye, and M. Mongeau, "A Hybrid Metaheuristic Optimization Algorithm for Strategic Planning of 4D Aircraft Trajectories at the Continental Scale," *IEEE Computational Intelligence Magazine*, vol. 9, no. 4, pp. 46–61, 2014.
- [20] J. Ellerbroek, M. Visser, S. B. J. Van Dam, M. Mulder, and M. M. van Paassen, "Design of an airborne three-dimensional separation assistance display," *IEEE Transactions on Systems, Man, and Cybernetics*, vol. 41, no. 5, pp. 863–875, 2011.
- [21] J. Lee and N. Moray, "Trust, Control Strategies and Allocation of Function in Human-Machine Systems," *Ergonomics*, vol. 35, no. 10, pp. 1243–1270, 1992.
- [22] J. K. Kuchar and L. C. Yang, "A review of conflict detection and resolution modeling methods," *IEEE Transactions on Intelligent Transportation Systems*, vol. 1, no. 4, pp. 179–189, 2000.
- [23] J. Ellerbroek, *Airborne Conflict Resolution In Three Dimensions*. PhD Thesis, Delft University of Technology, 2013.
- [24] J. Ellerbroek, M. M. van Paassen, and M. Mulder, "Evaluation of a separation assistance display in a multi-actor experiment," *Proceedings of the 16th International Symposium on Aviation Psychology*, pp. 1–12, 2011.
- [25] R. Trim, "Mode S : an introduction and overview," *Electronics & Communication Engineering Journal*, vol. 2, no. 2, pp. 53 – 59, 1990.
- [26] ICAO, "Doc 4444: PANS-ATM," November 2007.

- [27] J. M. Hoekstra, *Designing for Safety: the Free Flight Air Traffic Management Concept*. PhD Thesis, Delft University of Technology, 2001.
- [28] S. Ratcliffe, “‘Free Flight’ for Air Traffic in Europe,” *The Journal of Navigation*, vol. 52, no. May, pp. 289–295, 1999.
- [29] S. Ratcliffe, “Free-flight in Europe, Problems and Solutions,” *The Journal of Navigation*, vol. 54, no. 1966, pp. 213–221, 2001.
- [30] K. D. Bilimoria, K. S. Sheth, H. Q. Lee, and S. R. Grabbe, “Performance Evaluation of Airborne Separation Assurance for Free Flight,” *AIAA Guidance, Navigation, and Control Conference*, no. 2000-4265, 2000.
- [31] F. van Westrenen and J. Ellerbroek, “The Effect of Traffic Complexity on the Development of Near Misses on the North Sea,” *IEEE Transactions on Systems, Man, and Cybernetics*, vol. 47, no. 3, pp. 432–440, 2017.
- [32] Y. I. Jenie, E.-J. van Kampen, J. Ellerbroek, and J. M. Hoekstra, “Taxonomy of Conflict Detection and Resolution Approaches for Unmanned Aerial Vehicle in an Integrated Airspace,” *IEEE Transactions on Intelligent Transportation Systems*, vol. PP, no. 99, pp. 1–11, 2016.
- [33] RTCA, Inc., “Minimum performance standards - Airborne ground proximity warning equipment,” tech. rep., RTCA, Inc., Washington DC, May 1976.
- [34] M. S. Eby, “A Self-Organizational Approach for Resolving Air Traffic Conflicts,” *The Lincoln Laboratory Journal*, vol. 7, no. 2, pp. 239–253, 1994.
- [35] EUROCONTROL, *ACAS Guide*, 2.3 ed., May 2016.
- [36] Bundesstelle für Flugunfalluntersuchung, “Investigation Report,” tech. rep., Bundesstelle für Flugunfalluntersuchung, Braunschweig, May 2004.
- [37] Council of European Union, “Commission regulation (EU) no 1332/2011,” 2011.
- [38] J. M. Hoekstra, R. N. H. W. van Gent, and J. Groeneweg, “Airborne separation assurance validation with multiple humans-in-the-loop,” *5th USA/Europe Air Traffic Management R&D seminar*, vol. 251, pp. 1–10, 2003.
- [39] J. Maas, *A Quantitative Comparison of Conflict Resolution Strategies for Free Flight*. MSc Thesis, Delft University of Technology, 2015.
- [40] J. M. Hoekstra and F. Bussink, “Free Flight: How Low Can You Go?,” *Proceedings of the 21st Digital Avionics Systems Conference*, vol. 2, no. October, 2002.
- [41] L. Tychonievich, D. Zaret, J. Mantegna, R. Evans, E. Muehle, and S. Martin, “A Maneuvering-Board Approach to Path Planning with Moving Obstacles,” *Proceedings of the 11th international joint conference on Artificial Intelligence*, vol. 2, pp. 1017–1021, 1989.
- [42] P. Fiorini and Z. Shiller, “Motion planning in dynamic environments using the relative velocity paradigm,” *1993 IEEE International Conference on Robotics and Automation*, vol. 1, pp. 560–566, 1993.

- [43] J. Ellerbroek, M. M. van Paassen, and M. Mulder, "Coordination in airborne conflict resolution." presented at the 17th International Symposium on Aviation Psychology, May 2013.
- [44] Y. I. Jenie, E.-J. van Kampen, C. C. de Visser, J. Ellerbroek, and J. M. Hoekstra, "Selective Velocity Obstacle Method for Deconflicting Maneuvers Applied to Unmanned Aerial Vehicles," *Journal of Guidance, Control, and Dynamics*, vol. 38, no. 6, pp. 1140–1146, 2015.
- [45] M. M. van Paassen, J. G. D'Engelbronner, and M. Mulder, "Towards an Air Traffic Control Complexity Metric based on Workspace Constraints," *IEEE Systems, Man and Cybernetics International Conference*, pp. 654–660, 2010.
- [46] S. M. B. Abdul Rahman, M. M. van Paassen, and M. Mulder, "Using the Solution Space Diagram in Measuring the Effect of Sector Complexity During Merging Scenarios," *AIAA Guidance, Navigation, and Control Conference*, no. August, pp. 1–25, 2011.
- [47] J. G. d'Engelbronner, C. Borst, J. Ellerbroek, M. M. van Paassen, and M. Mulder, "Solution-Space-Based Analysis of Dynamic Air Traffic Controller Workload," *Journal of Aircraft*, vol. 52, no. 4, pp. 1146–1160, 2015.
- [48] C. Westin, B. Hilburn, and C. Borst, "Mismatches between Automation and Human Strategies: An Investigation into Future Air Traffic Management (ATM) Decision Aiding," *Proceedings of the First SESAR Innovation Days*, 2011.
- [49] C. Borst, C. Westin, and B. Hilburn, "An Investigation into the Use of Novel Conflict Detection and Resolution Automation in Air Traffic Management," *Proceedings of the Second SESAR Innovation Days*, 2012.
- [50] J. van den Berg, M. Lin, and D. Manocha, "Reciprocal Velocity Obstacles for Real-Time Multi-Agent Navigation," *Proceedings of IEEE International Conference on Robotics and Automation*, pp. 1928–1935, 2008.
- [51] J. Snape, J. van den Berg, S. J. Guy, and D. Manocha, "The Hybrid Reciprocal Velocity Obstacle," *IEEE Transactions on Robotics*, vol. 27, no. 4, pp. 696–706, 2011.
- [52] J. Sun, *ADS-B Decoding Guide*. Delft University of Technology, May 2017.
- [53] ICAO, *ADS-B Implementation and Operations Guidance Document*, 7 ed., September 2014.
- [54] E. Sunil, J. Ellerbroek, J. M. Hoekstra, A. Vidosavljevic, M. Arntzen, F. Bussink, and D. Nieuwenhuisen, "Analysis of Airspace Structure and Capacity for Decentralized Separation Using Fast-Time Simulations," *Journal of Guidance, Control, and Dynamics*, vol. 40, no. 1, pp. 38–51, 2017.
- [55] M. A. P. Tra, *The Effect of a Layered Airspace Concept on Conflict Probability and Capacity*. MSc Thesis, Delft University of Technology, 2016.
- [56] T. P. Langejan, *Effect of ADS-B Limitations and Inaccuracies on CD&R Performance*. MSc Thesis, Delft University of Technology, 2016.

-
- [57] K. D. Bilimoria, H. Q. Lee, Z.-H. Mao, and E. M. Feron, "Comparison of Centralized and Decentralized Conflict Resolution Strategies for Multiple-Aircraft Problems," *AIAA Guidance, Navigation, and Control Conference*, no. 2000-4268, 2000.
- [58] A. Wu, *Guaranteed Avoidance of Unpredictable, Dynamically Constrained Obstacles using Velocity Obstacle Sets*. MSc Thesis, Massachusetts Institute of Technology, 2011.
- [59] ICAO, *World Geodetic System - 1984 (WGS-84) Manual*, 2 ed., 2002.
- [60] I. E. Sutherland and G. W. Hodgman, "Reentrant Polygon Clipping," *Communications of the ACM*, vol. 17, no. 1, pp. 32–42, 1974.
- [61] K. Weiler and P. Atherton, "Hidden Surface Removal Using Polygon Area Sorting," *ACM SIGGRAPH Computer Graphics*, vol. 11, no. 2, pp. 214–222, 1977.
- [62] B. R. Vatti, "A Generic Solution to Polygon Clipping," *Communications of the ACM*, vol. 35, no. 7, pp. 56–63, 1992.
- [63] G. Greiner and K. Hormann, "Efficient Clipping of Arbitrary Polygons," *ACM Transactions on Graphics*, vol. 17, no. 2, pp. 71–83, 1998.

